

# **Kinetic Study of E-Selectin-Mediated Adhesion Under Flow**

A Thesis  
Presented to  
The Academic Faculty

By

Annica M. Wayman

In Partial Fulfillment  
Of the Requirements for the Degree  
Doctor of Philosophy in Mechanical Engineering

Georgia Institute of Technology

August 2006

Copyright © Annica Wayman 2006

# **Kinetic Study of E-Selectin-Mediated Adhesion Under Flow**

Approved By:

Dr. Cheng Zhu  
School of Mechanical Engineering and  
Department of Biomedical Engineering  
Georgia Institute of Technology

Dr. Don P. Giddens  
Department of Biomedical Engineering  
Georgia Institute of Technology

Dr. Andres J. Garcia  
School of Mechanical Engineering  
Georgia Institute of Technology

Dr. Marc K. Smith  
School of Mechanical Engineering  
Georgia Institute of Technology

Dr. Rodger P. McEver  
Oklahoma Medical Research Foundation  
and  
Department of Biochemistry and  
Molecular Biology  
University of Oklahoma Health Sciences  
Center

Date Approved: May 30, 2006

This thesis is dedicated to the memory of my father

**Maurice E. Warrick, Jr.**

## ACKNOWLEDGEMENTS

I am very thankful that I have reached this point of my Ph.D. studies. Without the support of several people along the way, I would not have made it this far.

I would first like to thank my advisor Dr. Cheng Zhu for his support of me throughout these years and providing me with the resources necessary to complete my thesis work. I also appreciate the support that my co-advisor, Dr. Don Giddens has given me. Additionally, I am grateful to the rest of my thesis committee members, Dr. Andres Garcia, Dr. Rodger McEver and Dr. Marc Smith for their time and guidance of my thesis project during these years.

My initial lessons in flow chamber assays came from Ms. Anne-Marie Benoliel, Dr. Anne Pierres and Ms. Dominique Touchard of Dr. Pierre Bongrand's laboratory. Without their time and attention, I would not have been able to even begin my thesis. The generosity of Dr. Rodger McEver and his lab technicians in supplying me with the reagents I needed for my experiments was essential to my work, so I thank you. Dr. Tadayuki Yago, a researcher in Dr. McEver's lab, helped me perfect my flow chamber techniques and was always willing to help me with any questions I had regarding my experiments. He was very instrumental in completing the site density work. His guidance was invaluable and much appreciated.

In addition, I would like to recognize the support of my lab members, the staff of the Woodruff School of Mechanical Engineering Department, especially Dr. William J. Wepfer, and the staff of the Institute of Bioengineering and Bioscience (IBB). A special recognition is in order for Johnafel Crowe, facilitator of the Microscopy and

Microanalysis Labs, who helped me greatly with my site density experiments and learning flow cytometry.

I would also like to thank the National Science Foundation Predoctoral Fellowship and National Institutes of Health Research Supplement for Underrepresented Minorities for their funding support. Also, the Georgia Tech FACES Fellowship program has supported me tremendously with financial and academic support. In addition, the support of ARCS Foundation this past year was greatly appreciated. This work was also supported by NIH grants AI 44902 and HL 65631.

On a personal note, I would like to thank all of my family and friends. My parents, Maurice and Deborah A. Warrick did such an excellent job shaping me into who I am and supporting me in all of my endeavors. I am so grateful for their hard work and love. I'd like to thank my brothers, Dion and Jaron, for keeping me grounded. Thank you to my son, Donovan, for making me laugh even after a rough day in the lab. And last but certainly not least, I would like to recognize my husband, Brian, who has really been my main source of encouragement throughout this process. I am so blessed to have him by my side. Thank you for your love and support.

## TABLE OF CONTENTS

ACKNOWLEDGEMENTS.....	IV
LIST OF TABLES .....	IX
LIST OF FIGURES .....	X
LIST OF ABBREVIATIONS.....	XIII
SUMMARY .....	XV
CHAPTER 1: INTRODUCTION.....	1
CHAPTER 2: BACKGROUND .....	4
2.1 Inflammation and Leukocyte Adhesion.....	4
2.2 Relevance of Selectin-Mediated Adhesion in Pathology.....	6
2.3 Selectins .....	7
2.4 Mechanokinetics of Selectin-Mediated Binding.....	11
2.5 Dissociation of Selectin-Mediated Bonds.....	12
2.6 Significance of Catch/Slip Bond.....	15
2.7 Relevance of Dissociation Studies to Rolling Adhesion .....	16
2.8 E-selectin Binding.....	17
CHAPTER 3: MATERIALS AND METHODS .....	21
3.1 Proteins and Cells .....	21
3.2 Coupling of sLe <sup>x</sup> to Microspheres .....	22
3.3 Site Density.....	22
3.4 Flow Chamber Apparatus .....	23
3.5 Preparation of Flow Chamber Experiment .....	24

3.6 Observation of Selectin-Mediated Rolling .....	25
3.7 Tether Frequency and Cell Accumulation .....	26
3.8 Tether Lifetime Analysis .....	26
3.8 Average Rolling Velocity Measurements.....	28
3.8 Instantaneous Rolling Velocity Measurements .....	28
3.10 Determination of Lifetime of Rollingly Adherent Cells.....	29
3.11 Statistical Analysis.....	29
CHAPTER 4: AIM 1 RESULTS .....	31
4.1 Feasibility and Reliability of New Flow Chamber .....	31
4.2 E-selectin/Ligand Interaction is Specific and Calcium Dependent .....	32
4.3 E-selectin/Neutrophil Dissociation Displays Triphasic Force Dependence .....	35
4.4 E-selectin/sLe <sup>x</sup> Dissociation Displays Triphasic Force Dependence .....	41
CHAPTER 5: AIM 2 RESULTS .....	49
5.1 Triphasic Rolling Velocity Over Force for E-selectin/Neutrophil Rolling .....	49
5.2 Triphasic Rolling Velocity Over Force for E-selectin/Fixed Neutrophil Rolling ..	52
5.3 Triphasic Rolling Velocity Over Force for E-selectin/HL-60 Rolling.....	53
5.4 Triphasic Rolling Velocity Over Force for E-selectin/Colo-205 Rolling.....	55
CHAPTER 6: AIM 3 RESULTS .....	58
6.1 New Invertible Flow Chamber is Reliable for Experiments.....	59
6.2 Dissociation of HL-60 cells Rolling on E-selectin .....	59
6.3 Rolling Velocity of HL-60 cells on E-selectin in Normal and Inverted Orientation .....	65
6.4 Dissociation for Neutrophils Rolling on E-selectin.....	74

6.5 Rolling Velocity of Neutrophils on E-selectin in Normal and Inverted Orientation .....	78
CHAPTER 7: DISCUSSION.....	84
7.1 Existence of a Triphasic Dissociation Curve for E-selectin .....	84
7.2 Relevance of the Triphasic Dissociation Curve to Selectin Studies .....	89
7.3 Triphasic Rolling Velocity for Neutrophils, HL-60 and Colo-205 cells .....	93
7.4 Biphasic Dissociation Rate of Rollingly Adherent Cells.....	94
7.5 Relevance of the Dissociation of Rollingly Adherent Cells to Tether Formation..	96
7.6 Average Rolling Velocity in the Inverted Orientation.....	99
CHAPTER 8: CONCLUSIONS AND RECOMMENDATIONS .....	103
REFERENCES .....	110

## LIST OF TABLES

Table 4-1: Various sealing methods of the flow chamber tested.....	32
Table 4-2: P-values of Student's t-test for tether lifetime and off-rate data .....	40
Table 4-3: P-values obtained by comparing the slopes of each phase of the tether lifetime curves .....	41
Table 4-4: P-values obtained by comparing the slopes of each phase of the rolling velocity curves .....	48

## LIST OF FIGURES

Figure 2-1: Depiction of the cascade of adhesion events .....	4
Figure 2-2: Illustration of the three selectin types and their ligands.....	8
Figure 3-1: Plot of the site density measured for varying concentrations of sEs .....	23
Figure 3-2: Schematic of the invertible flow chamber .....	24
Figure 4-1: Representative data for the initial tethering frequency for E-selectin/ Neutrophil interaction with E-selectin at $4.67 \text{ sites}/\mu\text{m}^2$ under various conditions .....	33
Figure 4-2: Representative data for the initial tethering frequency for E-selectin/HL-60 interaction with E-selectin at $37 \text{ sites}/\mu\text{m}^2$ under various conditions.....	34
Figure 4-3: Representative data of the cell accumulation after 5 minutes for E- selectin/HL-60 interaction under various conditions .....	35
Figure 4-4: Representative dissociation curves for the transient tethering of neutrophils to E-selectin at various shear stresses.....	36
Figure 4-5: Average tether lifetime measures of the E-selectin/Neutrophil interaction as a function of shear stress.....	37
Figure 4-6: Average dissociation rate constants for the E-selectin/Neutrophil interaction as a function of force .....	39
Figure 4-7: Flow cytometry results confirming the coupling of biotinylated $\text{sLe}^x$ on streptavidin-coated microspheres .....	42
Figure 4-8: Representative data for the initial tethering frequency for E-selectin/ $\text{sLe}^x$ interaction with E-selectin at $29 \text{ sites}/\mu\text{m}^2$ under various conditions.....	43

Figure 4-9: Representative dissociation curves for the transient tethering of sLe <sup>x</sup> -coated beads to E-selectin at various shear stresses .....	45
Figure 4-10: Average tether lifetime measures for the E-selectin/sLe <sup>x</sup> interaction as a function of shear stress .....	46
Figure 4-11: Average off-rate constants for the E-selectin/sLe <sup>x</sup> interaction as a function of force .....	47
Figure 5-1: Average rolling velocity for neutrophils rolling on E-selectin at 37 and 248 sites/ $\mu\text{m}^2$ at various shear stresses.....	51
Figure 5-2: Average rolling velocity for fixed neutrophils rolling on E-selectin at 248 sites/ $\mu\text{m}^2$ at various shear stresses.....	52
Figure 5-3: Average rolling velocity for HL-60 cells rolling on E-selectin at 248 sites/ $\mu\text{m}^2$ at various shear stresses.....	54
Figure 5-4: Average rolling velocity for Colo-205 cells rolling on E-selectin at 248 sites/ $\mu\text{m}^2$ at various shear stresses.....	56
Figure 6-1: Video images of HL-60 cells rolling on E-selectin at 127 sites/ $\mu\text{m}^2$ while inverted.....	60
Figure 6-2: Dissociation curves for the pooled data of HL-60 cells rollingly adherent on E-selectin at 127 sites/ $\mu\text{m}^2$ at various shear stresses .....	62
Figure 6-3: Dissociation rate constant from pooled data for rollingly adherent HL-60 cells on E-selectin at 127 sites/ $\mu\text{m}^2$ as a function of shear stress .....	63
Figure 6-4: Dissociation rate constants for rollingly adherent HL-60 cells on E-selectin at 73 sites/ $\mu\text{m}^2$ for one experiment and for 127 sites/ $\mu\text{m}^2$ with pooled data .....	64
Figure 6-5: Average rolling velocity of rollingly adherent HL-60 cells on E-selectin at 127 sites/ $\mu\text{m}^2$ while inverted .....	65

Figure 6-6: Instantaneous rolling velocity plots for three representative HL-60 cells each in the normal and inverted orientation on 127 sites/ $\mu\text{m}^2$ of E-selectin at 0.25 dynes/ $\text{cm}^2$ .....	66
Figure 6-7: Instantaneous rolling velocity plots for three representative HL-60 cells each in the normal and inverted orientation on 127 sites/ $\mu\text{m}^2$ of E-selectin at 0.1 dynes/ $\text{cm}^2$ .....	68
Figure 6-8: Instantaneous rolling velocity plots for three representative HL-60 cells each in the normal and inverted orientation on 127 sites/ $\mu\text{m}^2$ of E-selectin at 0.5 dynes/ $\text{cm}^2$ .....	70
Figure 6-9: Comparison of the average rolling velocities for the normal and inverted orientation at 127 sites/ $\mu\text{m}^2$ of E-selectin .....	71
Figure 6-10: Average distance HL-60 cells travel while continuously rolling on E-selectin at 127 sites/ $\mu\text{m}^2$ in normal orientation .....	73
Figure 6-11: Dissociation curves for the pooled data of neutrophils rollingly adherent on E-selectin at 127 sites/ $\mu\text{m}^2$ at various shear stresses.....	76
Figure 6-12: Dissociation rate constant from pooled data for rollingly adherent neutrophils on E-selectin at 127 sites/ $\mu\text{m}^2$ and for one experiment at 73 sites/ $\mu\text{m}^2$ as functions of shear stress .....	77
Figure 6-13: Average rolling velocity from one experiment for neutrophils rolling on E-selectin at 127 sites/ $\mu\text{m}^2$ while inverted.....	79
Figure 6-14: Instantaneous rolling velocity plots for three representative neutrophils each in the normal and inverted orientation on 248 sites/ $\mu\text{m}^2$ and 127 sites/ $\mu\text{m}^2$ , respectively, of E-selectin at 0.25 dynes/ $\text{cm}^2$ .....	80
Figure 6-15: Instantaneous rolling velocity plots for three representative neutrophils each in the normal and inverted orientation on 248 sites/ $\mu\text{m}^2$ and 127 sites/ $\mu\text{m}^2$ , respectively, of E-selectin at 0.15 dynes/ $\text{cm}^2$ .....	82

## LIST OF ABBREVIATIONS

sEs	Soluble E-selectin
PSGL-1	P-selectin Glycoprotein Ligand-1
sLe <sup>x</sup>	sialyl Lewis-x
sLe <sup>a</sup>	sialyl Lewis-a
ESL-1	E-selectin Ligand-1
mAb	monoclonal antibody
k <sub>off</sub>	Dissociation rate constant
k <sup>o</sup> <sub>off</sub>	Unstressed dissociation rate constant
k <sub>off(RA)</sub>	Dissociation rate constant for rollingly adherent cells
AFM	Atomic Force Microscope
SPR	Surface Plasma Resonance
SEM	Standard Error Mean
HSA	Human Serum Albumin
BSA	Bovine Serum Albumin
HBSS	Hank's Balanced Salt Solution
Lec	Lectin
EGF	Epidermal Growth Factor
IL-1	Interlukin-1
TNF	Tumor Necrosis Factor
PNAd	Peripheral Node Addressin
GlyCAM-1	Glycosylation-dependent Cell Adhesion Molecule-1

VEGFR	Vascular Endothelial Growth Factor Receptor
HPC	Hematopoietic Progenitor Cells
NeuNAc	N-acetylneuraminic acid
Fuc	Fucose
A/D	Analog to Digital

## SUMMARY

During inflammation and thrombosis, leukocytes tether to and roll on vascular surfaces and platelets through selectin molecules under shear flow. This selectin family of cell adhesion molecules includes P-, E-, and L-selectin. The association and dissociation of two or more selectin-mediated bonds under mechanical load produce the rolling motion of the leukocytes. Although much has been uncovered about the properties of selectins, the complete story of the selectin-mediated adhesion process is yet to be told. The goal of this research is to gain a more quantitative understanding of this receptor-ligand binding through the study of the dissociation kinetics of E-selectin-mediated adhesion using flow chamber techniques.

From transient tethering experiments, the dissociation rate of E-selectin-mediated adhesion was found to have a triphasic shear dependence at low shear stresses, where the bond transitioned from a slip to a catch then again to a slip bond. This trend was further supported by observations of the average rolling velocity of cells adhering to E-selectin at various shear stresses. A triphasic force dependence of the rolling velocity was revealed that showed that regions of increasing rolling velocity corresponded to the slip bond regime where tether lifetime decreased with increasing shear stress. Decreasing rolling velocity coincided with the catch bond regime, a regime of prolonged tether lifetime with increasing shear stress.

An invertible flow chamber was used in hopes of directly quantifying the dissociation rate of rollingly adherent cells on E-selectin to compare it to the dissociation rate data obtained through transient tethering experiments. However, tether formation, which

relates to the association rate, and its role in the stability of rolling seemed to be a key factor in the dissociation rate of rollingly adherent cells over the low shear stress range.

Overall, this thesis work shows that for the dissociation of transiently tethering cells to E-selectin at low shear forces, a slip/catch/slip bond exists, which seems to govern the rolling velocity of cells on E-selectin substrates. This dissociation behavior of E-selectin is similar to what has been found for P- and L- selectin, with the exception of the slip bond that precedes the catch bond. Thus, knowing the dissociation rate of E-selectin can provide additional insight into the catch bond phenomenon for the three selectins. Furthermore, the dissociation of rollingly adherent cells to E-selectin substrates may also have a biphasic and possibly triphasic dependence on shear stress. These results provide supporting evidence of a shear threshold for E-selectin as well as data to suggest that tether formation, in coordination with off-rate, determine the rolling velocity behavior of cells adhering to E-selectin.

## CHAPTER 1

### INTRODUCTION

Leukocyte recruitment during inflammation begins with their rolling adhesion to vascular surface through selectin molecules. Rolling occurs through the fast association and dissociation of selectins with their ligands. Selectin-mediated bonds also have mechanical properties that influence the kinetics when in a stressed environment like the circulatory system.

The dissociation rates of selectin-mediated interactions have been well studied at moderate to high shear stresses. However, the dissociation kinetics at low shear forces have only recently been studied and found to include catch bonds for P- and L-selectin. The dissociation rate for E-selectin-mediated adhesion has yet to be fully revealed. Moreover, past studies have determined the dissociation rate of selectin/ligand interactions using non-rolling cells. Although these results seem to be consistent with the relative rolling velocities obtained for each of the selectins, direct observation of the dissociation of rollingly adherent cells has not been done. Therefore, the goal of this thesis work is to better understand the dissociation kinetics of E-selectin-mediated adhesion for both transiently tethering and rollingly adherent cells using flow chamber assays.

***Aim 1:** Determine the force dependence of the dissociation kinetics for E-selectin/ligand interactions during transient tethering at low forces.*

This study aims to understand the dissociation kinetics at low forces. Evidence suggests that a transition from a more commonly seen slip bond to a catch bond exists for selectins as force decreases in the low force range. This has been shown for P- and L-selectin with the atomic force microscope and flow chamber. For E-selectin, early micropipette data indicates a trend similar to P- and L-selectin, but includes a third transition back to a slip bond as force decreases further. This has yet to be shown with E-selectin in flow chamber studies. Therefore, this aim intends to measure the dissociation rate or tether lifetime for E-selectin/ligand interaction under low forces using the flow chamber. Tether lifetimes for neutrophils and sialyl Lewis-x-coated beads was measured over a range of shear forces and found to vary with force in a triphasic manner.

***Aim 2:** Determine the force dependence of the rolling velocity for E-selectin/ligand interactions at low forces.*

For L-selectin, the transition between a catch and slip bond governs the rolling velocity of the cells through the shear threshold. So for this aim, the rolling velocity of cells mediated by E-selectin will be measured over a low shear force range. Revealing the dependence of the cell's rolling velocity on shear force would provide confirmation of the results for the dissociation kinetics obtained in Aim 1 because of what has been seen for L-selectin. In addition, the results would offer a possible reason for the triphasic dissociation kinetics of E-selectin found in Aim 1. The rolling velocities of neutrophils, fixed neutrophils and other cell types to E-selectin were determined and shown to also have a triphasic dependence on force.

***Aim 3:** Measure the dissociation kinetics of rollingly adherent cells mediated by E-selectin using an invertible flow chamber.*

Rolling involves multiple tethers forming and dissociating sequentially. Although selectin-mediated rolling has been extensively studied, the complex nature of its kinetics makes quantitatively determining the mechanisms involved in rolling quite challenging. Studies that look at the dissociation portion of the rolling mechanism are done with transiently tethering (non-rolling) cells as in Aim 1 of this thesis. However in this aim, a uniquely designed invertible flow chamber was used to study the dissociation kinetics of rollingly adherent cells. By measuring the number of rolling cells bound over time while inverted, the lifetime or dissociation rate of rollingly adherent HL-60 cells and neutrophils to E-selectin as a function of shear stress was determined. This new approach to studying the dissociation kinetics of rollingly adherent cells has actually led to further insight into the association kinetics of selectin-mediated binding.

## CHAPTER 2

### BACKGROUND

#### *2.1 Inflammation and Leukocyte Adhesion*

Inflammation is the body's reaction to tissue injury and infection. During the inflammation process, leukocytes are recruited to the local site of injury through a cascade of events as shown in Figure 2-1. Early in the inflammatory response, leukocytes flowing through the postcapillary venules at about 1mm/s tether to and roll on the local vasculature. This tethering and rolling is mediated by specific interactions

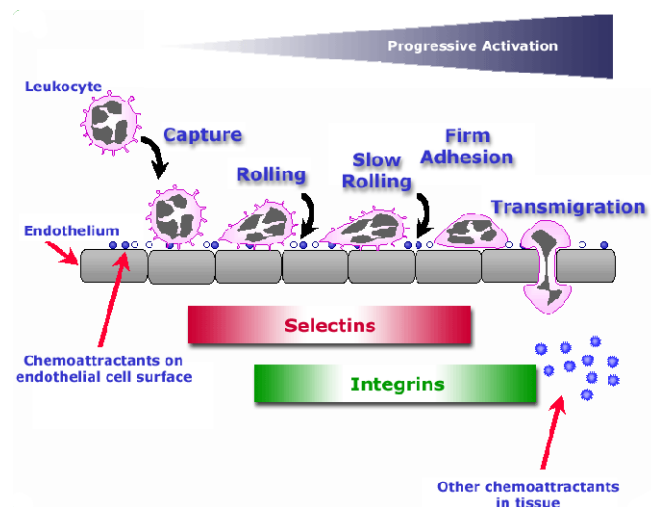


**Figure 2-1:** Depiction of the cascade of adhesion events that occurs during the inflammatory response (Ley 2003)

between selectins and their ligands, molecules that are both expressed on the leukocytes and on the vascular surface (Lawrence et al. 1991; Ley et al. 1991; von Andrian et al. 1991; McEver et al. 1995). These surface molecules are expressed either constitutively or induced by cytokines and other mediators (Springer 1994). Selectins are a family of molecules able to support temporary adhesion under a wide range of mechanical loads (Springer 1995; Chen et al. 1997). This family of selectins includes P-, E-, and L-selectin. Through this rapid selectin-ligand interaction, leukocytes roll along the vascular surface at velocities 10 to 100 times slower than its free stream velocity. The slower rolling prolongs the exposure of leukocytes to locally presented chemokines. Chemokines cause the activation of integrin molecules which mediate firm adhesion of the leukocytes to the vascular surface (Larson et al. 1990; Springer 1994). Integrins, heterodimeric molecules that consist of a  $\alpha$  and  $\beta$  subunit, are involved in various cell and extracellular matrix adhesion processes and signal transduction. Of the several integrin subfamilies that exist, the  $\beta_2$  integrins such as  $\alpha_L\beta_2$  and  $\alpha_M\beta_2$ , are known to mediate the firm adhesion and neutrophil activation during the inflammatory response (Schmits et al. 1996; Lu et al. 1997). Following this firm adhesion through the integrin molecules, the leukocyte emigrates through the endothelium of the tissue to the site of injury.

Similar trafficking of blood-borne cells occurs with lymphocyte homing and hematopoietic progenitor cells (HPC) entering the bone marrow (Springer 1994; Frenette et al. 1998; Mazo et al. 1998). Insight into cell trafficking requires an understanding of the molecular interactions that are involved. The first of these molecular interactions centers on the selectin family of molecules.

## ***2.2 Relevance of Selectin-Mediated Adhesion in Pathology***

With selectins playing a primary role in leukocyte trafficking, they are found to be relevant in certain pathologies. Cancer metastasis involves cellular adhesion of cancer cells instead of normal leukocytes. Certain types of cancer cells, particularly most human colon cancer cells, are known to express selectin ligands, including sLe<sup>x</sup> and mediate adhesion through E-selectin (Lauri et al. 1991; Kojima et al. 1992; Bevilacqua et al. 1994). In implantation of allografts, xenografts or tissue engineered grafts, graft rejection primarily involves inflammation where leukocyte adhesion plays a role and E-selectin has been seen expressed in certain tissues such as kidneys and heart (Bevilacqua et al. 1994). Pathologies such as ischemia-reperfusion injury, atherosclerosis, rheumatoid arthritis and several vasculitis-related diseases involve enhanced leukocyte-endothelium adhesion, thus the role of selectins in these diseases is likely. In fact, distinct selectin expression has been found in these diseased areas (Bevilacqua et al. 1994). Additionally, with the growing interest in stem cell transplantation, understanding the role of selectin-mediated adhesion in the homing of HPC to the bone marrow is important in finding more efficient transplantation procedures (Voermans et al. 2000).

In atherosclerosis, which is among the leading causes of death in the United States, leukocyte rolling on endothelium has been found to be highly dependent on P-selectin and also influenced by E-selectin (Eriksson et al. 2001). O'Brien et al. found E-selectin to be the only molecule seen more in atherosclerotic plaques than control coronary arteries examined (O'Brien et al. 1996). In addition, studies of monocyte adhesion in a stenotic model showed that the presence of E-selectin allowed adhesion at higher wall shear stresses, and adhesion was most abundant in the stenosis and tapered

regions for both steady and pulsatile flow (Hinds et al. 2001). Hence, the understanding of selectin-mediated adhesion in the hydrodynamic environment has the potential to open the pathways to a better knowledge of several pathologies related to the inflammation process and development of therapies for their treatment.

### ***2.3 Selectins***

The selectin family are type I membrane glycoproteins. Included in this selectin family are three types: P-, E-, and L-selectin. All selectins have a N-terminal C-type ( $\text{Ca}^{2+}$  dependent binding) lectin (Lec) domain that is followed by an epidermal growth factor (EGF)-like domain, a series of consensus repeats, a transmembrane domain and a cytoplasmic tail (McEver et al. 1995). Each selectin is distinct in the number of consensus repeats that it contains. P-selectin contains 9 while E-selectin contains 6 and L-selectin contains 2 consensus repeats.

P-selectin is stored in the Weibel-Palade bodies of endothelial cells and the  $\alpha$  granules of platelets (Springer 1995). The exposure to stimuli like histamine and thrombin causes the redistribution of P-selectin on the endothelial cells (Bevilacqua et al. 1994). Natively, P-selectin extends 38nm from the cell surface and has been shown to require a sufficient length to facilitate adhesion (Ushiyama et al. 1993; Patel et al. 1995). Similarly, E-selectin is expressed on endothelial cells upon stimulation with cytokines like interleukin-1 (IL-1) or tumor necrosis factor (TNF), extending 27nm above the cell surface (Hensley et al. 1994; Springer 1994). L-selectin, only extending approximately 10-12nm (Patel et al. 1995), is constitutively expressed on the microvilli tip of all

circulating leukocytes except for a subpopulation of memory lymphocytes (Erlandsen et al. 1993; Borregaard et al. 1994; Springer 1994).

As shown in Figure 2-2, the ligands that each of the three selectins binds to varies. However, a glycan epitope commonly found on all of the ligands of the three selectins is sialyl Lewis-x (sLe<sup>x</sup>). This carbohydrate structure contains a sialic acid and fucose component (Phillips et al. 1990; Polley et al. 1991; Zhou et al. 1991; Foxall et al. 1992). The most well characterized sLe<sup>x</sup> containing ligand is the homodimeric mucin, P-selectin glycoprotein ligand-1 (PSGL-1), which binds to all the selectins. PSGL-1 is constitutively expressed on the microvilli tips of leukocytes, extending 50-60nm from the surface (McEver et al. 1984; Moore et al. 1995). This glycoprotein is 240kDa with multiple N- and O-linked glycans. Branched, core-2 O-linked structures are decorated with sLe<sup>x</sup> and in the N-terminal region is a cluster of three tyrosine residues (Kumar et al. 1996; Bruehl et al. 1997; Moore 1998).

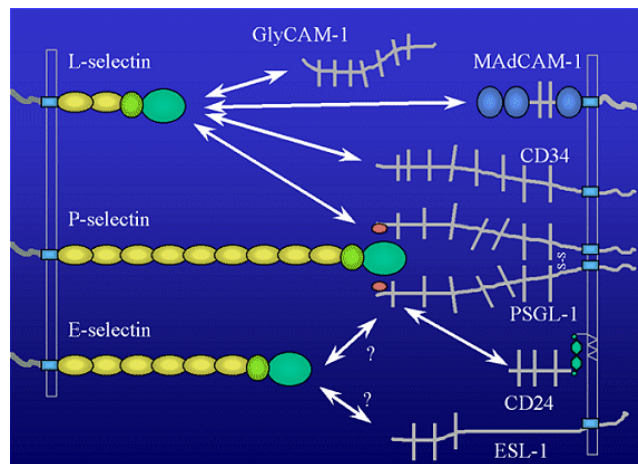


**Figure 2-2:** Illustration of the three selectin types and their ligands (Ley 2003)

P-selectin appears to have the highest affinity to PSGL-1 with an approximate  $K_D=320 \pm 20\text{nM}$  (Mehta et al. 1998) whereas E-selectin's very low affinity to PSGL-1 is 50 times lower than P-selectin/PSGL-1 (Moore et al. 1994). Through modeling of the co-crystal structure of the Lec and EGF domain of P- and E-selectin with the N-terminal domain of PSGL-1, two amino acid residues on P-selectin were found to interact critically with the sulfates on the tyrosine residues on PSGL-1. These residue interactions in the E-selectin/PSGL-1 complex is not as developed and may contribute to the lower affinity of E-selectin/PSGL-1 compared to P-selectin/PSGL-1. L-selectin lacks one of the residues to bind to the second tyrosine on PSGL-1 suggesting a weaker affinity of L-selectin to PSGL-1 than P-selectin (Somers et al. 2000).

The affinity of selectins binding to only the  $sLe^x$  portion is much lower than with the full PSGL-1 with  $K_D$  of 7.8, 3.9 and 0.72 mM for P-, L- and E-selectin, respectively (Poppe et al. 1997). This indicates that other components of PSGL-1 contribute to selectin-mediated binding. From this and other static culture experiments, E-selectin shows to have the highest relative affinity to  $sLe^x$  among the three selectins (Phillips et al. 1990; Polley et al. 1991; Foxall et al. 1992). The better affinity of E-selectin to  $sLe^x$  may result from the unique positioning of the N-acetylneuraminic acid (NeuNAc) residue and the fucose (Fuc) binding in the E-selectin/ $sLe^x$  complex (Somers et al. 2000).

For selectin-mediated binding to occur, the Lec and EGF domain are necessary and sufficient to mediated rolling. A finite region near the one bound  $Ca^{+2}$  on the Lec domain is likely the ligand interaction site. Other critical amino acid residues on the Lec domain seem to also be directly involved in the ligand recognition (Graves et al. 1994). Despite the limited association between the Lec and EGF domain suggesting that the

interface is flexible, EGF may modulate adhesion as well (Kansas 1996; Somers et al. 2000). P-selectin is additionally known to require at least five consensus repeats within the structure to sufficiently mediate neutrophil rolling. The consensus repeats serve to extend the P-selectin into optimal position for interaction with PSGL-1 (Patel et al. 1995). This was further quantified with P- and E-selectin with two-dimensional binding where a lower association rate was obtained when the binding domains of the selectins and their antibodies were lowered or randomly oriented on the membrane surface (Huang et al. 2004). L-selectin, despite only having two consensus repeats, is located on the microvilli tip of leukocytes, making it accessible for binding.

Selectin-mediated binding to PSGL-1 also depends on the presentation and modification of sLe<sup>x</sup> on PSGL-1 (Pouyani et al. 1995; Sako et al. 1995; McEver et al. 1997; Yang et al. 1999). Without tyrosine sulfation of PSGL-1, P-selectin-mediated rolling is drastically reduced (Rodgers et al. 2001) and may be required for rolling to occur (Goetz et al. 1997; Ramachandran et al. 1999). Similar binding requirements have been suggested for L-selectin as well (McEver et al. 1997; Yang et al. 1999). Interestingly, E-selectin is not dependent on tyrosine sulfation to mediate rolling (Pouyani et al. 1995; Sako et al. 1995; Rodgers et al. 2001).

In addition to the molecular interaction requiring certain residues and being positioned properly, cellular features such as cell contact area, microvilli extension and membrane extrusions also contribute to the selectin-mediated rolling. The deformation of rollingly adherent leukocytes under flow has been observed both *in vivo* and *in vitro* (Firrell et al. 1989; Lei et al. 1999). Additionally, neutrophils rolling on P-selectin exhibit membrane extrusions whose dynamic alternation are important for stabilizing

rolling (Ramachandran et al. 2004). Experiments with microspheres and fixed cells further confirmed the importance of cellular contributions. Microspheres coupled with sLe<sup>x</sup> or PSGL-1 or fixed cells expressing selectin ligands exhibited less robust and stable rolling on selectin surfaces (Brunk et al. 1997; Greenberg et al. 2000; Rodgers et al. 2000; Yago et al. 2002).

#### ***2.4 Mechanokinetics of Selectin-Mediated Binding***

Selectin binding depends on the unique kinetic and mechanical properties of each selectin-ligand pair. The formation and breakage of bonds between the selectin and its ligand is characterized by the kinetic parameters of association ( $k_{on}$ ) and dissociation rates ( $k_{off}$ ), respectively. The rapid association and dissociation of two or more selectin-mediated bonds subjected to an applied force results in leukocyte rolling on the cell surface that is a 10-100 fold reduction from the free stream velocity of the cells (von Andrian et al. 1991; Alon et al. 1997). An increase in the selectin or ligand density decreases the rolling velocity but an increase in wall shear stress ( $\tau_w$ ) above the required shear slowly increases the velocity of rolling (Chen et al. 1997; Puri et al. 1997). The tethering efficiency and strength of the rolling adhesion is similar among the three selectins. But, L-selectin is found to mediate the fastest rolling that is 7.5-9-fold faster than P-selectin and 8-11.5-fold faster than E-selectin-mediated rolling. Thus despite some overlap in structure and function between the three selectins, they each have distinct kinetic properties that result in unique leukocyte rolling behavior. The complexity of rolling involves understanding the mechanically coupled kinetics of both the association and dissociation of the selectin-mediated bond.

## ***2.5 Dissociation of Selectin-Mediated Bonds***

### **2.5.1 Bell Model**

The dissociation rate ( $k_{\text{off}}$ ) of the selectin/ligand interactions has been well studied. Bell proposed that in first order dissociation kinetics,  $k_{\text{off}}$  increases exponentially with increasing bond force according to the equation (Bell 1978):

$$k_{\text{off}} = k_{\text{off}}^{\circ} \exp(\sigma F_b / kT)$$

where  $k_{\text{off}}^{\circ}$  is the unstressed off-rate,  $\sigma$  represents the range of the energy well that defines the bound state,  $F_b$  is the bond force which can be calculated from  $\tau_w$  through lever arm measurements and static analysis (Alon et al. 1997),  $k$  is Boltzmann's constant and  $T$  is the absolute temperature. Selectin flow chamber experiments that suggest single tether formation due to a low adhesion probability that cannot support rolling exhibit first order dissociation kinetics. This is shown by a linear plot of the number of cells bound versus the tether lifetime of the interaction for a specified bond force. The dissociation rate,  $k_{\text{off}}$ , obtained from these slopes for varying bond forces shows that  $k_{\text{off}}$  increased exponentially with increasing bond force, fitting the Bell model well at moderate to high wall shear stresses. Using the Bell model, the extrapolated dissociation rate constant at zero force,  $k_{\text{off}}^{\circ}$ , obtained from previous experiments is  $0.95\text{s}^{-1}$  for P-selectin,  $0.70\text{s}^{-1}$  for E-selectin and  $6.6\text{-}8.0\text{s}^{-1}$  for L-selectin (Alon et al. 1995; Alon et al. 1997; Puri et al. 1998). The faster  $k_{\text{off}}^{\circ}$  of L-selectin correlates with its 7.5-9-fold and 8-11.5-fold faster rolling velocity over P- and E-selectin, respectively (Alon et al. 1997). However, recent

experiments have shown that at low shear forces, the dissociation rate with respect to force does not follow the Bell equation, which results in a different  $k_{\text{off}}^{\circ}$ .

### **2.5.2 Catch/Slip Bond Dissociation**

Dembo et al. proposed that membrane-to-surface adhesion of proteins could exist in three different bond type called ideal bonds, slip bonds, and catch bonds. An ideal bond's lifetime is independent of force. A slip bond is characterized by shortened bond lifetime as increased force is applied which is exhibited in the Bell model dissociation studies discussed earlier. With a catch bond, the bond lifetime is prolonged with increasing force (Dembo et al. 1988). This type of bond was theorized to exist but counterintuitive and different from what had been seen previously for the dissociation of selectin-mediated adhesion. However, Marshall et al. reveal a catch bond for P-selectin-mediated interactions when the bond lifetime is measured at forces as low as 6pN using atomic force microscope (AFM) and flow chamber (Marshall et al. 2003). Between 6 and 60 pN, the P-selectin/PSGL-1 interaction begins as a catch bond and transitions to a slip bond. A catch/slip bond transition has also been seen with AFM and in flow chamber studies using beads coated with L-selectin at forces between approximately 4 and 200 pN (Sarangapani et al. 2004).

Because of the catch bond regime, the Bell equation is not appropriate for modeling the dissociation rate constant at low shear stress. New models have been explored to explain the catch bond. One model proposes that the P-selectin/PSGL-1 bond has two pathways of dissociation, one fast and the other slow, where force history initiates a mechanochemical switch that determines its pathway (Evans et al. 2004).

The development of new models is essential to better understanding the dissociation rate constant at zero force,  $k_{\text{off}}^{\circ}$  for the catch/slip curve. The values obtained when extrapolating  $k_{\text{off}}^{\circ}$  from P- and L-selectin off-rate curves with the catch bond are significantly higher than the  $k_{\text{off}}^{\circ}$  seen in other studies which do not rely on the Bell model. In micropipette experiments,  $k_{\text{off}}^{\circ}$  was determined to be  $0.55\text{s}^{-1}$  (Zhu et al. 2002) and  $0.9\text{ s}^{-1}$  (Huang et al. 2004) for P-selectin binding to HL-60 cells expressing PSGL-1. Using surface plasma resonance (SPR), a direct measurement of  $k_{\text{off}}^{\circ} = 1.4 \pm 0.1\text{s}^{-1}$  was obtained for the P-selectin/PSGL-1 interactions (Mehta et al. 1998). The  $k_{\text{off}}^{\circ}$  estimated for L-selectin binding to glycosylation-dependent cell adhesion molecule-1 (GlyCAM-1) using SPR was  $\geq 10\text{s}^{-1}$  (Nicholson et al. 1998). All of these measures are comparable to previous results obtained using the Bell model but are substantially lower than that estimated from the catch/slip curve.

Therefore, the question of how dissociation in the catch bond region integrates with  $k_{\text{off}}^{\circ}$  still remains unknown. Preliminary experiments with the micropipette using E-selectin within the range of 10 and 28 pN shows that a third region may exist where the bond returns to a slip bond state (Piper 1997). Thus, the tether lifetime of E-selectin appeared to begin as a slip bond and then transition into a catch bond as force was increased. The existence of a slip bond prior to the catch bond regime would result in a  $k_{\text{off}}^{\circ}$  lower than if the catch bond regime was the initial dissociation region as force is increased from zero. Observing a slip/catch/slip dissociation curve for E-selectin may imply that a slip bond precedes the catch bond regime for P- and L-selectin also at lower forces due to their similar structure and function. Yet, the dissociation rate curve of E-selectin at low forces has not been fully determined.

## ***2.6 Significance of Catch/Slip Bond***

Selectin-mediated interaction has been shown to require a shear threshold in order for binding to occur. This was first seen with L-selectin where the maximum accumulation of rolling neutrophils or T lymphocytes on peripheral node addressin (PNAd), a ligand for L-selectin, was at  $1 \text{ dyn/cm}^2$ . Below this shear stress, the cells roll more rapidly as shear stress is decreased and at  $0.4 \text{ dynes/cm}^2$ , stable tethers cannot form (Finger et al. 1996). Interestingly, this threshold can be abolished by using periodate to chemically modify the sialic acid in the L-selectin interaction (Puri et al. 1998). Similarly, a threshold has been proposed with P- and E-selectin at  $0.5$  and  $0.25 \text{ dynes/cm}^2$  respectively (Lawrence et al. 1997). The physiologic role of this threshold in binding is thought to promote the formation of additional bonds in needed areas but prevent inappropriate cell binding in areas of low shear stress such as the sinusoids and large veins (Finger et al. 1996). Yet whether the mechanism of the shear threshold phenomenon is due to flow-enhanced tether formation (Lawrence et al. 1997; Chang et al. 1999; Chen et al. 1999; Chen et al. 2001) was still in question. Some hypothesized that the shear threshold was a result of catch bonds.

Recent investigation shows that for L-selectin, catch bonds are the means through which flow-enhanced rolling adhesion occurs. Above the shear threshold, prolonged bond lifetime (catch bond) is associated with slower rolling velocities and more regular rolling steps as shear is increased. Once the optimal shear stress of L-selectin is reached, the transition to a slip bond is seen with rolling velocity increasing and rolling regularity decreasing (Yago et al. 2004). The structural and functional similarities of the three selectins leads to the question of whether catch bonds play a similar role in the flow-

enhanced adhesion of P- and E-selectin. Although the shear threshold is more pronounced for L-selectin, correlation of the off-rate with the rolling velocity with increasing force for P- and E-selectin would also be expected. This would provide additional supporting evidence of the existence of catch bonds while also relating catch bonds to the rolling velocity for all three selectins.

### ***2.7 Relevance of Dissociation Studies to Rolling Adhesion***

Knowing about the dissociation of single tethered cells provides insight into selectin-mediated rolling, but rolling is supported by two or more tethers. A stabilization of the rolling velocity with increasing shear stress suggested an increase in bond number as shear stress increases (Chen et al. 1999). This could mean that the dissociation rate of rollingly adherent cells differs from that of cells adherent through a single tether. However, this question has not yet been addressed well.

Finding a way to measure the dissociation rate of rollingly adherent cells presents a challenge. Chen et al. used the instantaneous velocity data to measure the lifetime of neutrophils rolling on various densities of PNAd. From their dissociation curves, the kinetics of the interaction at 2 dynes/cm<sup>2</sup> and above did not follow first order kinetics (non-linear plot) suggesting that multiple bonds were present and making the determination of  $k_{\text{off}}$  difficult. With each PNAd density tested, as shear was increased above 2 dynes/cm<sup>2</sup>, the curve deviated more from a linear plot indicating that bond number increased as shear stress increased (Chen et al. 1999). Though for rolling supported by two or few tethers and/or at 1 dyne/cm<sup>2</sup> or less, first order dissociation kinetics may be displayed and dissociation rate constant data collected.

Lawrence et al. used a flow chamber which they inverted after stable rolling was achieved (Lawrence et al. 1997). The detachment of rolling cells from P- and E-selectin substrates when the shear stress was reduced to 0.1 dynes/cm<sup>2</sup> during inversion was observed (Lawrence et al. 1997). But, quantitative data on the dissociation rate of the rollingly adherent cells over a range of shear stresses was not acquired.

Being able to quantify the dissociation of rollingly adherent cells will provide insight into the dissociation rate data collected previously for non-rolling cells. Although the dissociation rate obtained with non-rolling cells has been well correlated to the rolling velocity of rollingly adherent cells, this has not been compared to direct dissociation measurements of rollingly adherent cells. The comparison of these results may verify that the dissociation rate of the rear bond determines the rolling velocity of the cell or introduce other factors that may be important in depicting the rolling behavior of cells on selectin surfaces.

### ***2.8 E-selectin Binding***

P- and L- selectin have proven to play a more vital role in the primary tethering and rolling of leukocytes during inflammation than E-selectin (Lawrence et al. 1991; Luscinskas et al. 1996; Smith et al. 1999). In the absence or blocking of L- or P-selectin, leukocyte adhesion is abolished whereas removing or blocking E-selectin only reduces adhesion, both in vivo and in vitro. However, E-selectin may be critical in rolling stabilization and firm adhesion of the leukocytes (Ley et al. 1998; Milstone et al. 1998). In addition, E-selectin may be of primary importance in cutaneous tropism of human skin-homing T-cells (Picker et al. 1990; Berg et al. 1991; Picker et al. 1991; Weninger et

al. 2000) and the homing of HPC to the bone marrow (Schweitzer et al. 1996; Frenette et al. 1998; Mazo et al. 1998; Naiyer et al. 1999) due to E-selectin being constitutively expressed on the post-capillary venules in these areas.

During inflammation, E-selectin is thought to be responsible for the slow rolling of leukocytes on vascular surfaces. The leukocyte rolling velocity in E-selectin deficient mice was 3-5-fold higher and the flux of rolling leukocytes was over 2-fold higher than that in mice with all three selectins present. The number of adherent leukocytes was also reduced (Kunkel et al. 1996). In a few studies, mice lacking E-selectin showed some impairment of the inflammatory function (Kunkel et al. 1996; Munoz et al. 1997; Ley et al. 1998). However, mice lacking both E-selectin and the  $\beta_2$  integrin, responsible for the firm adhesion to follow selectin binding, have severe inflammatory disorders and defects in hematopoiesis. This is not seen with mice deficient in both P-selectin and the  $\beta_2$  integrin (Forlow et al. 2000). Therefore, slower rolling of cells through E-selectin may be important to allowing ample exposure time of cells to local chemoattractants for the continuation of the inflammation cascade (Kunkel et al. 1996; Ley et al. 1998).

Although PSGL-1 binds to E-selectin, its interaction has a 50-fold lower affinity than the P-selectin/PSGL-1 interaction (Moore et al. 1994). In fact, several studies indicate that PSGL-1 may not be the primary ligand for E-selectin. E-selectin mediated adhesion still occurred in PSGL-1 deficient mice (Yang et al. 1999). Additionally, PSGL-1 coated microspheres perfused through mouse venules lacking or blocking E-selectin were still able to roll exhibiting a higher rolling velocity than in the presence of E-selectin (Norman et al. 2000).

Interestingly, the interaction of E-selectin with only the epitope that decorates PSGL-1, sLe<sup>x</sup>, results in rolling. Microspheres coated with sLe<sup>x</sup>, sLe<sup>a</sup> and sulfated Le<sup>x</sup> all were sufficient for rolling on E-selectin/IgG chimera (Brunk et al. 1997). PSGL-1 has only a fraction of the total sLe<sup>x</sup> on the leukocyte so binding of E-selectin to portions of the leukocyte other than PSGL-1 is possible (Norgard et al. 1993). Some data suggest that L-selectin, which is constitutively expressed on leukocytes and presents sLe<sup>x</sup>, binds to E-selectin (Picker et al. 1991; Kunkel et al. 1996). Other ligands on the surface of leukocytes, such as E-selectin ligand-1 (ESL-1), have also been explored as a possible primary ligand for E-selectin where the  $K_D = 62\mu\text{M}$  (Wild et al. 2001). CD44, which is expressed on HPC, mediated adhesion to E-selectin over a wider range of shear than PSGL-1 binding to E-selectin (Dimitroff et al. 2001).

The dissociation rate of E-selectin is the slowest of the three selectins with  $k_{\text{off}}^{\circ}=0.70\text{s}^{-1}$  for E-selectin/neutrophil interaction using the Bell model. Using micropipette, where unstressed  $k_{\text{off}}$  can be measured directly,  $k_{\text{off}}^{\circ}=0.92 \pm 0.23\text{s}^{-1}$  for E-selectin binding to HL-60 cells that express PSGL-1 and  $k_{\text{off}}^{\circ}=0.44 \pm 0.10\text{s}^{-1}$  for E-selectin interacting with Colo-205 cells which have sLe<sup>x</sup> and sLe<sup>a</sup> (Long et al. 2001). Other micropipette experiments resulted in  $k_{\text{off}}^{\circ}=0.9\text{s}^{-1}$  for E-selectin/HL-60 cell interaction and  $k_{\text{off}}^{\circ}=0.35\text{s}^{-1}$  for E-selectin/Colo-205 cell interaction (Piper 1997; Huang et al. 2004).

This kinetic study of selectins focuses on E-selectin. Knowledge gained for P- and L-selectin, such as the catch/slip bond transition for the dissociation of their interactions, has yet to be fully determined for E-selectin. Correlation of the dissociation rate of the rear bonds to rolling velocity through the shear threshold for E-selectin, as

observed for L-selectin, would aid in understanding the relationship of off-rate to rolling velocity and the shear threshold phenomenon for E-selectin. Comparing that information to direct measurements of the dissociation of rollingly adherent cells using an invertible flow chamber would then provide greater insight into leukocyte rolling on E-selectin that could hopefully be used to generate a complete description of selectin-mediated rolling.

## CHAPTER 3

### MATERIALS AND METHODS

#### ***3.1 Proteins and Cells***

Human soluble E-selectin (sEs) was isolated from transfected CHO cells (Xia et al. 2004). For blocking E-selectin-mediated adhesion, the anti-human E-selectin monoclonal antibody (mAb) ES1 was used (Patel et al. 1995). Both were generous gifts from Dr. Rodger McEver.

Human neutrophils were freshly isolated from healthy donors through using Dextran 70 (BBraun Irvine, CA) followed by separation from the lymphocytes using Ficoll-Hypaque (Histopaque 77; Sigma Diagnostics St. Louis, MO) as done previously (Zimmerman et al. 1985). Neutrophils are suspended in a solution of 0.5% human serum albumin (HSA) (Sigma Diagnostics St. Louis, MO) in Hanks Balanced Saline Solution (HBSS) (Sigma Diagnostics St. Louis, MO) to a diluted concentration of 0.5-1.0x10<sup>6</sup>cells/mL. Neutrophils must be used within approximately 6 to 8 hours of their extraction.

Human promyelocytic leukemic (HL-60) cells were a generous gift from Dr. Rodger McEver. This continuous cell line expresses PSGL-1 and rolls identically to neutrophils on selectins (Bevilacqua et al. 1987; Moore et al. 1995). However, its expression of L-selectin is limited which allows more control of cell aggregation during an experiment (Ley et al. 1995). Human colon adenocarcinoma (Colo-205) cells were obtained from American Type Culture Collection (Rockville, MD). Both were cultured using RPMI 1640 media (Cellgro Herndon, VA) supplemented with 10% fetal calf or

bovine serum, 1% L-Glutamine and 1% Penicilin-Streptomycin (Sigma Diagnostics St. Louis, MO). Cells are diluted to a concentration of approximately  $1.0 \times 10^6$  cells/mL in PBS solution for experimentation.

### ***3.2 Coupling of sLe<sup>x</sup> to Microspheres***

In order to focus on the molecular interaction of selectins, the cellular contributions to the adhesion process should be eliminated. Beads coated with the ligand or the binding portion of the ligand is one way of removing cellular contributions. For this study, streptavidin-coated 6 $\mu$ m diameter beads (Polyscience Warrington, PA) were coupled with a multivalent biotinylated sialyl Lewis-x (sLe<sup>x</sup>, GlycoTech Gaithersburg, MD), a carbohydrate epitope that is present in selectin ligands. Frequent mixing of the beads during incubation with the biotinylated sLe<sup>x</sup> allowed uniform coating of the beads. To ensure the coupling of the beads, flow cytometry was used. The sLe<sup>x</sup>-coated beads were incubated with 20  $\mu$ l of a fluorescently-conjugated anti- sLe<sup>x</sup> monoclonal antibody HECA-452 (BD Pharmingen San Diego, CA). The level of FITC on sLe<sup>x</sup>-coated beads was compared to that on plain beads using flow cytometry to confirm the presence of sLe<sup>x</sup> on the beads.

### ***3.3 Site Density***

A radioimmunoassay was used to approximate the effective site density of E-selectin on the glass substrate used during experiments. Iodination of the anti-E-selectin

mAb ES1 was done as described by Ushiyama et al. (Ushiyama et al. 1993). Circular glass slides similar to those used in the flow chamber were coated with sEs. The binding of  $^{125}\text{I}$ -labeled ES1 to sEs was measured to determine the available binding sites of sEs on the surface using various concentrations of sEs (Figure 3-1).

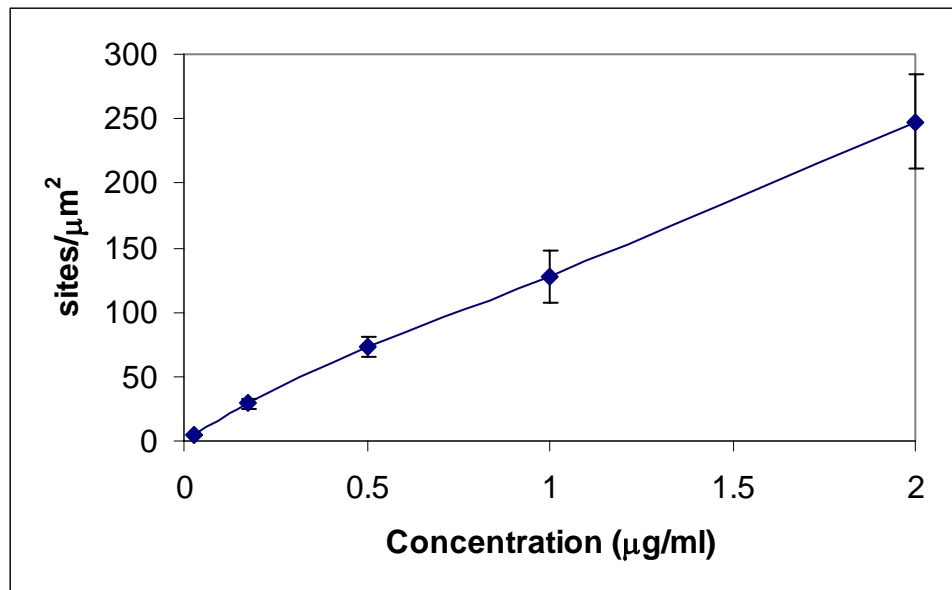


**Figure 3-1:** Plot of the site density measured for varying concentrations of sEs using a radioimmunoassay

### ***3.4 Flow Chamber Apparatus***

To determine the kinetic parameters subjected to mechanical loads, a parallel plate flow chamber is used as shown in Figure 3-2. The chamber was uniquely constructed for this thesis project. To achieve a durable chamber, the exterior unit consists of two Lexan parts 7.457cm long, 3.73cm wide and 0.589cm thick that house a

rigid gasket. The gasket, 0.0381cm thick plastic shim, is cut to create a chamber of that height. Cover glass of 0.16 to 0.19mm thickness and with dimensions of 22x60 mm (Fisher Scientific Pittsburgh, PA) is the substrate for coating the soluble molecules. The most unique design feature of this flow chamber is the ability of the observed surface to remain in the microscope focus after being inverted, allowing for continuous observation of the cells during an experiment. Inverted flow chambers have been used similarly in one previous study by Lawrence et al. (Lawrence et al. 1997) but has not be utilized since.

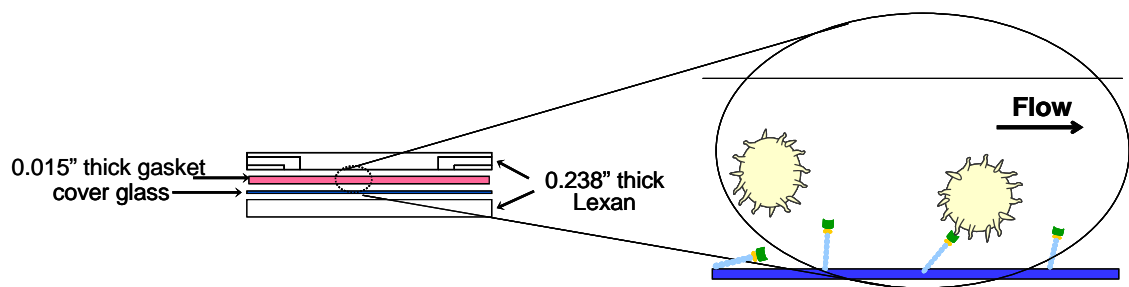


**Figure 3-2:** Schematic of the invertible flow chamber.

### ***3.5 Preparation of Flow Chamber Experiment***

Glass slides are cleaned by submerging them in piranha solution (70% sulfuric acid + 30% hydrogen peroxide (30%)) for 30 minutes and rinsing with distilled water. Using HBSS, sEs is diluted to the specific concentration and E-selectin site density needed for the experiment. For transient tethers, a low sEs density is used to only allow brief contact of the cells or beads with E-selectin where rolling cannot occur. This is

required for the formation of single tethers. For neutrophils, transient tethering occurred at 4.67 sites/ $\mu\text{m}^2$  and 29 sites/ $\mu\text{m}^2$  for sLe<sup>x</sup>-coated beads. Higher densities were used for rolling experiments. A 200 $\mu\text{l}$  volume of the sEs is placed on the glass surface and directly adsorbs to the slides. The sEs incubates on the slide for a minimum of two hours. To reduce nonspecific adhesion, the glass slides are incubated for 30 minutes with 1% bovine serum albumin (BSA, Calbiochem La Jolla, CA) in phosphate buffer saline (PBS) (Sigma Diagnostics St. Louis, MO) or 1% HSA in HBSS. For experiments to inhibit adhesion of E-selectin using a blocking mAb, 20 $\mu\text{g/ml}$  of ES1 is then added to the slide and allowed to incubate for 30 minutes to an hour. Tween 20 (Sigma Diagnostics St. Louis, MO) diluted to 0.5% in HBSS is incubated for 5 minutes as a final step for experiments with microsphere perfusion to prevent non-specific interaction of the microspheres with the glass slide (Geng et al. 1990). After each of the incubations, the slides are washed two to three times with HBSS.

The glass slide is assembled in the flow chamber with the gasket using screws. Barbed fitting are used to connect tubes from the cell supply to the inlet of the chamber and from the outlet of the chamber to the syringe, which is responsible for driving the flow. The chamber is first filled with PBS. Then the cell solution is perfused through the chamber.

### ***3.6 Observation of Selectin-Mediated Rolling***

A CCD analog camera with temporal resolution of 30 frames per second (AutomatiCam A106 Boyertown, PA) is mounted on an Olympus inverted microscope (Lake Success, NY). The flow chamber is placed on the microscope stage using a

customized stage adaptor. Experiments are recorded by a video cassette recorder (Panasonic) on VHS tapes for later analysis.

### ***3.7 Tether Frequency and Cell Accumulation***

To ensure the experiment captured the interaction of E-selectin with its ligand, control tests were conducted. For these control tests, we measured the tether frequency and cell accumulation to determine if binding was hindered. Tether frequency compares the number of cells that tether to the surface to the total number of cells that flow near the surface in the field of view. Obtaining the tethering frequency within the first minute of the experiment results in the initial tethering frequency. After 5 minutes of cell perfusion, the number of cells that have collected on the substrate due to tethering and rolling or the cell accumulation can be determined. Five different fields of view are observed and their cell number averaged together to obtain the cell accumulation measure. For transient tethering control experiments, the cell accumulation is not measured since cell rolling does not occur.

### ***3.8 Tether Lifetime Analysis***

To closely observe tether events, an analog to digital (A/D) converter (Pinnacle Systems Mountain View, CA) was used to import the video segments into the computer. The software that accompanied the A/D converter was used to control the acquisition of the video segments as well as frame-by-frame playback of them. Each frame is 33ms. Once a tether event is identified, meaning when a cell or bead pauses on the substrate, the

lifetime of that tether is quantified. The tether lifetime begins with the first frame where the pause occurs and ends with the frame just before the cell or bead detaches and begins movement again. For these transient tethering experiments, the pause of the cells or beads is brief (<1second).

The lifetimes of 50-100 transient tethers of neutrophils to E-selectin were measured and averaged for each constant wall shear stress that ranged from 0.05-0.8 dynes/cm<sup>2</sup>. These lifetime measurements can also be used in obtaining the dissociation curve, which is the  $\ln(\# \text{ of tethers with a lifetime } \geq t)$  vs.  $t$ , for each shear stress. This plot exhibits a straight line, consistent with first order dissociation kinetics. From the negative reciprocal of the slope of the plot for each shear stress, another indicator of tether lifetime can also be obtained. A third indicator is the standard deviation of lifetimes, which equals the mean lifetime and negative reciprocal of the slope for an exponential distribution. The dissociation rate constant is obtained from the negative of the slope of the dissociation curve.

The tether force is estimated as described previously (Alon et al. 1997; Yago et al. 2002) assuming similar tether properties between the three selectin-mediated adhesions with neutrophils. Briefly, the lever arm of tethered neutrophils was measured using flow reversal and used to derive the tether angle (Yago et al. 2002). With the tether angle, the tether force can then be determined using the exact solution of the Stokes equation for neutrally buoyant spheres (Goldman et al. 1967) resulting in the relationship between the shear stress on the cell and the tether force. A similar method is used to estimate the tether force for beads transiently adhering to E-selectin. By also assuming that the tether properties between the Colo-205 cells and neutrophils are similar, the dimensionless

parameter,  $F_{t\infty}/(r^2\mu\gamma)$ , determined previously (Yago et al. 2004) can be used to find the ratio of the tether force to the wall shear stress for Colo-205 cells.  $F_{t\infty}$  represents the maximum tether force that develops,  $r$  is the radius,  $\mu$  is viscosity and  $\gamma$  is the shear rate.

### ***3.8 Average Rolling Velocity Measurements***

Selectin-mediated rolling is stochastic, meaning that each rolling step taken by the cell occurs at a different velocity. For this work, the average rolling velocity of the cell over several steps, typically measured for approximately 5-10 seconds, is observed under various conditions. This is done by measuring the distance the rolling cell travels on the substrate and dividing it by the time it takes to travel that distance. The average rolling velocity of a number of cells is examined for each condition tested.

### ***3.8 Instantaneous Rolling Velocity Measurements***

To measure the instantaneous rolling velocity of cells on E-selectin, the movements of cells were tracked using Image Pro Plus imaging software (Media Cybernetics Silver Spring, MD). Video clips were converted to digital images using the A/D converter and then processed with QED (Media Cybernetics Silver Spring, MD) and Image J (NIH Bethesda, MD) into an avi format compatible with Image Pro Plus. Filters were appropriately set in order for the cells to be properly selected and tracked. Each track was checked for its validity and accuracy in depicting the rolling behavior of the desired cell.

### ***3.10 Determination of Lifetime of Rollingly Adherent Cells***

E-selectin is coated at a density where cell rolling can be supported yet cell detachment can also occur when the chamber is inverted. In an ideal sense, the objective is to have rolling supported by two selectin-mediated tethers (Alon et al. 1997). A range of sEs between 0.5  $\mu\text{g/ml}$  and 1mg/ml was used to allow detachment of cells from the E-selectin substrate while inverted. After 3-5 minutes of cell perfusion, cells stably roll on the selectin-coated substrate. At this time, the chamber is flipped to its inverted orientation, where the substrate floor is now located on the ceiling of the chamber. This inhibits new cells entering the field of view from initiating rolling adhesion to the substrate. In addition, cells currently rolling have a greatly reduced chance of rebinding after detachment from the substrate while inverted. Thus in the inverted orientation, a measure of the lifetime of rollingly adherent cells is able to be determined.

Every 15 seconds after inversion, the number of rolling cells that remains on the substrate is quantified. The number of cells bound over time can then be plotted to show an exponential decay. So similar to the conventional analysis used for transient tethering cells, the natural log of the number of cells bound over time or  $\ln(\# \text{ of cells with a lifetime } \geq t)$  vs.  $t$  generates a linear plot for each shear stress. The slope of this line then provides information on the dissociation rate and lifetime of the tethers of rollingly adherent cells.

### ***3.11 Statistical Analysis***

The subtle change in the trend of the data and small shear stress increments tested emphasized the need for statistical analysis. To test whether the changes in the trends of

the tether lifetime and average rolling velocity data were statistically significant, the respective slopes of the monotonically increasing and decreasing phases adjacent to each other in one curve were compared. Linear regression was used to obtain the slopes and other statistical parameters for each line segment. A t-statistic can be calculated for testing the hypothesis of equal slopes by using the following equation:

$$t = \frac{b_1 - b_2}{S_{b_1-b_2}}$$

where

$$S_{b_1-b_2} = \sqrt{\left( \frac{(s^2_{Y.X})_P}{(\sum x^2)_1} + \frac{(s^2_{Y.X})_P}{(\sum x^2)_2} \right)}$$

The  $(s^2_{Y.X})_P$  is the pooled residual mean squared which is found by dividing the sum of the residual sum of squares for both linear curves by the sum of the residual degrees of freedom for the two lines. P-values can then be obtained through the use of a two-tailed t-distribution table with the degrees of freedom equaling the sum of the residual degrees of freedom (Zar 1974).

## CHAPTER 4

### RESULTS: AIM 1

Before collecting any data, the newly designed flow chamber had to be characterized and confirmed to be satisfactory for conducting experiments. So, this chapter begins by discussing tests done to finalize the design of the flow chamber and ensure its proper function. Equally important are the control experiments which prove that the cell adhesion being observed in the flow chamber is specifically being mediated by E-selectin. Control experiments for neutrophils, HL-60 cells and sLe<sup>x</sup> coated beads are included in this chapter. However, the focus of this chapter is on the study of the dissociation kinetics of E-selectin-mediated transient tethers. The tether lifetimes of neutrophils and sLe<sup>x</sup> coated beads on E-selectin are quantified and found to exhibit a triphasic pattern, transitioning from a slip bond to a catch bond and back to a slip bond, as force is increased.

#### ***4.1 Feasibility and Reliability of New Flow Chamber***

The newly designed flow chamber was tested to ensure proper performance for experiments. Various sealing methods were evaluated for their air and water tightness as shown in Table 4-1. The use of a 381 $\mu$ m thick gasket with vacuum grease, highlighted in Table 4-1, proved to be the best sealing method for the flow chamber and was used throughout all the experiments.

**Table 4-1:** Various sealing methods of the flow chamber tested

Type of Sealing	Air Tightness	Water Tightness	Other Observations
<b>0.0075" Gasket</b>			
<i>Plain</i>	leaks	leaks	
<i>Silicon Caulk - lining inner edges</i>	still had small air bubbles	satisfactory	could see transparency bunched on sides
<i>Silicon Caulk - covering whole gasket</i>	seems good (no small bubbles)	leaks	
<b>Silicon Sheet</b>	good	good	hard time keeping inlet/outlet open (silicon flattens over opening)
<b>0.015" Gasket</b>			
<i>Plain</i>	leaks	leaks	
<i>With vacuum grease</i>	seems good	good	

#### ***4.2 E-selectin/Ligand Interaction is Specific and Calcium Dependent***

Soluble E-selectin was immobilized on a glass substrate that was placed along the lower wall of the flow chamber. Neutrophils which express PGSL-1 and possibly other ligands for E-selectin were perfused through the chamber and observed interacting with E-selectin coated on the surface at 4.67 sites/ $\mu\text{m}^2$ . The tether frequency for the initial minute of the experiment was measured for 0.2, 0.4, 0.6 and 0.8 dynes/cm<sup>2</sup> as shown in Figure 4-1 for a representative experiment. Without E-selectin present on the substrate or by adding the E-selectin blocking antibody, ES1, interaction of neutrophils with the substrate was reduced or abolished. This is exhibited in Figure 4-1 where the tethering frequency for these conditions is lower than when neutrophils are perfused over E-selectin alone for 0.2, 0.4, 0.6 and 0.8 dynes/cm<sup>2</sup>. Because the interaction of E-selectin is known to be calcium-dependent, Figure 4-1 also shows the addition of EDTA, which chelates the calcium reducing the binding of neutrophils to E-selectin at the three shear stresses tested.

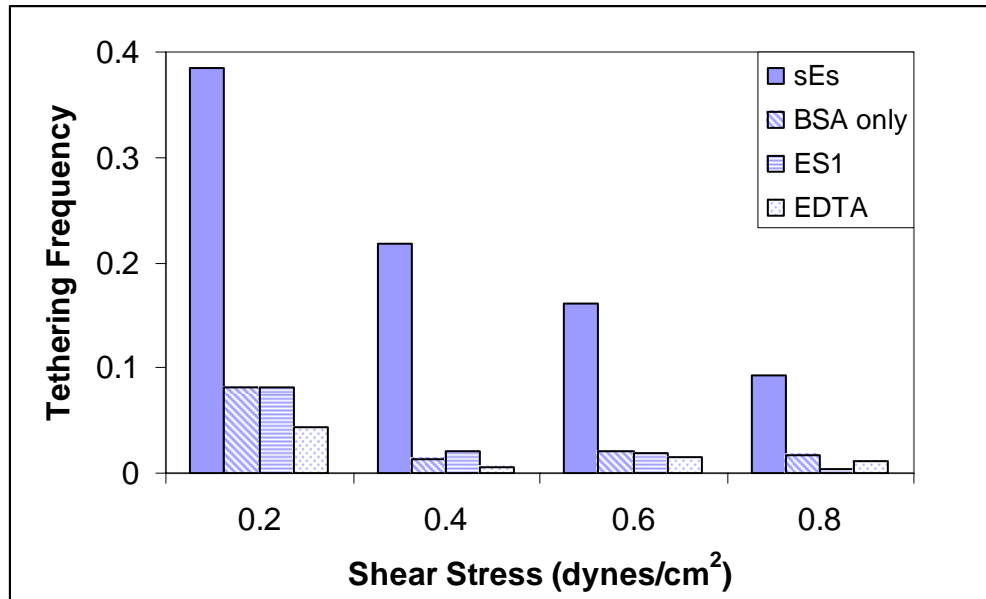


**Figure 4-1:** Representative data for the initial tethering frequency for E-selectin/Neutrophil interaction with E-selectin at 4.67 sites/ $\mu\text{m}^2$ , E-selectin with EDTA present, E-selectin with a blocking antibody to E-selectin, ES1, present and without E-selectin present at 0.2, 0.4, 0.6 and 0.8 dynes/cm<sup>2</sup>

HL-60 cells are a continuous cell line that is similar to neutrophils in the surface molecules expressed and its adhesion behavior to selectins. Use of HL-60 cells with a higher density of E-selectin, where rolling adhesion could occur, also shows specificity of binding between the cell's surface ligands and E-selectin. In Figure 4-2 the initial tethering frequency for HL-60 cells flowing over E-selectin substrate of 37 sites/ $\mu\text{m}^2$  was measured and compared to HL-60 cells perfusing over substrates with an irrelevant IgG antibody instead of E-selectin or with the addition of EDTA. Figure 4-2 shows a representative experiment. Overall, the initial tethering frequency is higher for HL-60

cells tethering to E-selectin than what is shown in Figure 4-1 for neutrophils due to the higher site density used. However, the tethering frequency

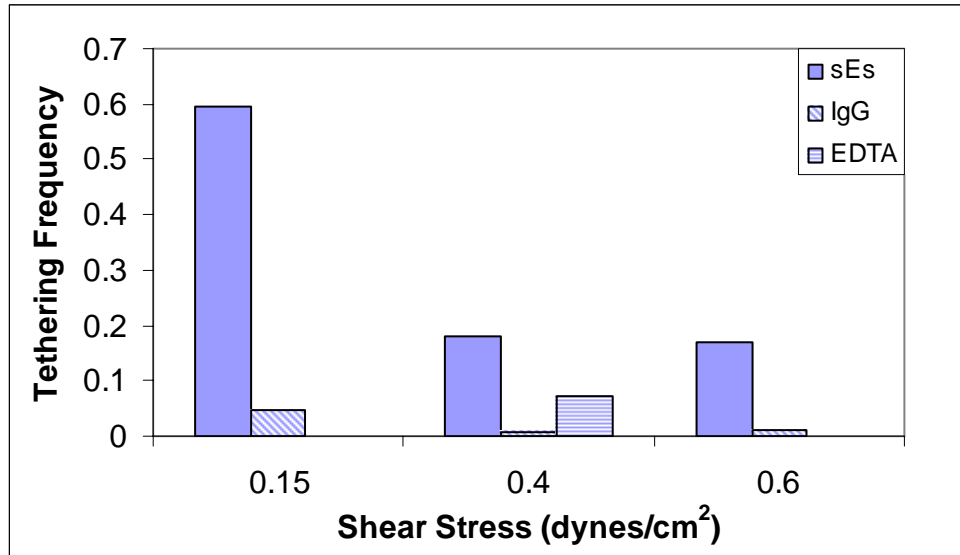


**Figure 4-2:** Representative data for the initial tethering frequency for E-selectin/HL-60 Interaction with E-selectin at 37 sites/ $\mu\text{m}^2$ , an irrelevant IgG antibody present instead of E-selectin and with E-selectin plus EDTA present at 0.15, 0.4, and 0.6 dynes/cm<sup>2</sup>

is reduced for each shear stress tested when an irrelevant antibody is present on the surface instead of E-selectin or EDTA is present. In Figure 4.3, the cell accumulation after 5 minutes of perfusion of HL-60 cells is described for the various control conditions for a representative set of data. Again, cell accumulation is shown to be reduced when E-selectin is not present in a calcium environment. Thus, the binding of E-selectin to its ligands expressed on neutrophils and HL-60 cells is specific and calcium-dependent.

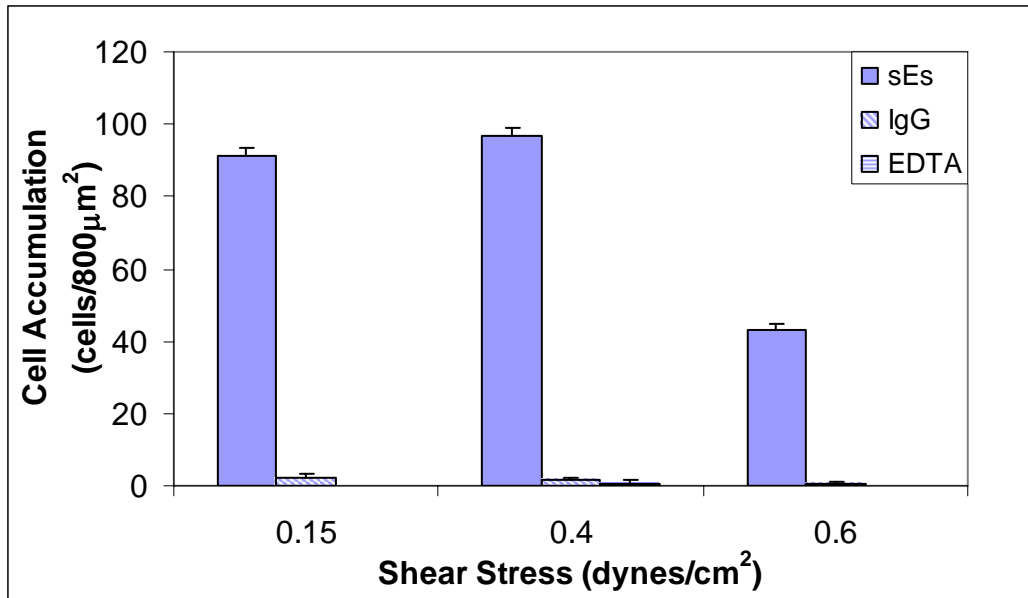


**Figure 4-3:** Representative experiment of the cell accumulation after 5 minutes for E-selectin/HL-60 interaction with EDTA, blocking antibody to E-selectin, ES1, and without E-selectin present at 0.15, 0.4, and 0.6 dynes/cm<sup>2</sup>. The average and SEM of the five fields of view observed for each condition are shown

#### ***4.3 E-selectin/Neutrophil Dissociation Displays Triphasic Force Dependence***

Neutrophils were perfused over E-selectin at a density of 4.67sites/um<sup>2</sup>. At this E-selectin density, rolling of neutrophils could not occur. Instead, brief contacts of the neutrophil with the surface is seen and known as transient tethers. With transient tethering of the neutrophils with the E-selectin substrate, the lifetime of a single tethering event between the cell and the substrate could be observed.

The lifetimes of 50-100 tethering events of neutrophils to E-selectin were measured for each constant wall shear stress that ranged from 0.05-0.8 dynes/cm<sup>2</sup>. For each shear stress, 2-3 independent experiments were done except at 0.15 dynes/cm<sup>2</sup>

where only one experiment was conducted. From those measurements, we obtained dissociation curves for each shear stress by plotting the natural log of the number of

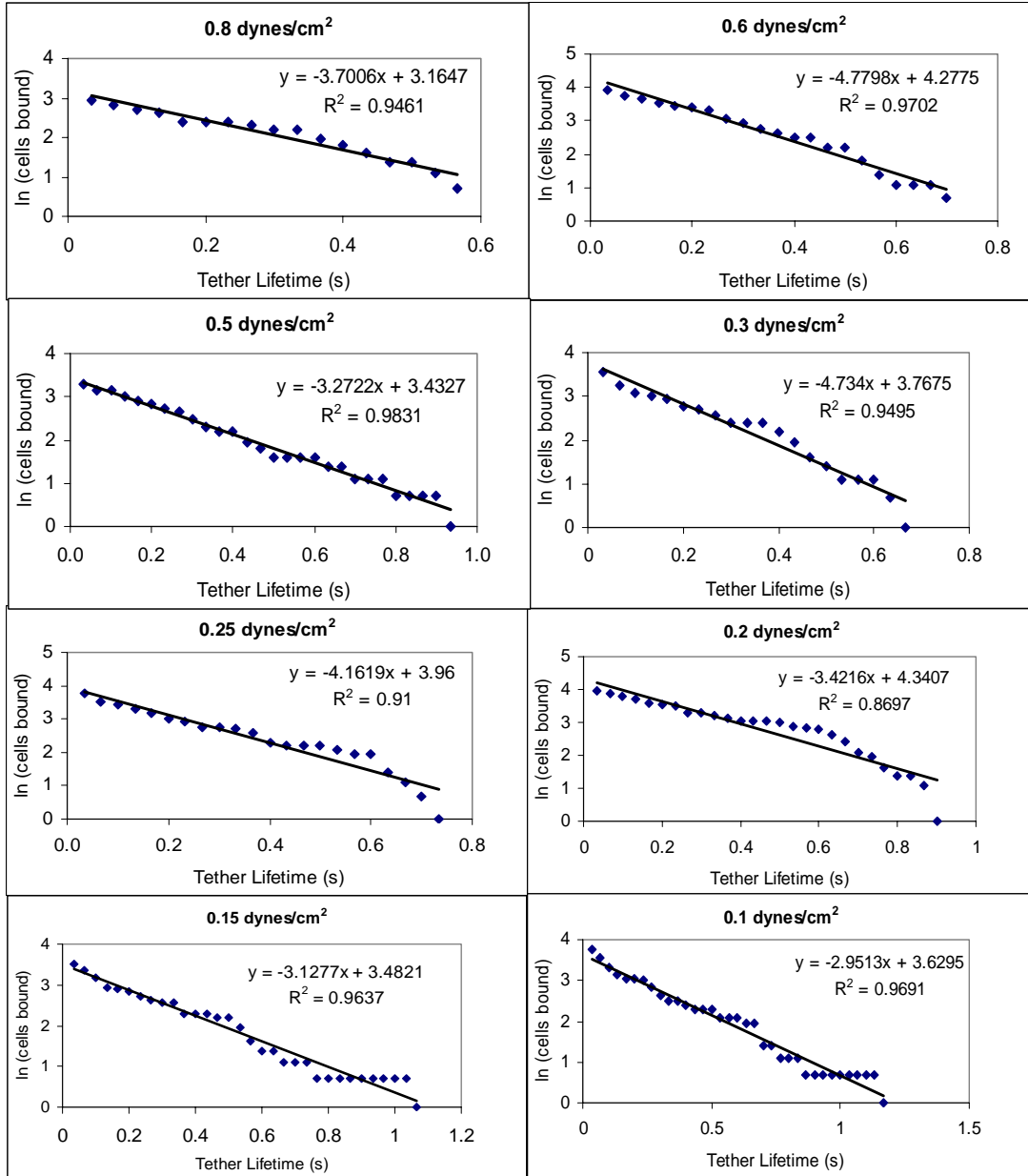


**Figure 4-4:** Representative dissociation curves for the transient tethering of neutrophils to E-selectin at various shear stresses

tethers with a lifetime greater than time,  $t$  versus  $t$ . Figure 4-4 shows the dissociation curves for a representative tether lifetime experiment. From the plots, the data can be seen to correlate well to a straight line, which is consistent with first order kinetics. This analysis is repeated for each experiment.

The negative reciprocal of the slopes ( $-1/\text{slope}$ ) from the dissociation curves is one indicator of tether lifetime. The tether lifetime can also be obtained from simply averaging the tether lifetimes measured directly from the experiment. A third indicator is the standard deviation of lifetimes, which equals the mean lifetime and negative reciprocal of the slope for an exponential distribution. Figure 4-5 presents the average

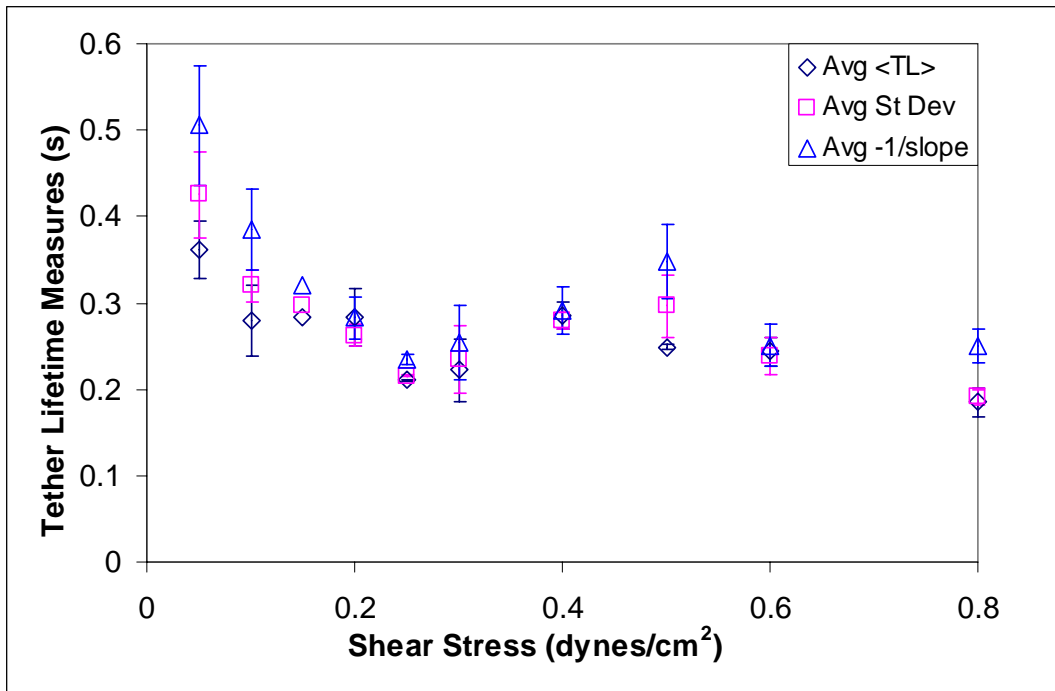


**Figure 4-5:** Average tether lifetime measures with SEM of the E-selectin/ Neutrophil interaction as a function of shear stress

over the 2-3 experiments of the  $-1/\text{slope}$ , average tether lifetime and standard deviation of lifetimes as a function of wall shear stresses with their standard error mean (SEM). At the highest shear stresses tested, the lifetime decreases as the shear stress increases. This is the slip bond characteristic most commonly seen in selectin dissociation studies. At the moderate range of shear stresses, however, the lifetime seems to increase as the shear stress increases, a hallmark of catch bonds. And at the very low shear stresses, the bond seems to return to slip bond behavior. Thus, the tether lifetime of neutrophils with E-selectin seems to exhibit a triphasic behavior, where the interaction changes from a slip bond to a catch bond and returns to a slip bond as shear is increased.

The adhesion events observed were small in number compared to the total flux of cells across the field of view. Such adhesion events have been experimentally and statistically shown to be independent, equivalent and mediated by a low number of discrete, quantal binding units that are likely to be single bonds (Long et al. 2001; Zhu et al. 2002). Therefore, the lifetimes measured can be assumed to be a single bond between E-selectin and its ligand. Using that assumption allows further analysis of the dissociation rate constant for E-selectin binding to neutrophils. From the negative of the slope of the dissociation curve of Figure 4-6, the dissociation rate constant,  $k_{\text{off}}$ , for E-selectin and its neutrophil ligand can be obtained. The  $k_{\text{off}}$  as a function of tether force is presented in Figure 4-6, also showing a triphasic trend. The tether force is estimated as described in the Materials and Methods section with the tether force  $F_t \approx 125 \text{ pN per dyne/cm}^2$ . By extrapolating the curve to zero shear stress, the unstressed off-rate,  $k_{\text{off}}^0$ , an intrinsic property of the E-selectin binding due to the absence of force can be estimated to be  $1.03\text{s}^{-1}$ .

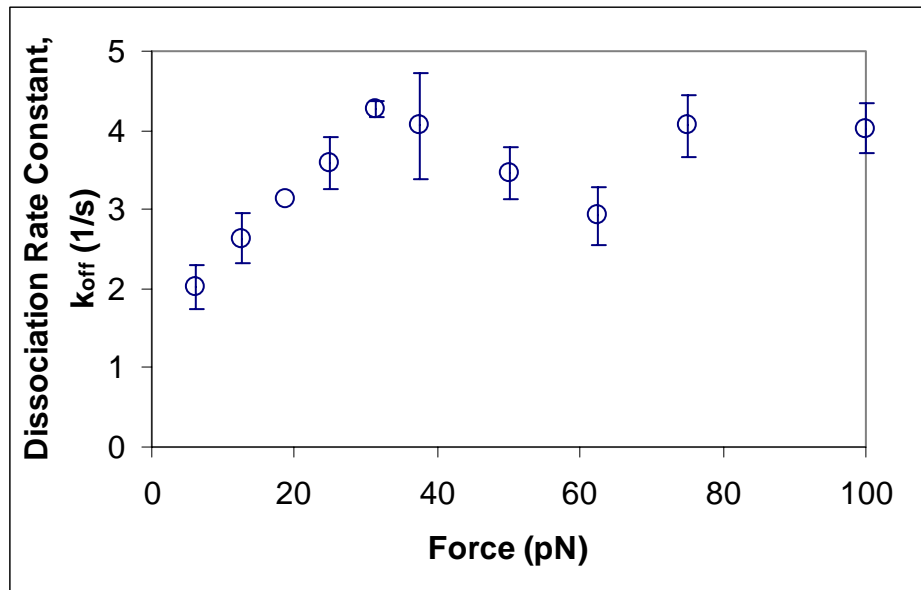


**Figure 4-6:** Average dissociation rate constants with SEM for the E-selectin/ Neutrophil interaction as a function of force

The triphasic trend of the data is gradual. So, statistical methods were employed to test whether the changes from slip to catch and back to slip bond are statistically significant. The use of a Student's t-test for comparing the difference in values between neighboring points was not effective for this data set. P-values calculated for points along the curve for each tether lifetime measure and  $k_{off}$  are shown in Table 4-2. Neighboring points with small increments in shear stress have high p-values indicating no statistical significance in their points. But, as points farther away from each other are compared, the p-values generally decrease with some showing statistical significance with  $p < 0.05$  (highlighted in Table 4-2). Large error in the tether lifetime or  $k_{off}$  at one of the shear stresses caused higher p-values for non-neighboring points in one or two

instances. However, the narrow wall shear stress range of the slip/catch/slip transition and the mild dependence of tether lifetime and  $k_{off}$  on shear causes most of the p-values of non-neighboring points to not reach significance as the shear stress interval between them is increased with some having a higher p-value than points closer together. This will be discussed more in Chapter 7. But overall, using the Student's t-test to assess the statistical significance in the difference of points along the curve was found to be ineffective.

**Table 4-2:** P-values of Student's t-test for tether lifetime and off-rate data

TL	St Dev	1/slope	koff	TL	St Dev	1/slope	koff	TL	St Dev	1/slope	koff
0.05 to 0.1 dynes/cm <sup>2</sup>				0.05 to 0.2 dynes/cm <sup>2</sup>				0.05 to 0.25 dynes/cm <sup>2</sup>			
0.262191	0.283495	0.190775	0.276904	0.220767	0.220767	0.220767	0.044521	0.045494	0.059808	0.053804	0.016565
0.25 to 0.2 dynes/cm <sup>2</sup>				0.25 to 0.1 dynes/cm <sup>2</sup>							
0.193521	0.230799	0.053349	0.221141	0.231083	0.083803	0.031665	0.03899				
0.25 to 0.3 dynes/cm <sup>2</sup>				0.25 to 0.4 dynes/cm <sup>2</sup>				0.25 to 0.5 dynes/cm <sup>2</sup>			
0.772607	0.702458	0.673683	0.793049	0.04143	0.18508	0.020694	0.147799	0.004162	0.11774	0.154304	0.067625
0.5 to 0.4 dynes/cm <sup>2</sup>				0.5 to 0.3 dynes/cm <sup>2</sup>							
0.151365	0.382105	0.690644	0.379063	0.538487	0.257188	0.360793	0.276292				
0.5 to 0.6 dynes/cm <sup>2</sup>				0.5 to 0.8 dynes/cm <sup>2</sup>				0.4 to 0.8 dynes/cm <sup>2</sup>			
0.81599	0.115703	0.234937	0.14034	0.065864	0.172031	0.104422	0.147943	0.049915	0.351959	0.020393	0.348926

Instead of comparing values at each point along the curve, the trend that the data points follow in different phases can be shown to be statistically significantly different. One way is by comparing the changing slopes of the triphasic curve. Each phase of the curve is a monotonically increasing or decreasing line. Therefore, the slopes of each phase of the curve were obtained through linear regression of that data and then compared to see if any significant differences existed between the two slopes. To begin, linear regression analysis for each of the tether lifetime measures and  $k_{off}$  was done. The F-statistic was observed to see that the data for each phase significantly fit a

monotonically increasing or decreasing linear model. For most phases of the curve for each of the measures, the data followed a monotonically increasing or decreasing trend with 95-99% confidence. All but one of the phases that did not follow a statistically significant linear trend occurred at the higher shear stresses where fewer tether lifetime data points were collected. The slopes of the data determined through linear regression were then compared by calculating a t-statistics as described by Zar (Zar 1974) which is used to obtain the p-values. Table 4-3 shows the p-values obtained when the three phases of the curve are compared for each tether lifetime measure and  $k_{off}$ . The two slopes for each transition prove to be statistically different with  $p < 0.05$  for every comparison. Thus, the slip/catch/slip transition of the E-selectin-mediated bond appears to be significant.

**Table 4-3:** P-values obtained by comparing the slopes of each phase of the tether lifetime curve

<b>p-values</b>	<b>&lt;TL&gt;</b>	<b>-1/slope</b>	<b>St Dev</b>	<b><math>k_{off}</math></b>
<i>Slip<sub>1</sub>/Catch</i>	0.018	0.0003	0.0005	<0.0001
<i>Catch/Slip<sub>2</sub></i>	0.0043	0.04	0.0048	0.0411

#### ***4.4 E-selectin/sLe<sup>x</sup> Dissociation Displays Triphasic Force Dependence***

To further test if the triphasic slip/catch/slip bond transition of the dissociation of E-selectin from its ligand is a molecular property, beads coupled with sLe<sup>x</sup>, a carbohydrate epitope that is present in selectin ligands were perfused over the surface instead of neutrophils. Using beads removes cellular effects such as flattening of contact

area and membrane extrusions that may contribute to the observed lifetime vs. shear stress data.

Streptavidin-coated 6 $\mu$ m diameter beads were coupled with biotinylated sLe<sup>x</sup>. To ensure the presence of sLe<sup>x</sup> on the beads, the beads were incubated with a FITC conjugated anti- sLe<sup>x</sup> antibody and the fluorescence was measured using flow cytometry. The histogram, shown in Figure 4-7, provides confirmation that the beads have sLe<sup>x</sup> present on them.

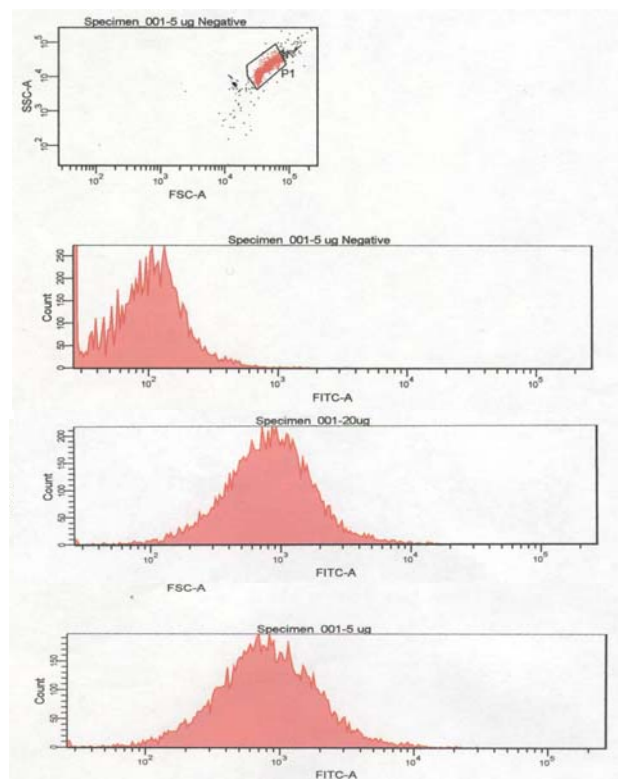


**Figure 4-7:** Flow cytometry results confirming the coupling of biotinylated sLe<sup>x</sup> on streptavidin -coated microspheres

The sLe<sup>x</sup> – coated beads were tested for specific binding to E-selectin. A higher density of E-selectin was necessary for sLe<sup>x</sup> – coated beads to tether to the surface. By increasing the E-selectin site density to 29 sites/μm<sup>2</sup>, sLe<sup>x</sup> – coated beads displayed some tethering frequency to the surface (Figure 4-8) at various shear stresses. Plain beads that

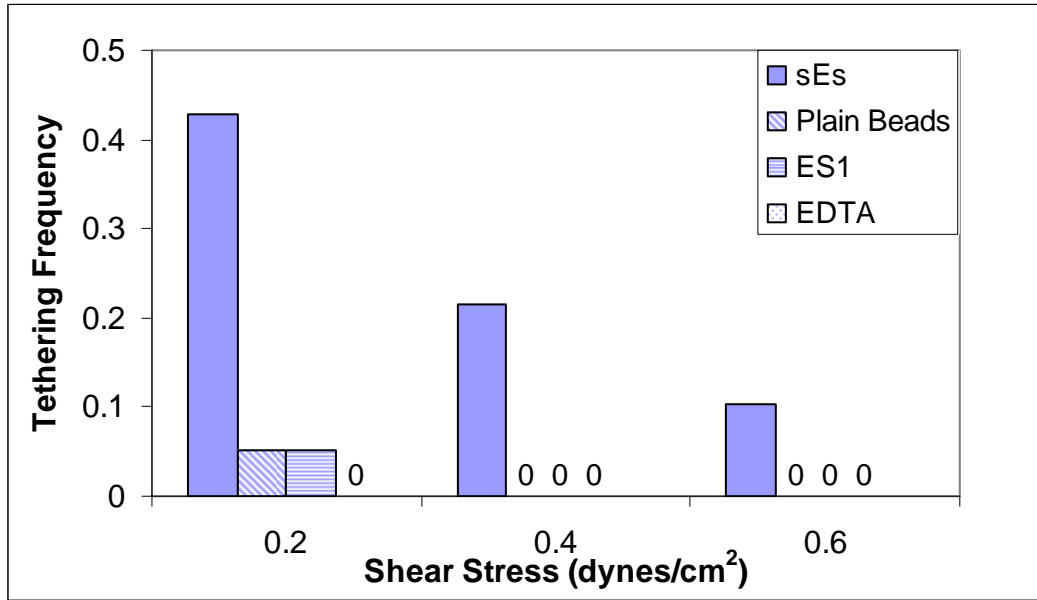


**Figure 4-8:** Representative data for the initial tethering frequency for E-selectin/sLe<sup>x</sup> interaction with E-selectin at 29 sites/μm<sup>2</sup>, E-selectin with EDTA present, E-selectin with a blocking antibody to E-selectin, ES1, present and without E-selectin present at 0.2, 0.4, and 0.6 dynes/cm<sup>2</sup>

are not coupled with sLe<sup>x</sup> were perfused through the chamber at 0.2, 0.4 and 0.6 dynes/cm<sup>2</sup> and their initial tethering frequency to E-selectin substrates was also measured as shown in Figure 4-8 for a representative set of data. Additionally, sLe<sup>x</sup> – coated beads perfused over E-selectin surfaces at the same shear stresses with EDTA or ES1 present

were also observed for their initial tethering frequency. These conditions reduced or abolished tethering frequency compared to sLe<sup>x</sup> – coated beads perfused over E-selectin with calcium present at the same shear stresses. Thus, the interaction of the sLe<sup>x</sup> – coated beads with the E-selectin substrate is specific.

The transient tethering of 50-100 sLe<sup>x</sup> – coated beads on E-selectin at 29 sites/ $\mu\text{m}^2$  was observed for shear stresses ranging from 0.05 to 0.8 dynes/cm<sup>2</sup>. For each shear stress, 2-4 independent experiments with 50-100 tethering events each were collected. From the observations of each experiment, dissociation curves were plotted (Figure 4-9) for each shear stress tested. The correlation of the data to a linear curve indicates that the dissociation is again first order. The average and SEM of the direct measurements of tether lifetime and lifetime measures obtained from our dissociation curves is summarized in Figure 4-10 over the shear stress range of 0.05-0.8 dynes/cm<sup>2</sup>. Compared to the lifetime measures for the E-selectin/neutrophil interaction, the lifetimes of the sLe<sup>x</sup> – coated beads binding to E-selectin are shorter. In Figure 4-11, the  $k_{\text{off}}$  as a function of tether force is plotted for the E-selectin/sLe<sup>x</sup>- coated beads interaction. The

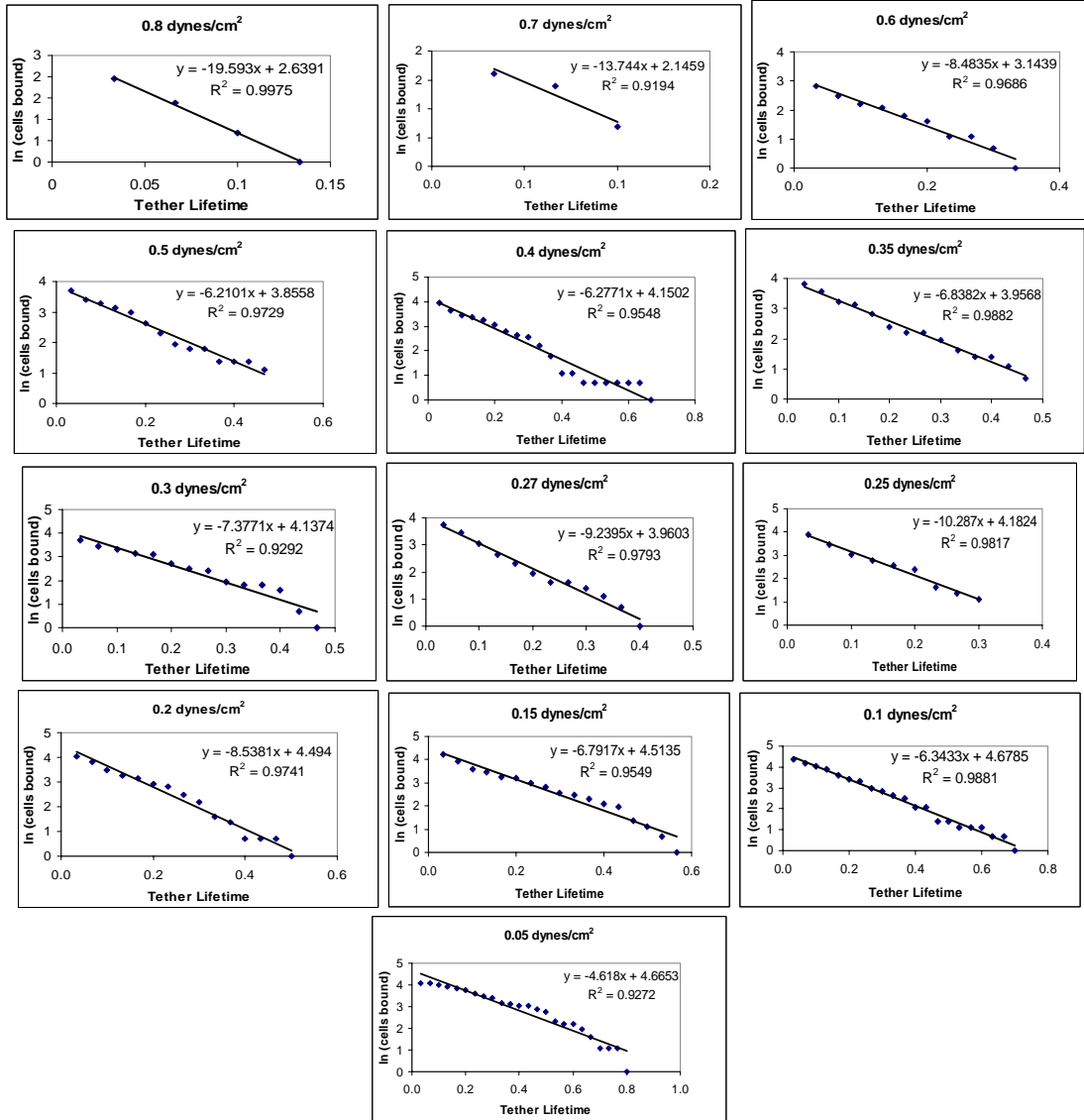


**Figure 4-9:** Representative dissociation curves for the transient tethering of sLe<sup>x</sup>-coated beads to E-selectin at various shear stresses

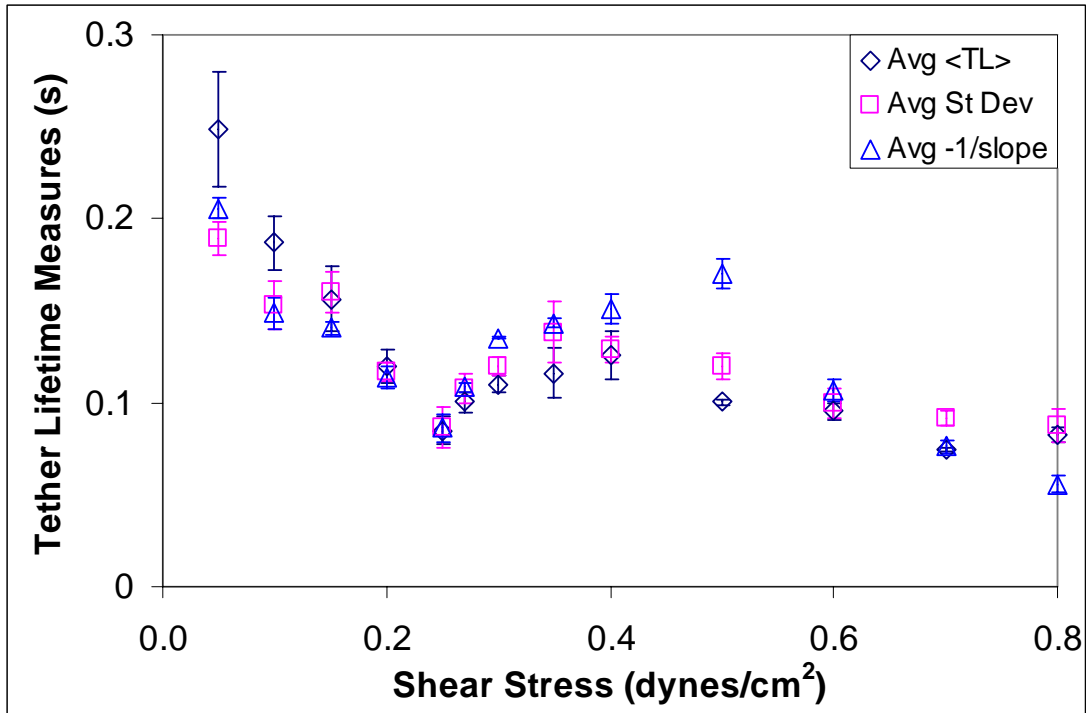


**Figure 4-10:** Average tether lifetime measures for the E-selectin/sLe<sup>x</sup> interaction as a function of shear stress

tether force is estimated as described in the Materials and Methods section with the tether force  $F_t \approx 119$  pN per  $\text{dyne}/\text{cm}^2$ . Figure 4-11 also reveals that the  $k_{\text{off}}$  and extrapolated  $k_{\text{off}}^0$  are higher than with the E-selectin/neutrophil interaction. This shorter lifetime and higher off-rate when only the sLe<sup>x</sup> epitope is involved in binding suggests that components of neutrophil ligands other than just the sLe<sup>x</sup> epitope contribute to its binding with E-selectin.

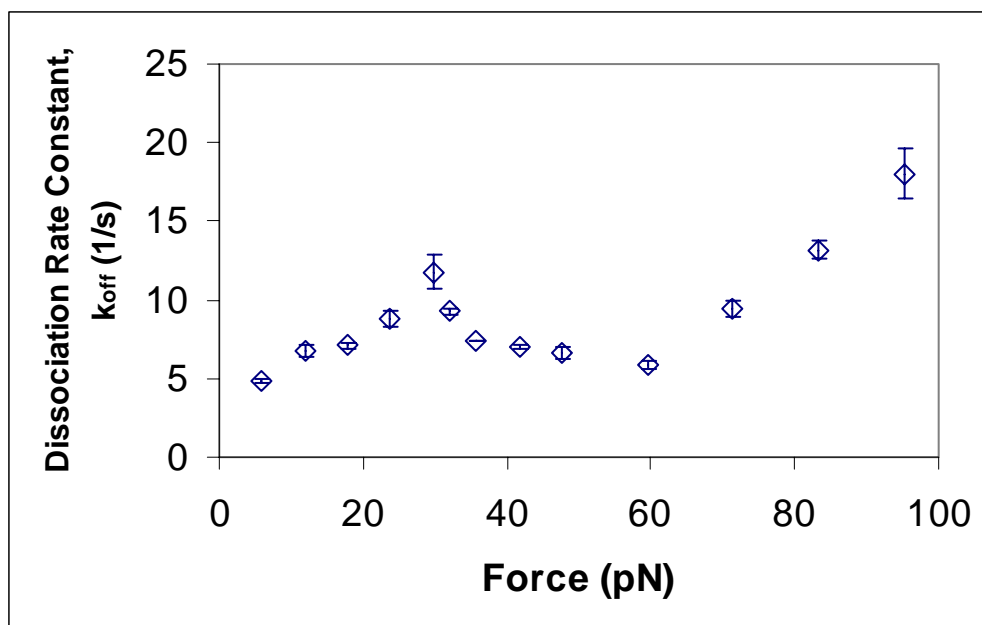


**Figure 4-11:** Average off-rate constants for the E-selectin/sLe<sup>x</sup> interaction as a function of force

Despite shorter lifetimes, the dissociation of the E-selectin/sLe<sup>x</sup> interaction exhibits a triphasic dependence on shear stress similar to the E-selectin/neutrophil interaction. Again the transitions between the three phases are subtle. However, statistically comparing the difference in the two slopes in the slip to catch bond transition, as well as in the catch to the second slip bond transition indicates that the changes in phases are significant. The F-statistic that resulted from linear regression analysis showed that the data in all the phases for each tether lifetime measure and  $k_{off}$  significantly followed a monotonically increasing or decreasing linear trend with a confidence of 95-99% (one phase from one measure resulted in 90% confidence). In Table 4-4, the difference in the slopes between two phases is statistically significant with  $p < 0.004$  for every comparison. Furthermore, the similarity of the curve to that of the E-

selectin/neutrophil lifetime curve provides confidence that despite the subtle transitions, the triphasic trend of the dissociation of the E-selectin-mediated adhesion exists. The existence of the triphasic trend with sLe<sup>x</sup>-coated beads binding to E-selectin indicates that the slip/catch/slip transition is a property of the E-selectin itself and not due to cellular features. So, the dissociation of E-selectin-mediated adhesion appears to transition from a slip bond to a catch bond and then returns to a slip bond as shear stress is increased.

**Table 4-4:** P-values obtained by comparing the slopes of each phase of the tether lifetime curve

<b>p-values</b>	<b>&lt;TL&gt;</b>	<b>-1/slope</b>	<b>St Dev</b>	<b>k<sub>off</sub></b>
<i>Slip<sub>1</sub>/Catch</i>	<0.0001	0.0001	0.0014	0.0009
<i>Catch/Slip<sub>2</sub></i>	0.0025	0.0004	0.0039	0.0002

## CHAPTER 5

### RESULTS: AIM 2

The data in the previous chapter on the tether lifetime of E-selectin-mediated adhesion indicates that a triphasic transition of bond dissociation occurs over the low range of shear force. This was shown with neutrophils and sLe<sup>x</sup>-coated beads. To further examine this phenomenon, the rolling velocity of cells on E-selectin was investigated. Off-rate has been shown to determine the rolling velocity of cells with L-selectin (Alon et al. 1997). In addition, catch bonds have been shown to govern L-selectin-mediated rolling through the shear threshold where their catch and slip bond regimes align well with regions of decreasing and increasing rolling, respectively, with increasing force (Yago et al. 2004). This provides evidence that the bond, whether catch or slip, correlates to the changes in the rolling velocity with changing forces. In this chapter, the rolling velocities of unfixed and fixed neutrophils and other cell types on E-selectin were measured at low shear forces. The results support the triphasic trend seen with the E-selectin-mediated dissociation kinetics. In addition this data provides further insight into the role of the triphasic bond dissociation in E-selectin-mediated rolling.

#### ***5.1 Triphasic Rolling Velocity Over Force for E-selectin/Neutrophil Rolling***

The average rolling velocity for approximately 15-30 neutrophils at each shear stress, although less than 5 cells for 0.05 dynes/cm<sup>2</sup>, was measured by timing the travel of a cell over a specified distance. This was done at 37 and 248 sites/μm<sup>2</sup>, both of which promote rolling adhesion along E-selectin substrates. Figure 5-1 shows the average and

SEM of the average rolling velocity at various shear stresses for both site densities tested. As expected, the neutrophils roll faster on the substrate with a lower site density of E-selectin than that with more E-selectin, with difference in the rolling velocities appearing to actually increase as shear stress increases.

The curves of the average rolling velocities as a function of shear stress at both 37 and 248 sites/ $\mu\text{m}^2$  of E-selectin displays a triphasic trend. Similar to that for the dissociation kinetics of E-selectin-mediated bonds, the moderate changes in the rolling velocity as wall shear stress increases and the narrow shear stress range where transitions in the data occur lead to concerns with proving statistical significance of the existence of the transitions. Because of these subtle transitions and the small increments of shear stresses tested, the Student's t-test was not effective in showing the significance of differences between neighboring point values in the triphasic curve of the average rolling velocity. By comparing the slopes of the phases of the curve as done for the dissociation data in Chapter 4, the triphasic trend is found to be significant with  $p=0.0005$  and  $p=0.03$  for the transitions at the low to moderate and moderate to high shear stresses, respectively for 37 sites/ $\mu\text{m}^2$  of E-selectin. For E-selectin at 248 sites/ $\mu\text{m}^2$ ,  $p<0.0001$  and  $p=0.0005$  for the transitions at the low to moderate and moderate to high shear stresses, respectively.

In Figure 5-1 at the very low shear stresses, the velocity increases with shear. In the previous tether lifetime data, the tether lifetime is decreasing as shear is increased in this region, typical of a slip bond. In the middle range, the average rolling velocity decreases with increasing shear, which is where the catch bond is largely observed. Interestingly, the catch regime for the neutrophils rolling on 37 sites/ $\mu\text{m}^2$  of E-selectin is

slightly smaller than the catch region for the neutrophils rolling on 248 sites/ $\mu\text{m}^2$ . Finally, at the higher shears tested, the average rolling velocity again increases with increasing shear. This is the regime where the bond returns to a slip bond.

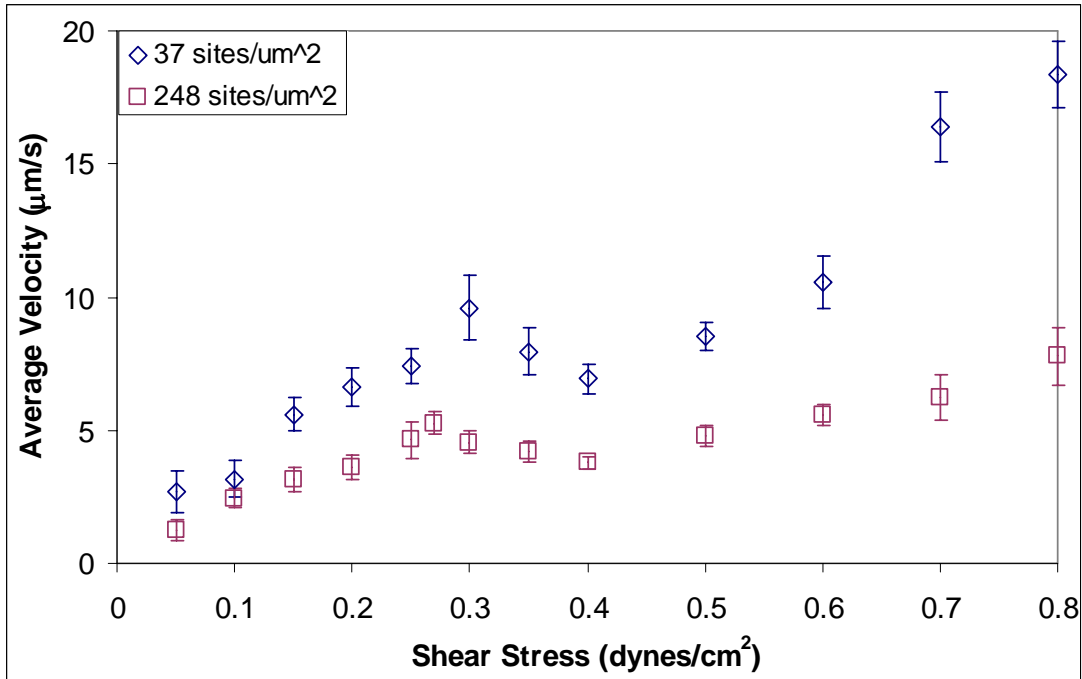


**Figure 5-1:** Average and SEM of the measurements of the average rolling velocity for neutrophils rolling on E-selectin at 37 and 248 sites/ $\mu\text{m}^2$  at various shear stresses

Thus, the average rolling velocity of neutrophils on E-selectin seems to correlate well to the slip/catch/slip transition seen for the dissociation kinetics of E-selectin providing supporting evidence that the triphasic shear force dependence of E-selectin dissociation exists. Furthermore, this suggests that the slip/catch/slip bond may govern the rolling velocity of E-selectin/neutrophil rolling as seen with L-selectin-mediated rolling.

### 5.2 Triphasic Rolling Velocity Over Force for E-selectin/Fixed Neutrophil Rolling

To address concerns that this triphasic pattern of rolling velocity over shear is due to cellular behavior instead of E-selectin binding, the experiment was repeated with fixed neutrophils. By using 1% formaldehyde, proteins on the membrane are crosslinked and the cell stiffens thus reducing cellular effects. Fixed neutrophils required a minimum of 248 E-selectin sites/ $\mu\text{m}^2$  for sufficient rolling to occur. At this density, the fixed neutrophils rolled approximately twice as fast as the unfixed neutrophils (Figure 5-2). In

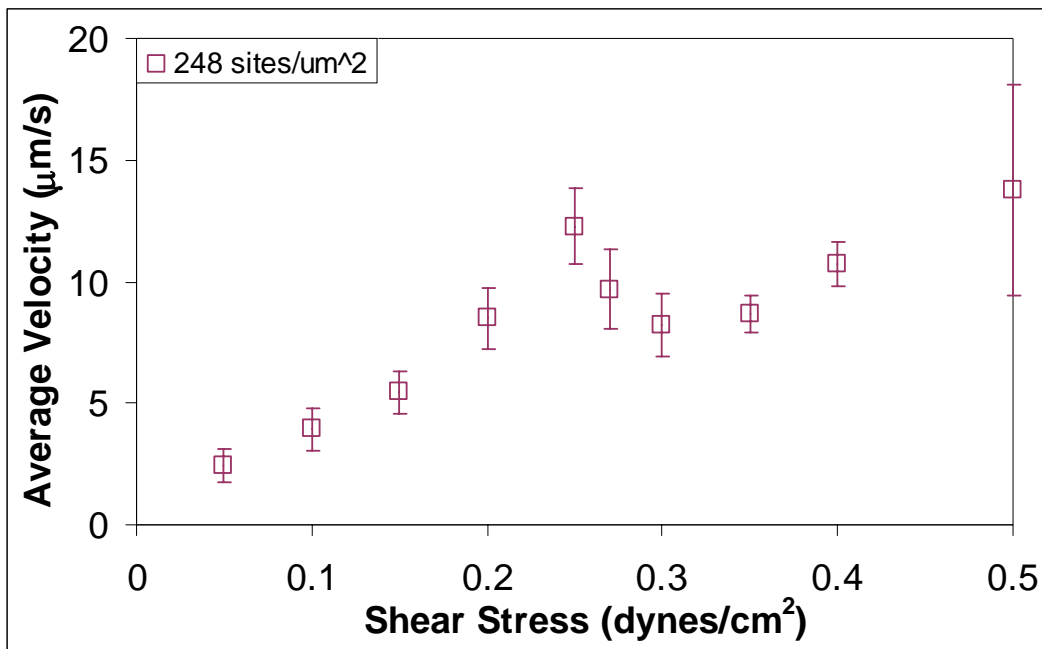


**Figure 5-2:** Average and SEM of the measurements of the average rolling velocity for fixed neutrophils rolling on E-selectin at 248 sites/ $\mu\text{m}^2$  at various shear stresses

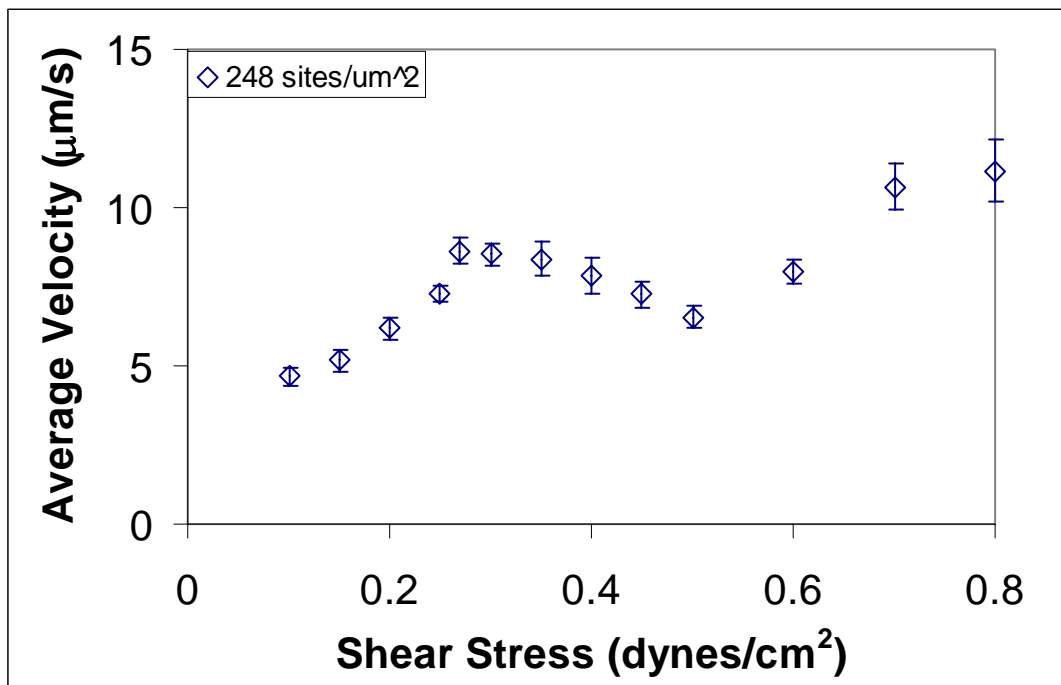
addition, some cells were found to skip across the substrate more than roll. At higher shear stresses the few cells that tethered primarily skipped instead of rolling. For the shear stresses that rolling cells were able to be observed, between 5 and 15 cells per shear stress, the average rolling velocity measurements were averaged for each shear stress (Figure 5-2). The average rolling velocity followed a significant triphasic trend ( $p=0.009$  for the slope comparison of both transitions) over force similar to that seen for unfixed neutrophils. This signifies that the triphasic velocity curve may be a property of E-selectin binding and not a result of the cellular features like tether extrusions.

Figure 5-1 already showed that the unfixed neutrophils rolling on 37 sites/ $\mu\text{m}^2$  rolled faster and had a slightly smaller catch regime than the unfixed neutrophils on 248 sites/ $\mu\text{m}^2$ . However, the fixed neutrophils roll faster and have a smaller decreasing velocity regime than the unfixed cells rolling on 37 sites/ $\mu\text{m}^2$ . Despite the variation in size of the decreasing velocity region for the three curves of average rolling velocity, this regime spans within a similar range of shear stresses for the unfixed neutrophils at both E-selectin densities and the fixed neutrophils on E-selectin.

### ***5.3 Triphasic Rolling Velocity Over Force for E-selectin/HL-60 Rolling***

HL-60 cells are precursory white blood cells that are known to roll on selectins in a similar manner to neutrophils. Measuring the average rolling velocity of HL-60 cells in the same range of shear will help to determine whether the triphasic trend occurs when different cell types bind to E-selectin. Figure 4-3 displays the average and SEM of the average rolling velocities for HL-60 cells rolling on E-selectin at 248 sites/ $\mu\text{m}^2$ . At each shear stress, the average rolling velocity of 20 cells was measured. HL-60 cells are larger

than neutrophils and roll faster on similar densities of E-selectin. Yet, the rolling velocity of HL-60 cells on E-selectin displays a significant triphasic curve ( $p < 0.0005$  for the slope comparison of both transitions) comparable to that seen for unfixed and fixed neutrophils. Furthermore, the regime of decreasing velocity for the HL-60 cells is fairly similar to that for unfixed neutrophils rolling on matched densities of E-selectin with decreasing velocity region of the HL-60 cells extended a little. This data suggest that the slip/catch/slip transition of E-selectin/ligand bonds occurs among other cell types as well.



**Figure 5-3:** Average and SEM of the measurements of the average rolling velocity for HL-60 cells rolling on E-selectin at 248 sites/ $\mu\text{m}^2$  at various shear stresses

#### ***5.4 Triphasic Rolling Velocity Over Force for E-selectin/Colo-205 Rolling***

Although the slip/catch/slip trend is consistent when looking at tether lifetime and average rolling velocity of neutrophils, fixed and unfixed, sLe<sup>x</sup>-coated beads and HL-60 cells, the question still remained if the data agreed with early micropipette experiments. Using micropipette, the data suggests that E-selectin-mediated dissociation with Colo-205 cells begins as a slip bond and is followed by a catch bond between 10 and 28 pN (Piper 1997). The tether force is estimated as described in the Materials and Methods section with  $F_t \approx 435 \text{ pN per dyne/cm}^2$  assuming a cell radius of  $7.94 \text{ }\mu\text{m}$  for Colo-205 cells (Piper 1997). Therefore, the force range used with micropipette converts to a wall shear stress between  $0.025\text{-}0.065 \text{ dynes/cm}^2$ , which is lower than the shear stresses tested in previously discussed flow chamber experiments with other cell types. In addition to sLe<sup>x</sup>, Colo-205 cells are known to have sialyl Lewis-a (sLe<sup>a</sup>) which can also bind to E-selectin (Piper et al. 1998). So investigating the rolling velocity of Colo-205 cells on E-selectin could provide additional insight into the results obtained by micropipette and the overall phenomenon of the slip/catch/slip bond.

Experiments were done with Colo-205 cells rolling on E-selectin substrates at  $248 \text{ sites}/\mu\text{m}^2$ . The average rolling velocity measurement for 20-25 cells for each shear stress, with the exception of  $0.6$  and  $0.8 \text{ dynes/cm}^2$  where the average rolling velocity of 10-12 cells were measured, were averaged and plotted in Figure 5-4. Observation of cell tethering and rolling was difficult below  $0.05 \text{ dynes/cm}^2$  with the flow chamber. Therefore, the average rolling velocity of Colo-205 cell on E-selectin was not measured below  $0.05 \text{ dynes/cm}^2$  ( $21.8\text{pN}$ ).

Again, the average rolling velocity as shear stress is increased exhibits a significant triphasic trend with  $p < 0.0001$  and  $p = 0.03$  for the slope comparisons of the transition between low to moderate and moderate to high shear stresses, respectively. The decreasing velocity regime resembles that seen for the fixed neutrophils where it is a quite small region beginning around  $0.25 \text{ dynes/cm}^2$ . The Colo-205 cells are also similar to the

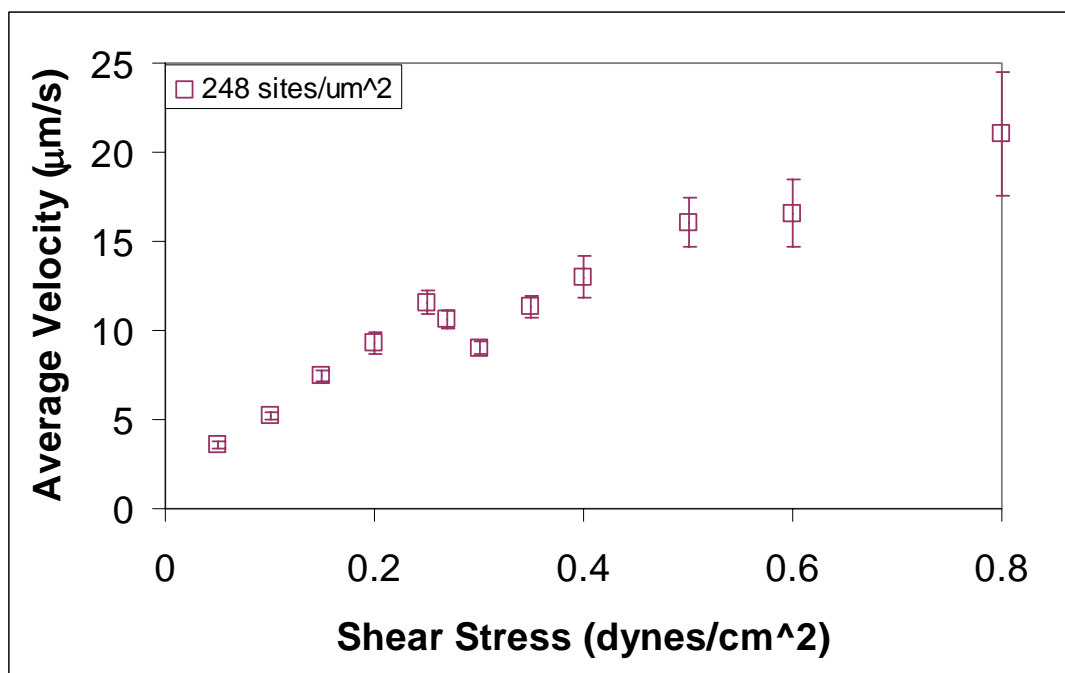


**Figure 5-4:** Average and SEM of the measurements of the average rolling velocity for Colo-205 cells rolling on E-selectin at  $248 \text{ sites}/\mu\text{m}^2$  at various shear stresses

fixed neutrophils by exhibiting faster average rolling velocities than neutrophils and HL-60 cells. They are larger than both the neutrophils and HL-60 cells, too.

Figure 5-4 suggests that E-selectin dissociation from Colo-205 cells also transitions from a slip bond to a catch bond and back to a slip bond. However, the region of faster and slower rolling are at higher forces than where the slip and catch regions were seen in earlier micropipette experiments. Because shear stresses lower than 0.05 dynes/cm<sup>2</sup> were not able to be tested with the flow chamber, uncertainty still exists regarding the correlation of the micropipette data and the flow chamber data.

Despite the possible discrepancy with the Colo-205 cells in where the slip/catch/slip region exists between the average rolling velocity data obtained with flow chamber and the tether lifetime data collected with micropipette experiments, both sets of data exhibit curves that begin with adhesion behavior characteristic of a slip bond and then followed by a catch bond. Seeing this pattern with a third cell type strengthens the idea that the triphasic trend of E-selectin dissociation is not cell specific and a property of the selectin itself.

## CHAPTER 6

### RESULTS: AIM 3

In Chapter 4, the dissociation kinetics of E-selectin-mediated adhesion was studied using the conventional method of observing transiently tethering cells. Similar to previous studies, the off-rate obtained in Chapter 4 proved to be relevant to rollingly adherent cells. Chapter 5 showed that the regimes of faster dissociation (slip bond) corresponded to increasing rolling velocities while regions of slower dissociation (catch bond) were linked to cells of decreasing rolling velocities.

Aim 3 attempts to directly observe and quantify the dissociation kinetics of rollingly adherent cells  $k_{\text{off(RA)}}$ . In order to do this, the flow chamber was inverted during the experiment to prevent new adhesions from being formed and limit the probability of cell re-attachment once the final bond dissociates. Once inverted, the number of cells that remains bound over time is counted and analyzed to obtain the lifetime or dissociation of rollingly adherent cells at various shear forces. The data presented in this chapter illustrates that the dissociation of rollingly adherent cells can be quantitatively measured using the inverted flow chamber and correlates well to first order dissociation. This chapter will further show that the dissociation rate of rollingly adherent HL-60 cell and neutrophils also undergoes phase changes as force is increased. However, this regime change is quite different from the triphasic pattern seen in Aim 1. Further exploration of the data suggests that other factors may play a role in the dissociation of the rollingly adherent cells ( $k_{\text{off(RA)}}$ ) while inverted such as tether formation, membrane extrusions and microgravity.

### ***6.1 New Invertible Flow Chamber is Reliable for Experiments***

Early experiments inverting the flow chamber with HL-60 cells rolling on P-selectin revealed that tube disturbances interrupted the flow and caused cells to detach while the chamber was being inverted. As a result, the tubes were arranged in the same horizontal plane as the flow chamber to allow limited movement during inversion. With this experimental setup, cells continued to roll on the P-selectin substrate after inversion.

Although cells were observed rolling on the surface after inversion, concern regarding the percentage of cells that may have still detached while inverting needed to be addressed. The number of HL-60 cells remaining bound immediately after inversion at various densities of P-selectin was observed to be on average 37% with large variation between the densities tested. To improve the reliability and consistency of the inversion of the chamber, the tubes connected to the flow chamber were encased in slightly larger and stiffer tubes. This modification improved the number of cells remaining bound after inversion to nearly 100% on average with more consistency observed between P-selectin densities and even cell types. With this experimental setup, the flow chamber was sufficient to utilize for experiments.

### ***6.2 Dissociation of HL-60 cells Rolling on E-selectin***

Experiments were done by rolling HL-60 cells on E-selectin at  $127 \text{ sites}/\mu\text{m}^2$ . For most experiments, the flow began at  $0.25 \text{ dynes}/\text{cm}^2$  to allow rolling cells to accumulate on the surface. After 3-5 minutes, HL-60 cell rolling was stabilized and the number of

rollingly adherent cells was uniform across the working section of the flow chamber which is several centimeters in length along the flow direction. The chamber was then inverted to observe the dissociation of rollingly adherent cells. The purpose of inverting the chamber was to prevent freely flowing cells entering the field from initiating rolling. In addition, the inverted orientation reduces the chance of re-attachment once a rolling cell dissociates. Once the chamber was inverted, the shear stress was changed from 0.25 dynes/cm<sup>2</sup> to the desired level of shear, and the number of rolling cells that remained bound was observed to decrease over time. This decrease for a particular shear stress was found to be similar when experiments were initiated at a shear stress other than 0.25 dynes/cm<sup>2</sup>. Thus, starting the flow at 0.25 dynes/cm<sup>2</sup> and inverting the chamber at that shear seemed to have no affect on the results. At very low shear stresses such as 0.1 dynes/cm<sup>2</sup>, the decrease in the number of cells bound over time was noticeably faster

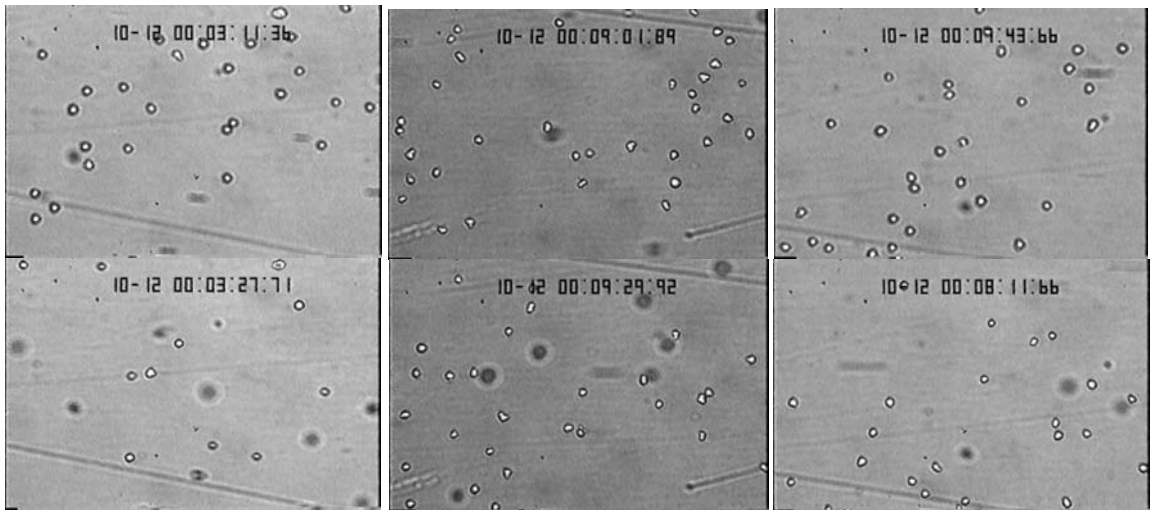


**Figure 6-1:** Video images of HL-60 cells rolling on E-selectin at 127 sites/ $\mu\text{m}^2$  while inverted for 0.15 (column one), 0.25 (column two) and 0.5 (column three) dynes/cm<sup>2</sup>. The top row is immediately after the inversion and shear stress change. The bottom row is 15 seconds later for 0.15 dynes/cm<sup>2</sup> and 30 seconds later for 0.25 and 0.5 dynes/cm<sup>2</sup>.

than for cells at 0.25 dynes/cm<sup>2</sup> (Figure 6-1). This was previously observed by Lawrence et al. (Lawrence et al. 1997) .

Bound cells were counted every 15 seconds for as long as several hundreds of seconds. Data from three experiments done on different days at similar densities of E-selectin were pooled together totaling between 70 and 140 cells observed for each wall shear stress. The semi-log plots of pooled number of cells that remained bound against time are shown in Figure 6-2 for various shear stresses. When fitted by a straight line, the data seems to be in good agreement to a linear curve. This signifies that the dissociation of rollingly adherent HL-60 cells on E-selectin follows first order dissociation.

Using first order dissociation analysis as done in Aim 1, the dissociation rate constants can be determined from the negative slopes of each semi-log plot. The dissociation rate constant for rollingly adherent HL-60 cells as a function of shear stress is displayed in Figure 6-3. Overall, the  $k_{\text{off(RA)}}$  are much lower than that obtained for neutrophils and sLe<sup>x</sup>-coated beads transiently tethering to E-selectin surfaces. This is expected since more E-selectin bonds are formed to support cell rolling. However, the trend of the curve over the shear stress range is quite surprising. At the very low shear stresses, the HL-60 cells seemed to come off faster thus resulting in a higher  $k_{\text{off(RA)}}$ . As shear stress was increased to 0.25 dynes/cm<sup>2</sup>, the cells remained rolling longer and the rolling cell dissociation rate constant was lower. Following 0.25 dynes/cm<sup>2</sup>, the cells began to dissociate faster again as shear stress was increased. Interestingly, this trend mirrors that seen in Aim 1 for lifetimes of cells transiently tethering (not rolling) to E-

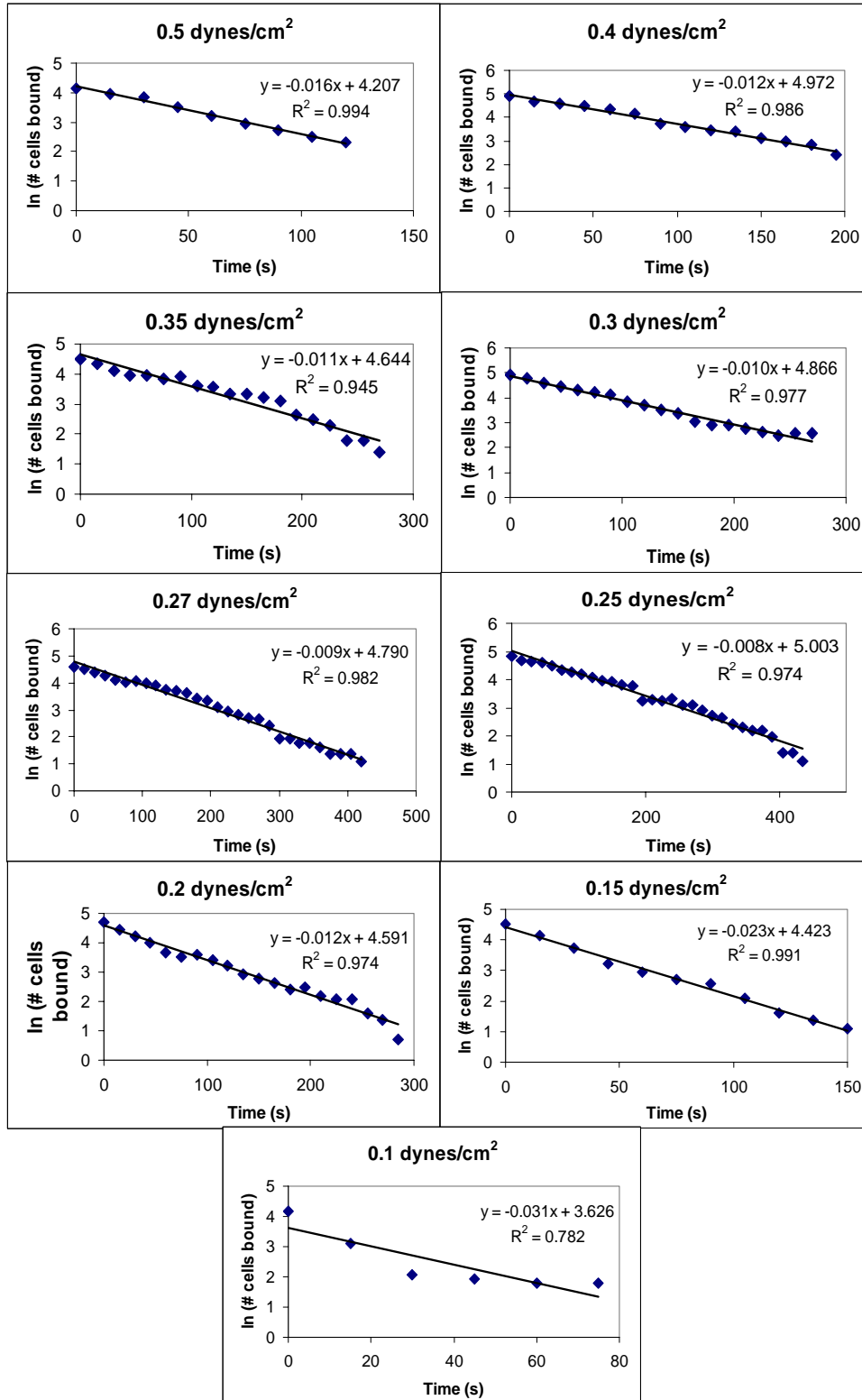


**Figure 6-2:** Dissociation curves for the pooled data of HL-60 cells rollingly adherent on E-selectin at  $127 \text{ sites}/\mu\text{m}^2$  at various shear stresses

selectin. For transiently tethering cells, longer tether lifetimes, meaning lower dissociation rate constants, were seen at the very low shear stresses and around

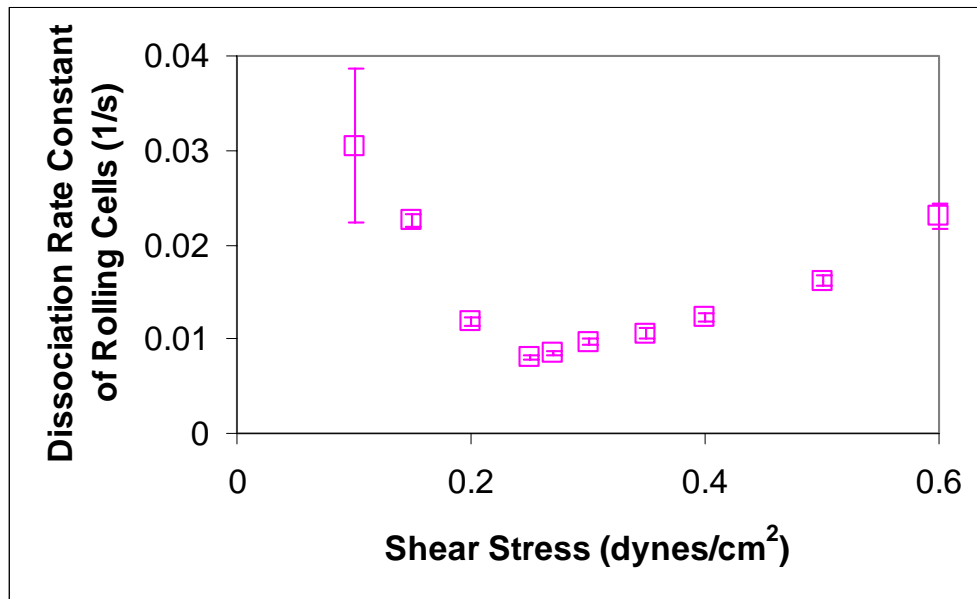


**Figure 6-3:** Dissociation rate constant from pooled data for rollingly adherent HL-60 cells on E-selectin at 127 sites/ $\mu\text{m}^2$  as a function of shear stress with SEM

0.25 dynes/cm<sup>2</sup>, the catch bond regime began where tether lifetime was prolonged with shear stress (Figure 4-5 and 4-6).

The data from each individual experiment, which included approximately 20-30 cells being observed at each shear stress, had some scatter due to the small number of cells being observed. However, each experiment still exhibited this reverse biphasic trend, adding confidence to this result. In addition, pooling the data together as done in Figure 6-3 provides a smooth biphasic trend line of  $k_{\text{off(RA)}}$  versus wall shear stress.

Further evidence of this reverse biphasic trend is shown in Figure 6-4 where the dissociation constant of rollingly adherent HL-60 cells on lower density of E-selectin is seen to follow the same trend. Seeing the dissociation of rollingly adherent HL-60 cells on E-selectin surfaces less than  $127 \text{ sites}/\mu\text{m}^2$  was challenging due to the rapid dissociation of the cells. However, the blue diamonds in Figure 6-4 represent one experiment where data were attained for E-selectin at  $73 \text{ sites}/\mu\text{m}^2$ . Although there is some scatter in the data due to the low number of cells (approximately 15-20 cells for each shear stress), the overall trend is consistent with the  $k_{\text{off(RA)}}$  seen for HL-60 cells rolling on  $127 \text{ sites}/\mu\text{m}^2$ .

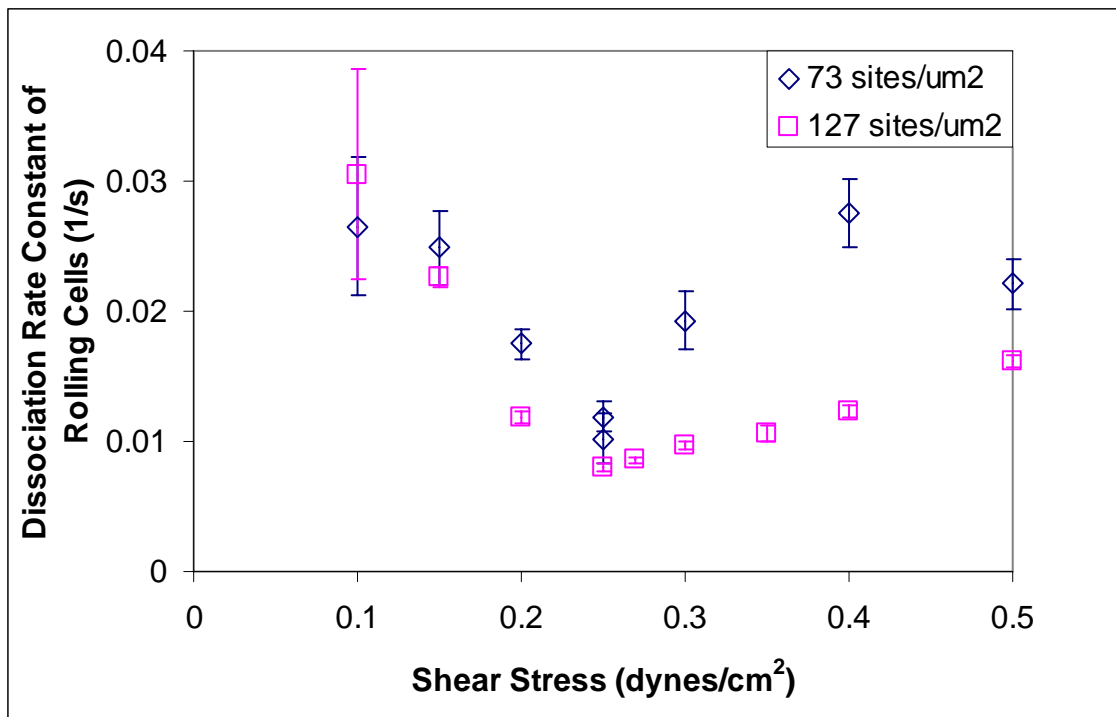


**Figure 6-4:** Dissociation rate constants for rollingly adherent HL-60 cells on E-selectin with SEM at  $73 \text{ sites}/\mu\text{m}^2$  for one experiment and for  $127 \text{ sites}/\mu\text{m}^2$  with pooled data

### 6.3 Rolling Velocity of HL-60 cells on E-selectin in Normal and Inverted Orientation

The average rolling velocity results in Aim 2 correlate well with the tether lifetime data in Aim 1, suggesting that the rolling velocity is governed by the tether lifetime. Therefore, to investigate the dissociation results for rollingly adherent cells further, the average rolling velocity of the HL-60 cells in the inverted orientation was measured. Figure 6-5 shows the average of rolling velocity measurements taken from two experiments. The average rolling velocity correlates with the dissociation results for rollingly adherent cells. As shear increased, increasing dissociation resulted in increasing rolling velocity where decreasing dissociation resulted in decreasing rolling velocity of the HL-60 cells on E-selectin. However, this consequently means that the rolling velocity curve as a

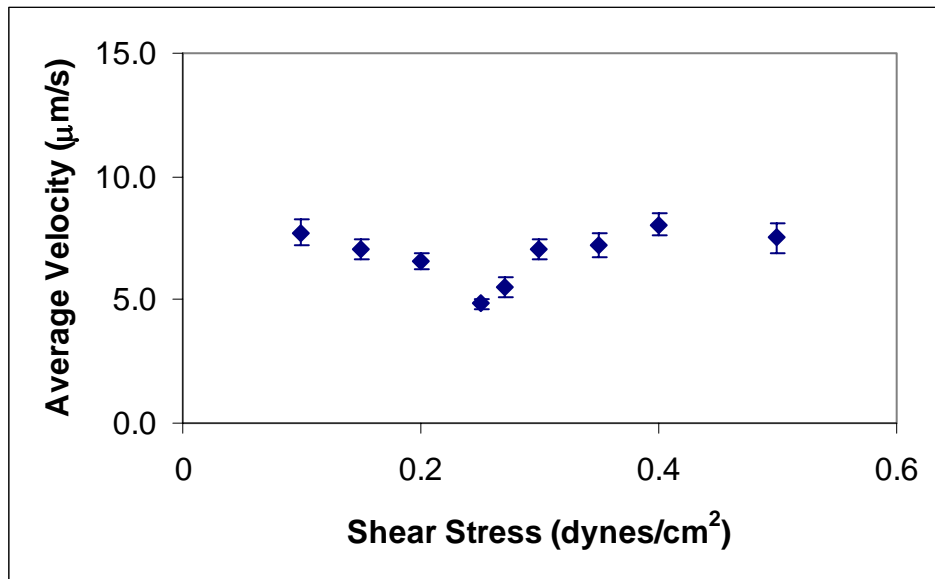


**Figure 6-5:** Average and SEM of the measures of the average rolling velocity from two experiments of rollingly adherent HL-60 cells on E-selectin at 127 sites/μm<sup>2</sup> while inverted

function of wall shear stress for the inverted orientation and normal orientation mirror each other. So both the rolling cell dissociation rate constant and rolling velocity curves in the inverted orientation, although consistent with each other, mirror the transiently tethering dissociation rate constant and rolling velocity curves in the normal orientation.

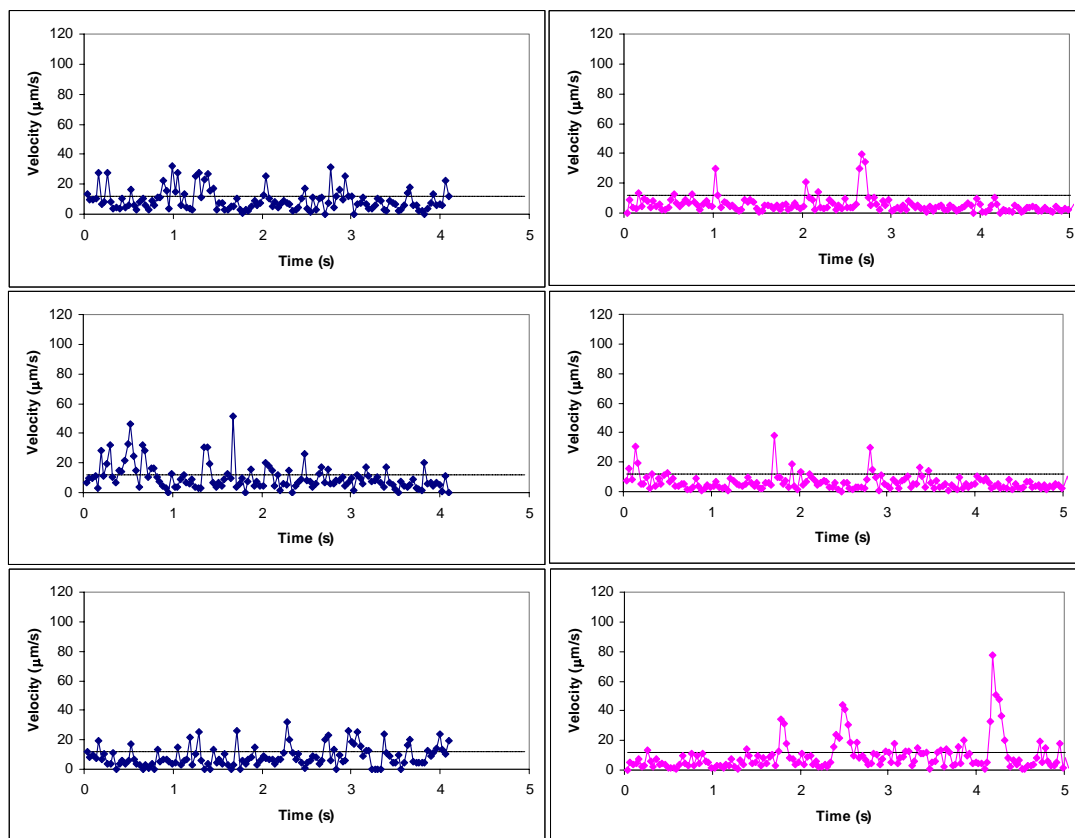


**Figure 6-6:** Instantaneous rolling velocity plots for three representative HL-60 cells in the normal orientation (left column, blue diamonds) and three cells in the inverted orientation (right column, pink diamonds) rolling on  $127 \text{ sites}/\mu\text{m}^2$  of E-selectin at  $0.25 \text{ dynes}/\text{cm}^2$

The instantaneous rolling velocities of the HL-60 cells in the inverted and normal orientation were analyzed and compared to hopefully provide further insight into this strange phenomenon. Figure 6-6 shows the instantaneous rolling velocities in both the normal (left column) and inverted (right column) orientation for  $0.25 \text{ dynes/cm}^2$ . The x-axis is the time during which the cell was tracked. The y-axis is the instantaneous velocity the cell travels between each time point which is every 33ms. Because of noise in the image and tracking software, immobile cells may still fluctuate slightly. However, the threshold velocity is represented on each graph where velocities below this line imply that the cell is stationary.

The first column of graphs in Figure 6-6, illustrated in blue diamonds, are three typical HL-60 cells rolling on  $127 \text{ sites}/\mu\text{m}^2$  of E-selectin at  $0.25 \text{ dynes/cm}^2$  in normal orientation. HL-60 cells that were not engaged with the surface flowed at a velocity of approximately  $160 \mu\text{m/s}$  but the y-axis is maximized at  $120 \mu\text{m/s}$  so the details of the rolling velocity can be reasonably seen. The stochastic rolling behavior that is usually seen with selectin-mediated rolling appears in Figure 6-6 with the HL-60 cells rolling on E-selectin. The pink diamonds in the second column are typical HL-60 cells also rolling on  $127 \text{ sites}/\mu\text{m}^2$  but in the inverted orientation. The magnification is a little higher due to modifications in the microscope setup, possibly allowing more detail in the rolling velocity to be captured. Overall, the rolling velocity in the inverted orientation seems to be fairly similar to the normal orientation with stochastic rolling motion exhibited. However, the cells in the inverted orientation seem to pause a bit longer in between steps during rolling. This would lead to the belief that the cells in the inverted orientation roll

slower than the cells in the normal orientation at similar densities. This will be explored later.

At  $0.1 \text{ dynes/cm}^2$ , where the rollingly adherent cells dissociated rapidly while inverted, a slight difference in the instantaneous rolling velocity between the normal and

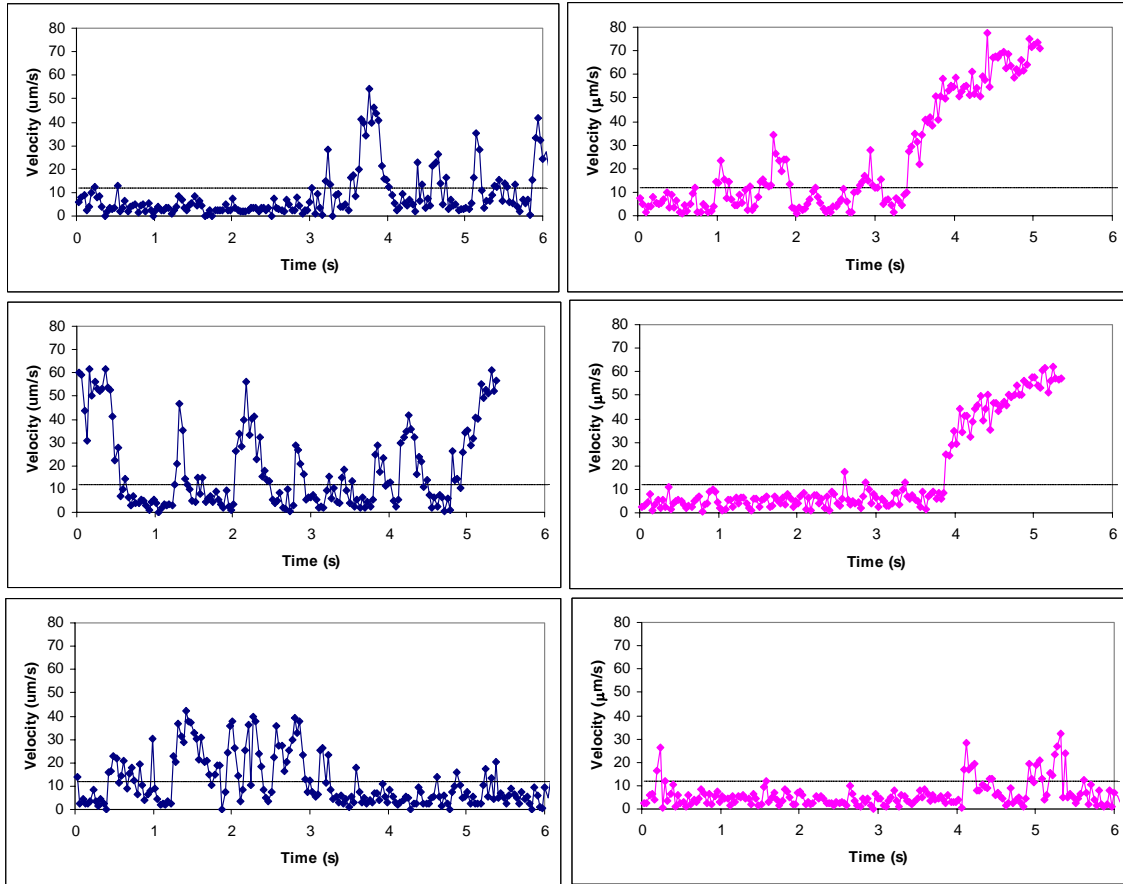


**Figure 6-7:** Instantaneous rolling velocity plots for three representative HL-60 cells in the normal orientation (left column, blue diamonds) and three cells in the inverted orientation (right column, pink diamonds) rolling on  $127 \text{ sites}/\mu\text{m}^2$  of E-selectin at  $0.1 \text{ dynes/cm}^2$

inverted orientation can be seen as well (Figure 6-7). The velocity at which free flowing HL-60 cells traveled at  $0.1 \text{ dynes/cm}^2$  immediately above the chamber floor was around  $60 \text{ }\mu\text{m/s}$ . The three rolling cells plotted in Figure 6-7 in the inverted orientation (second column, pink diamonds) seemed to pause slightly longer than that in the normal orientation similar to what was seen with  $0.25 \text{ dynes/cm}^2$ . Rolling velocities in the inverted orientation also had smaller values with shorter durations when movement occurred than those in the normal orientation. In fact, velocities in the normal orientation point towards cell rolling that is very irregular, with cells at times detaching and re-attaching.

Similar results are seen with  $0.5 \text{ dynes/cm}^2$ , the regime where rolling cells dissociate moderately faster than at  $0.25 \text{ dynes/cm}^2$ . Free flowing cells move at a velocity of approximately  $200 \text{ }\mu\text{m/s}$ . Comparing the instantaneous rolling velocities for the normal and inverted orientation, slightly longer pauses during rolling are seen in the inverted orientation but do not seem significantly different (Figure 6-8). In addition, the velocity values during movement when in the normal orientation were a bit larger in magnitude than velocities during movement in the inverted orientation. However, the velocities of the cells in the normal orientation compared to the free flowing cell velocity were still moderate. The cell's motion during rolling seems to involve mainly steps where the cell remains attached as bonds form and dissociate. The steps the cell takes may be larger than that seen for  $0.25 \text{ dynes/cm}^2$  since velocities were larger, but the velocity profile does not seem to imply that the cells were skipping as seen with  $0.1 \text{ dynes/cm}^2$ .

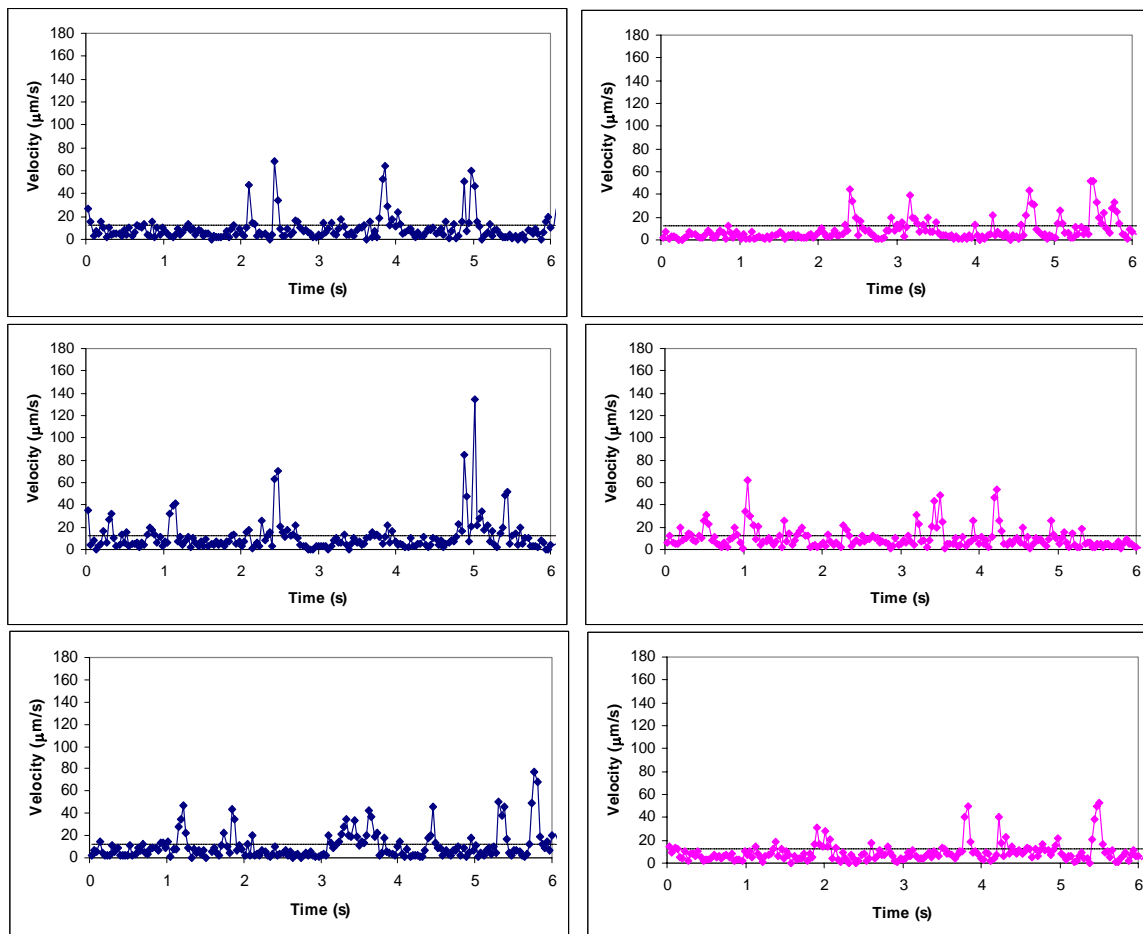


**Figure 6-8:** Instantaneous rolling velocity plots for three representative HL-60 cells in the normal orientation (left column, blue diamonds) and three cells in the inverted orientation (right column, pink diamonds) rolling on  $127 \text{ sites}/\mu\text{m}^2$  of E-selectin at  $0.5 \text{ dynes}/\text{cm}^2$

The instantaneous velocities of the three shear stresses shown, all appearing at extremes of the two regimes, showed some differences between the rolling velocity behavior of the normal and inverted orientation. The HL-60 cells rolling at three shears seemed to have longer pauses in the inverted orientation than in the normal orientation

which would suggest slower rolling. However, the average rolling velocity obtained from the instantaneous velocity plots, summarized in Figure 6-9, does not indicate that slower rolling in the inverted orientation compared to the normal orientation exists for all the shears. At 0.25 dynes/cm<sup>2</sup>, where the dissociation of rollingly adherent cells is slowest but the dissociation of transiently tethering cells is fastest, the average rolling velocity of the cells in the inverted orientation is significantly

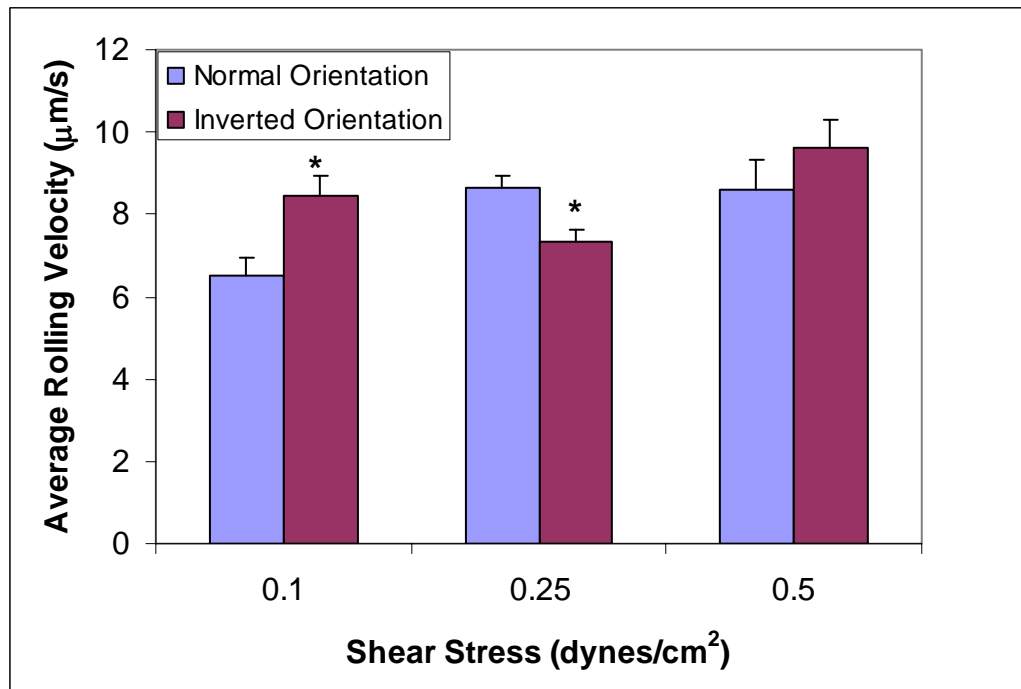


**Figure 6-9:** Comparison of the average rolling velocities for the normal and inverted orientation obtained from the instantaneous rolling velocity plots for 0.1 (n=11 and 7), 0.25 (n=13 and 14) and 0.5 dynes/cm<sup>2</sup> (n=11 and 20) at 127 sites/µm<sup>2</sup> of E-selectin with asterisk showing statistical significance (p<0.01)

slower (p<0.005; Student's t-test) than in the normal orientation. However, for 0.1 dynes/cm<sup>2</sup>, where dissociation is faster, the average rolling velocity of the cells in the

inverted orientation is actually significantly faster ( $p < 0.01$ ) than in the normal orientation. For  $0.5 \text{ dynes/cm}^2$ , the average rolling velocity in the inverted orientation appears to be faster than the normal orientation as well but the difference is not statistically significant.

The plots of the instantaneous rolling velocities highlighted another significant trend. In looking at the instantaneous rolling velocities in the normal orientation, the rolling behavior is distinct between the three shear stresses. This could provide insight into the biphasic curve of the dissociation of rollingly adherent cells.

At  $0.25 \text{ dynes/cm}^2$ , where the dissociation of rollingly adherent cells is slowest, the rolling is generally continual with small velocity values in comparison to its free flowing velocity that are indicative of rolling steps. In contrast, the rolling at  $0.1 \text{ dynes/cm}^2$  consists of large velocity values with some reaching the point of free flowing velocity. This would signify a cell in the “go” phase of rolling. The cells seem to “go” more frequently and for longer durations. In Figure 6-7, the cell travels at the higher velocities for up to 15-20 frames or 0.5-0.6 seconds. Some cells that were tracked but not shown here will travel at similar velocities for several seconds. This behavior indicates that the cell has brief contacts with the E-selectin surface while rolling with some detachment and re-attachment, or skipping, also occurring during rolling. Confirmation of this rolling behavior was made by comparing the instantaneous rolling velocity profiles to the movement of the cell in the video. So, the lack of the ability of the cell to remain in continuous contact with the surface at  $0.1 \text{ dynes/cm}^2$  may explain why dissociation of rollingly adherent cells in the inverted orientation is faster at this shear stress than at  $0.25 \text{ dynes/cm}^2$ .

At 0.5 dynes/cm<sup>2</sup>, larger velocities in the “go” phases were also seen. However, their magnitude was not as drastic as with 0.1 dynes/cm<sup>2</sup>. Additionally, durations of the “go” phases were much shorter than that for 0.1 dynes/cm<sup>2</sup>. This suggests that at 0.5 dynes/cm<sup>2</sup>, some skipping may occur but much briefer and less frequently so that rolling was more continuous than at 0.1 dynes/cm<sup>2</sup> but not as continuous as at 0.25 dynes/cm<sup>2</sup>. This correlates well to the results seen for  $k_{off(RA)}$  as a function of shear stress.

To further quantify the ability of a cell to continuously roll at these shear stresses, the rolling distance a cell traveled was measured for approximately 20 cells for each shear stress. Figure 6-10 shows that at the shear stresses where the dissociation of rollingly adherent cells is faster, the cells also roll for a shorter distance. A cell will

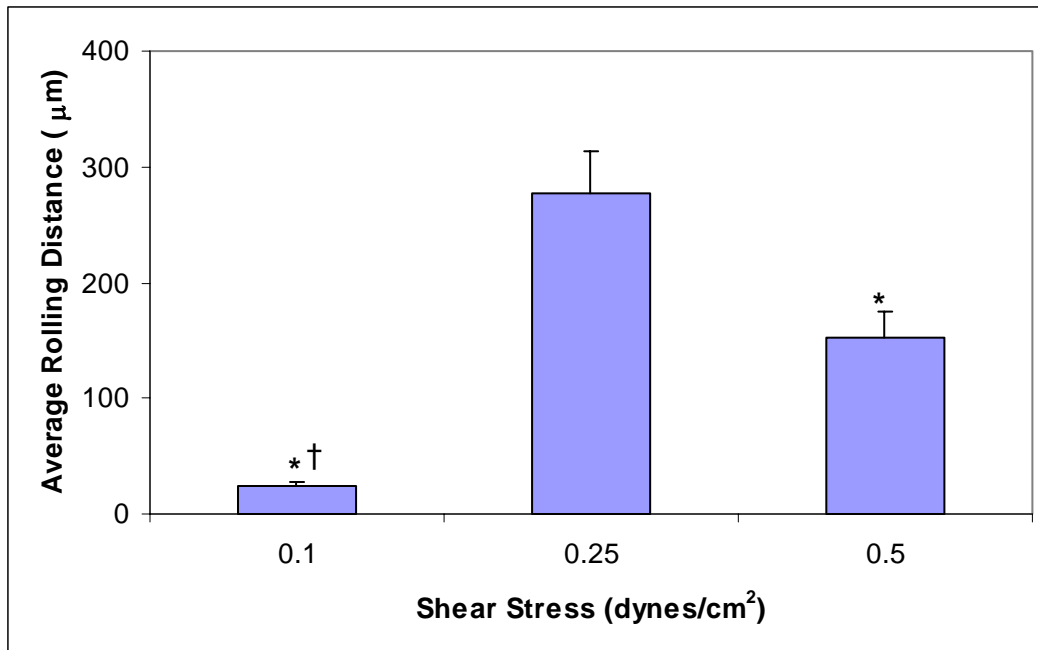


**Figure 6-10:** Average distance HL-60 cells travel while continuously rolling on E-selectin at 127 sites/μm<sup>2</sup> in normal orientation. The asterisks indicate shear stresses with average rolling distances significantly different than 0.25 dynes/cm<sup>2</sup> (p<0.005) and the cross represents the statistically significant difference between 0.1 and 0.5 dynes/cm<sup>2</sup> (p<0.0001)

continue to roll if bonds are able to form in the front before the rear bond dissociates.

Thus, a cell that travels a shorter distance while rolling would indicate that the front bond is unable to form before the rear bond dissociates. Since the  $k_{\text{off}}$  of E-selectin/ligand bonds with transiently tethering cells was smaller at 0.1 dynes/cm<sup>2</sup> than at 0.25 dynes/cm<sup>2</sup>, the fast  $k_{\text{off(RA)}}$  at 0.1 dynes/cm<sup>2</sup> would not be expected to be caused by  $k_{\text{off}}$  alone. This leads to the hypothesis that the measure of  $k_{\text{off(RA)}}$  may rather reflect E-selectin-mediated tether formation or the coordination between off-rate and tether formation. If so, then the results for the dissociation of cells transiently tethering and rollingly adherent are different due to the measurements reflecting different molecular kinetic parameters.

#### ***6.4 Dissociation for Neutrophils Rolling on E-selectin***

In order to strengthen the validity of the results, the dissociation of rollingly adherent neutrophils on E-selectin was measured. In early neutrophil experiments, the cells appeared to detach faster at 0.25 dynes/cm<sup>2</sup> than the HL-60 cells at the same shear stress and E-selectin site density, making it hard to observe a large number of cells after inversion. Better retention of accumulated cells after inversion was achieved at 0.5 dynes/cm<sup>2</sup> than at 0.25 dynes/cm<sup>2</sup>. So, most neutrophil experiments began at 0.5 dynes/cm<sup>2</sup> to allow the cells to accumulate and then changed to the desired shear stress immediately after inversion. Experiments where flow was initiated at 0.25 dynes/cm<sup>2</sup>

and then inverted were found to have similar results to experiments started at 0.5 dynes/cm<sup>2</sup> and then decreased to 0.25 dynes/cm<sup>2</sup> after inversion. Therefore, the wall shear stress at which the chamber is inverted does not affect the results.

Neutrophils bound over time while under a constant shear stress during inversion was observed and the wall shear stress was then varied over a range. Again, the number of cells bound decreased very rapidly over time at the very low shear stresses and seemed to have a modest decay at 0.25 dynes/cm<sup>2</sup> and 0.5 dynes/cm<sup>2</sup>.

Two experiments with neutrophils rolling on E-selectin at 127 sites/μm<sup>2</sup> were pooled together to result in 100-200 cells being included in the cell count per shear stress. Figure 6-11 shows the semi-log plots of the pooled number of cells bound over time for various shear stresses. The approximation of the data to a straight line is fairly good suggesting first order dissociation kinetics. But, the neutrophil data does deviate from a straight line more than the HL-60 cells. This was mostly due to an unusually long pause of certain neutrophils after the most significant dissociation of cells occurred. These neutrophils would appear to be firmly adherent, but after one to several minutes, the cell would begin to move and dissociate. This behavior was very different from that seen with the HL-60 cells, although, from the instantaneous rolling velocity plots, HL-60 cells in the inverted orientation also paused during rolling for extended periods. The instantaneous rolling velocity will be explored further for neutrophils later in this chapter.

By using the first order approximation of the data from Figure 6-11, the pink squares in Figure 6-12 representing the dissociation rate constant for rollingly adherent neutrophils on 127 sites/μm<sup>2</sup> at various shear stresses, are obtained. Comparing the results to that for HL-60 cells at 127 sites/μm<sup>2</sup> of E-selectin,  $k_{\text{off(RA)}}$  seems to fall in the

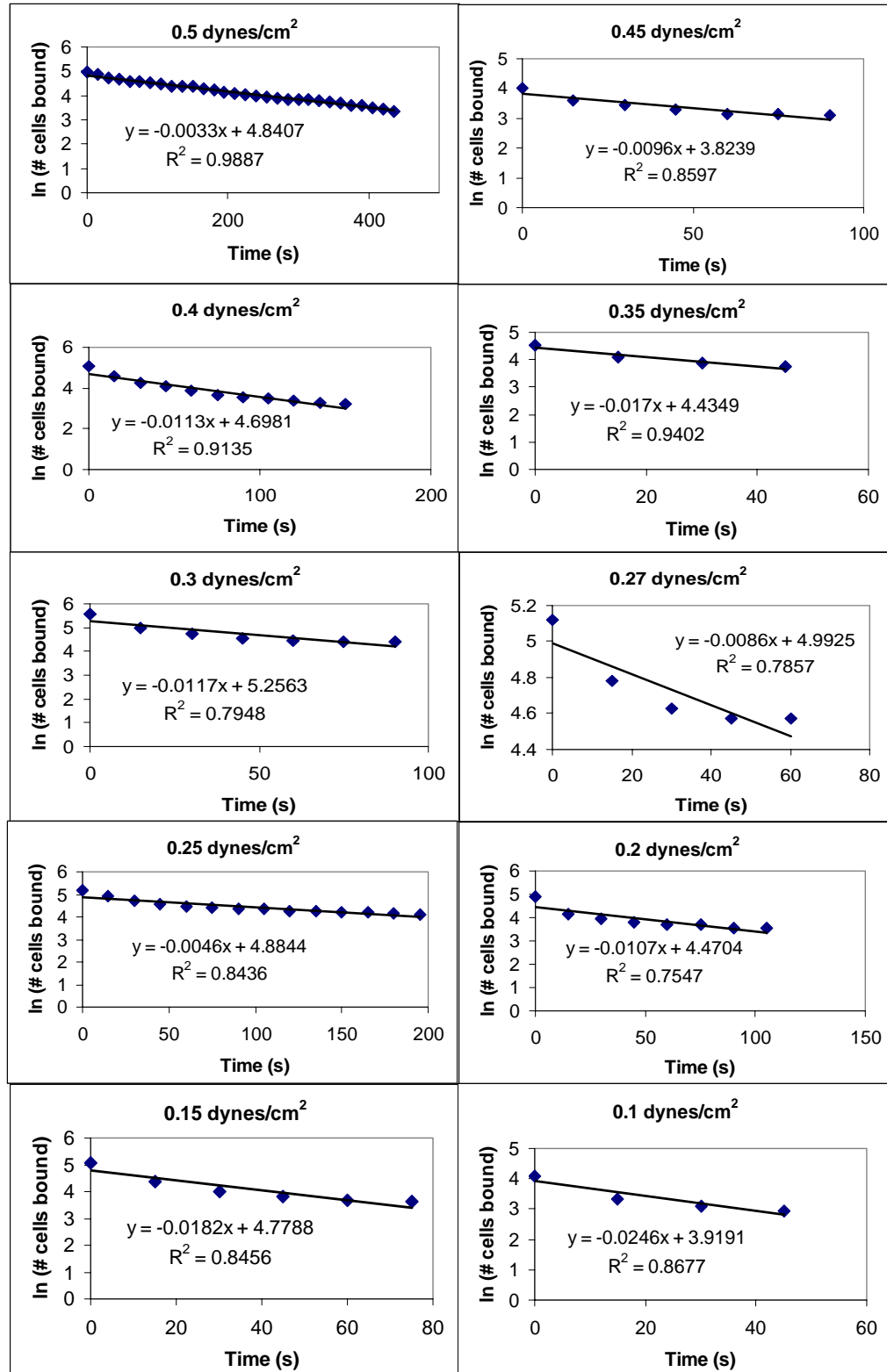


**Figure 6-11:** Dissociation curves for the pooled data of neutrophils rollingly adherent on E-selectin at 127 sites/ $\mu\text{m}^2$  at various shear stresses

same range. Again, this is much lower than that seen for transiently tethering neutrophils which is expected due to multiple bonds forming for rolling to occur. In addition to seeing similar  $k_{\text{off(RA)}}$  between the two cell types, the trend of the curve over the shear stress range is also similar. From the lowest shear stresses,  $k_{\text{off(RA)}}$  decreases as shear stress is increased to 0.25 dynes/cm<sup>2</sup>, meaning that the cells below 0.25 dynes/cm<sup>2</sup> detach faster. The dissociation rate constant then increases as shear stress is increased. This

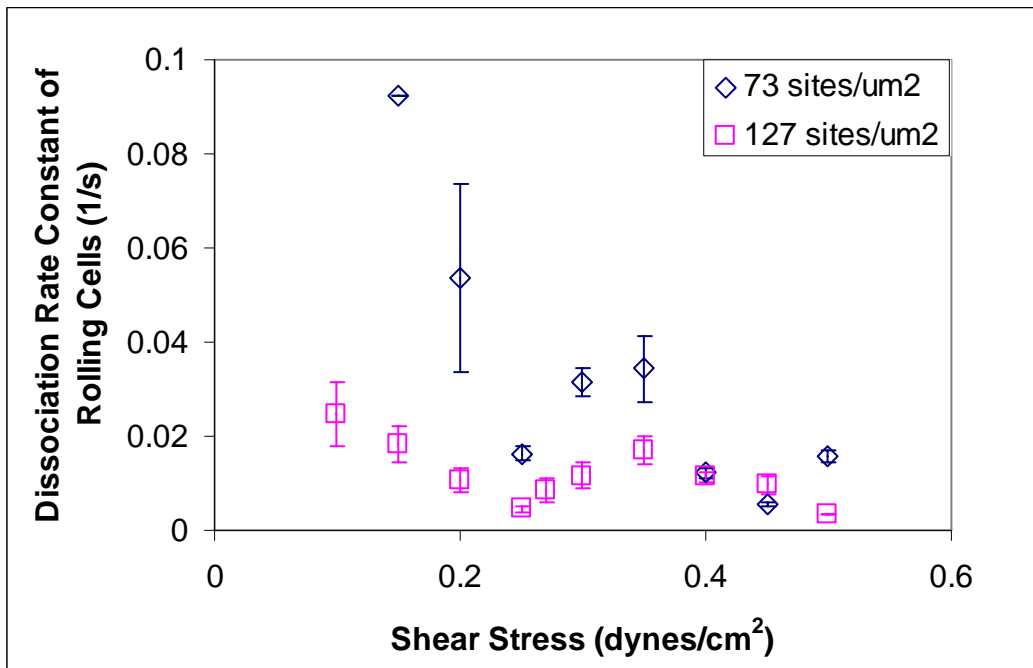


**Figure 6-12:** Dissociation rate constant with SEM for pooled data for rollingly adherent neutrophils on E-selectin at 127 sites/μm<sup>2</sup> and for one experiment at 73 sites/μm<sup>2</sup> as functions of shear stress

biphasic trend - first a decrease and then an increase in  $k_{\text{off(RA)}}$  with increasing shear stress - was also seen in the HL-60 cell experiments. One difference is that, beyond 0.35 dynes/cm<sup>2</sup>, the dissociation rate constant for rolling neutrophils decreases again whereas

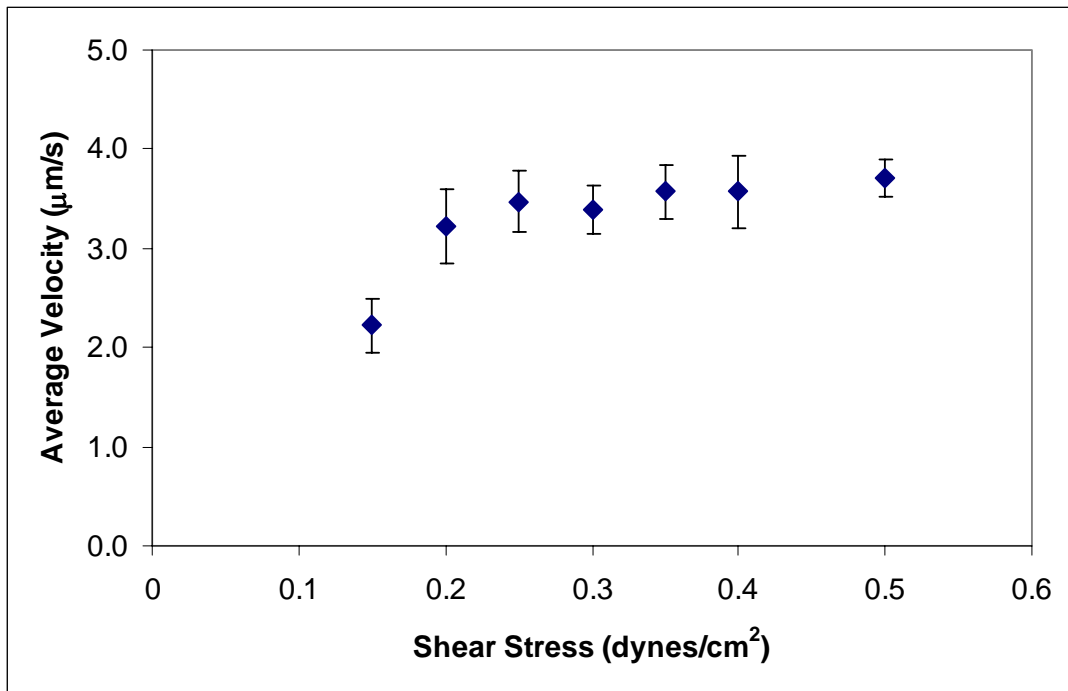
for HL-60 cells the constant continues to increase. This would mean that for neutrophils, the trend of  $k_{\text{off(RA)}}$  over shear stress is actually triphasic. Preliminary data suggests that for HL-60 cells, a triphasic curve may also exist where after 0.5 dynes/cm<sup>2</sup>,  $k_{\text{off(RA)}}$  decreases again with force. More data is needed to ensure the consistency of the trend beyond 0.5 dynes/cm<sup>2</sup>. But for HL-60 cells, a third phase may exist as well and begin at a higher shear stress than that for neutrophils.

Figure 6-12 also show the dissociation rate constant for rolling neutrophils on 73 sites/ $\mu\text{m}^2$  of E-selectin from one experiment. The curve follows the same trend seen for the neutrophils rolling on E-selectin at 127 sites/ $\mu\text{m}^2$ . Therefore, the similarity in the HL-60 and neutrophil curves at two E-selectin densities strengthens the contention that  $k_{\text{off(RA)}}$  follows a biphasic and possible triphasic trend where  $k_{\text{off(RA)}}$  decreases then increases as shear stress is increased.

### ***6.5 Rolling Velocity of Neutrophils on E-selectin in Normal and Inverted Orientation***

The average rolling velocity of neutrophils in the inverted orientation was measured for one of the experiment done at 127 sites/ $\mu\text{m}^2$  of E-selectin (Figure 6-13). The results were very different from that obtained for HL-60 cells rolling in the inverted orientation. Instead of a curve that mirrored the triphasic average rolling velocity curve exhibited in the normal orientation, the neutrophils displayed a flat curve. There seemed to be very little change in the rolling velocity over the range of shear stresses tested. The distinct behavior of the neutrophils where some cells pause for an extended period of time followed by a quick dissociation made collecting average rolling velocity

measurements difficult due to the short period of rolling. However, this behavior may signify that the cells could be rolling in a modified way while inverted. This may be the cause for the discrepancy in the average rolling velocity curves in the normal and inverted orientation for both the HL-60 cells and neutrophils.



**Figure 6-13:** Average and SEM of the measures for the average rolling velocity from one experiment for neutrophils rolling on E-selectin at 127 sites/ $\mu\text{m}^2$  while inverted

Because of the extended pauses times of the neutrophils before dissociation while inverted, the instantaneous rolling velocity of the cells in the inverted orientation was analyzed. The instantaneous rolling velocity of neutrophils in the normal orientation

from previous experiments was also collected for comparison. However, the previous experiments were done with E-selectin at 248 sites/ $\mu\text{m}^2$  and imaged with higher magnification. Although neutrophils rolling on the same density of E-selectin as utilized for the inverted experiments was not available, comparing the neutrophil rolling behavior of the two orientations at different densities still provided insight into the disparate rolling behaviors.

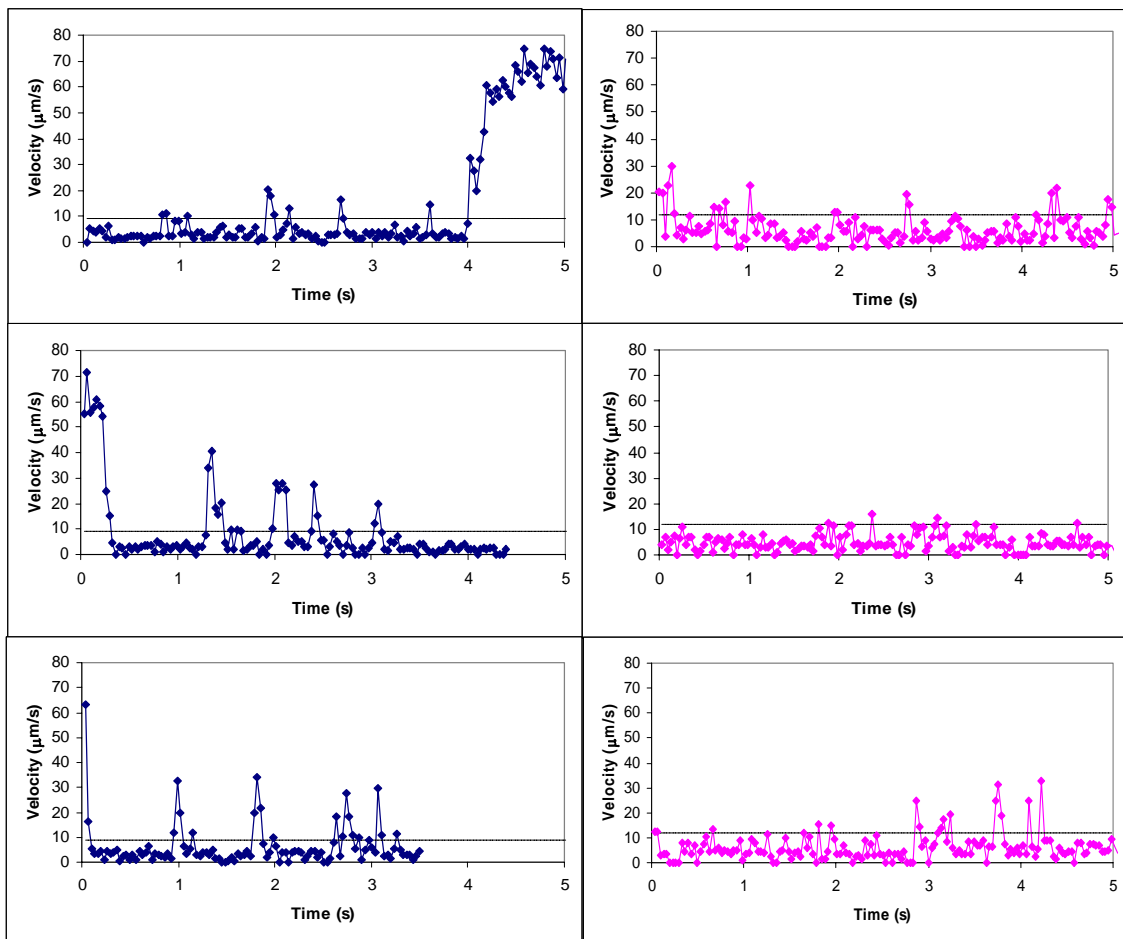


**Figure 6-14:** Instantaneous rolling velocity plots for three representative neutrophils in the normal orientation on 248 sites/ $\mu\text{m}^2$  of E-selectin (left column, blue diamonds) and three neutrophils in the inverted orientation (right column, pink diamonds) rolling on 127 sites/ $\mu\text{m}^2$  of E-selectin at 0.25 dynes/cm<sup>2</sup>

Figure 6-14 shows the velocity of neutrophils rolling on E-selectin at 0.25 dynes/cm<sup>2</sup>. Again, the dotted line represents the threshold velocity where below that line, cells are considered stationary. The left column with data shown in blue diamonds is neutrophils rolling on 248 sites/μm<sup>2</sup> in the normal orientation. Cells are shown continuously rolling with some stochastic motion of small magnitude and duration and attaching or detaching at the free flowing velocity of approximately 75 μm/s. The right column includes neutrophils rolling on E-selectin at 127 sites/μm<sup>2</sup> in the inverted orientation. While engaged with the surface, two of the cells do not appear to move much and the third cell pauses at first and then begins to roll.

For neutrophils flowing at 0.15 dynes/cm<sup>2</sup>, cells not bound to the surface flow at about 45 μm/s. The instantaneous rolling velocity of neutrophils rolling on E-selectin at 0.15 dynes/cm<sup>2</sup> is shown in Figure 6-15. Once more, in the inverted orientation (pink diamonds, right column), long pauses of the neutrophils during rolling is seen. The first cell shown in column two begins to move because it is detaching. Detachment occurs quickly due to the low shear stress. However, this movement is preceded by a pause of the cell. This rolling behavior in the inverted orientation is quite unlike that seen for the normal orientation.

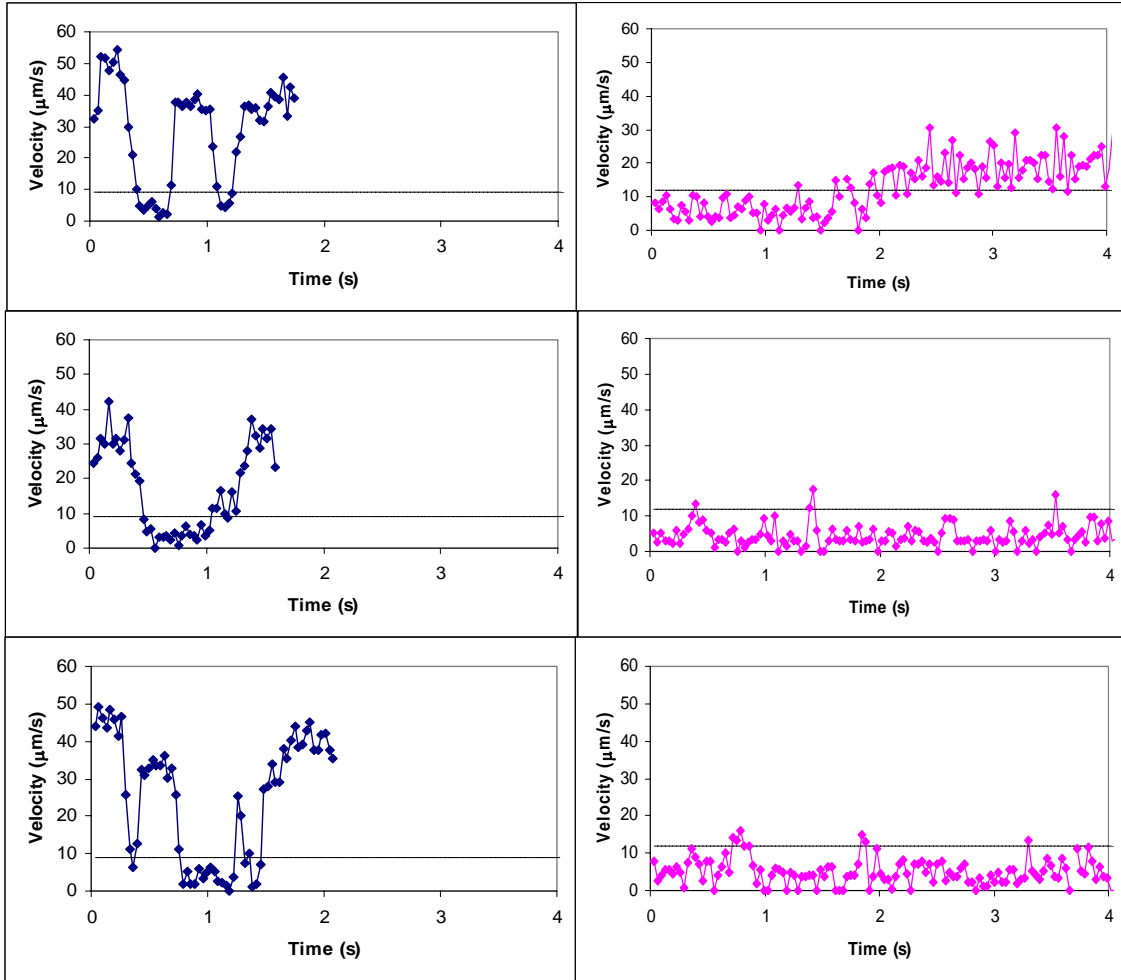


**Figure 6-15:** Instantaneous rolling velocity plots for three representative neutrophils in the normal orientation on 248 sites/ $\mu\text{m}^2$  of E-selectin (left column, blue diamonds) and three neutrophils in the inverted orientation (right column, pink diamonds) rolling on 127 sites/ $\mu\text{m}^2$  of E-selectin at 0.15 dynes/ $\text{cm}^2$

In the normal orientation, where neutrophils roll on 248 sites/ $\mu\text{m}^2$  at 0.15 dynes/ $\text{cm}^2$  (Figure 6-15 shown in left column with blue diamonds), very irregular rolling occurs. Brief rolling interactions with the surface were preceded and followed by attachment and re-attachment or skipping. This skipping was also seen with HL-60 cell rolling on E-selectin at 0.1 dynes/ $\text{cm}^2$ . At these low shear stresses, the rolling cells were

seen dissociating faster from the surface while inverted than cells at 0.25 dynes/cm<sup>2</sup>. So again, the increase or decrease in the stability of rolling that is seen for cells at a given shear stress seems to correlate to the slower or faster dissociation, respectively, of those rolling cells from the surface while inverted. Cells that roll more stably are able to form a new E-selectin-mediated tether in the front before the rear bond dissociates resulting in smoother, more continuous rolling. Thus, cells displaying less stable rolling, particularly at the low and moderately high shear stresses, may have a slower rate of tether formation that causes the rear bond to dissociate before the front bond forms. Hence, the trend of the  $k_{\text{off(RA)}}$  curve seems to be closely related to rolling stability and shear-dependent tether formation .

## CHAPTER 7

### DISCUSSION

#### *7.1 Existence of a Triphasic Dissociation Curve for E-selectin*

The data in Aim 1 suggests that slip/catch/slip transitional bonds for E-selectin/ligand interactions exist. Micropipette data with Colo-205 cells interacting with E-selectin provided early evidence that E-selectin/ligand interaction might behave as catch bonds. In this experiment, a slip bond followed by a catch bond was observed for forces between 10 and 28 pN (Piper 1997). A catch bond followed by a slip bond was seen for P- and L-selectin interacting with PSGL-1 at forces in the range of 6-60 pN and 4-200 pN, respectively (Marshall et al. 2003; Sarangapani et al. 2004). Because of the similarity between the three selectins and the early micropipette data with E-selectin, the tether lifetime data for cells transiently tethering on E-selectin would be expected to begin as a slip bond, then transition to a catch bond and return to a slip bond. The E-selectin/neutrophil and sLe<sup>x</sup>-coated beads/E-selectin data did follow this trend.

Although a triphasic trend resulted from both the E-selectin/neutrophil and sLe<sup>x</sup>-coated beads/E-selectin experiments, the increase of lifetime with force in the catch bond regime is moderate. One explanation for this could involve the uncertainty that still remains regarding the primary ligand for E-selectin. E-selectin is known to interact with PSGL-1 but with less affinity than P-selectin interacting with PSGL-1 (Mehta et al. 1998). From the data presented here, it has been shown that E-selectin can sufficiently interact with sLe<sup>x</sup> which is an epitope on PSGL-1. But other ligands, like ESL-1 may

have a stronger affinity to E-selectin and result in a stronger triphasic trend of the tether lifetime.

Despite the subtle transitions, the data presented here demonstrate that the triphasic curve exists. Neutrophil experiments were repeated over the shear stress range and found to have consistent results. Repeat tether lifetime experiments done with sLe<sup>x</sup>-coated beads also showed the triphasic trend with each phase of the curve matching well to the neutrophil results.

Additionally, the average rolling velocity measurements collected for unfixed and fixed neutrophils rolling on E-selectin supported the triphasic trend of the tether lifetime data seen for the neutrophils and sLe<sup>x</sup>-coated beads well. For selectins, higher off-rates have been known to mediate faster rolling. For example, L-selectin has higher off-rates than P- and E-selectin and mediates faster rolling than those two selectins (Alon et al. 1997). Similarly, changes in off-rate of a selectin type because of shear stress would lead one to expect the rolling velocity to change accordingly with shear stress. For L-selectin, cells are found to roll slower as force is increased in the catch bond regime where lifetimes are prolonged by increasing force. In the slip bond regime where lifetime is shortened with increasing force, faster rolling is seen (Yago et al. 2004). Because three tether lifetime regimes were seen with E-selectin, the rolling velocity would be expected to also have a triphasic curve with the velocity trend in each phase being inversely related to the tether lifetime trend in that range of shear. As Figure 5-1 and 5-2 reveal, as shear stress is increased, regions of increasing rolling velocity are associated with decreasing tether lifetime, while decreasing rolling velocity was found in areas of increasing tether

lifetime. Furthermore, this trend is seen for HL-60 and Colo-205 cells. This provides strong evidence of the triphasic trend of E-selectin-mediated dissociation over shear.

The subtle trend of the curve emphasizes the importance of using proper statistics to test the statistical significance of the changes in the trend of the curve. The use of the Student's t-test to show that the difference between tether lifetime measures for each shear stress is statistically significant did not prove effective in this case. Because of the subtle trend and frequent phase changes of the curve, small increments of shear stress were tested to give higher resolution to the curve. Each data point along the curve represents discrete points that are part of a continuum along the trend line. However, the smaller the shear stress increment, the smaller the difference is in the tether lifetime between neighboring points. This would result in a high p-value indicating no statistically significant difference in the tether lifetime between the two points. Table 4-2 shows the p-values using t-test analysis of the tether lifetime measures (average tether lifetime, standard deviation, inverse of the slope) and off-rate for shear stresses along the triphasic curve. For neighboring points having a small shear stress increment, the p-values indicate that the results between the two shear stresses are not statistically significantly different. But, as points farther apart are compared, lower p-values are generally seen. This correlation of the p-values to the shear stress increment becomes more complex due to the mild dependence of the tether lifetime on shear stress and the narrow range of the shear stress where the slip/catch/slip transition occurs. Therefore, statistical significance between even non-neighboring points is hard to observe using the Student's t-test.

Better proof of the data following a triphasic trend was found using other statistical methods to analyze the data. The triphasic curve can also be viewed as three straight lines that are monotonically increasing or decreasing. If each phase of the curve is analyzed separately as a monotonically increasing or decreasing line, most of the data is found to significantly follow a linearly increasing or decreasing curve with 95-99% confidence. The tether lifetime data for neutrophils at high shear stresses was not found to be statistically significantly linear. However, fewer data points were collected in this region due to the focus of this study on the lower shear stresses where the slip/catch transition would occur. Previous experiments have shown the dissociation kinetics for E-selectin-mediated adhesion at higher shear stresses where the bond behaves as a slip bond (Alon et al. 1997; Puri et al. 1997; Smith et al. 1999). Thus, proving that the tether lifetime data at the higher forces is monotonically decreasing, as is true for a slip bond, is not as much of a concern. For sLe<sup>x</sup>-coated beads, more tether lifetime data was collected and the data in all regimes significantly followed a monotonically increasing or decreasing curve. The slope of each of those straight line segments can then be compared to the adjacent line segment to test whether their slopes are significantly different. In Section 4.2 and 4.3, when comparing the trend line of the data in the slip bond regime to that in the catch bond regime, the slopes of the regression lines are found to be statistically significantly different with p-values reaching only as high as 0.04 for neutrophils and 0.004 for sLe<sup>x</sup>-coated beads. Therefore, the transitions from monotonically increasing to decreasing and back to increasing trends in the triphasic curve seem statistically significant.

One limitation of this method involves the determination of the inflection point where the data transitions from monotonically decreasing to increasing or from increasing to decreasing. From the Student's t-test, the difference in the tether lifetime between neighboring points is not found to be statistically different. Thus, the inflection point, although chosen because of its tether lifetime value, is not statistically distinct as the local maximum or minimum.

If the statistical analysis is done by including either of the points neighboring the chosen inflection point in the linear regression analysis, the results are quite different. For the neutrophil tether lifetime data, the data in the first slip bond phase for the various tether lifetime measures and  $k_{\text{off}}$  is found to have a statistically significant linear trend with a 90% confidence interval or more whereas the catch and second slip bond regime data does not demonstrate statistical linear significance. When comparing the slopes of the three phases, the slope of the data in the first slip bond regime appears to be statistically different from the slope of the data in the catch bond regime when either neighboring point to the optimal inflection point is included in the slope of the data with  $p < 0.05$  for all but one measure in one case. Statistical difference is not found when comparing the slopes of the catch bond regime to the second slip bond regime with any of the tether lifetime measures in any of the cases. Although significance between the slopes is still demonstrated in the first slip/catch transition when either neighboring point is included in the slope, the weaker significance in the second transition as well as with the linear trend of the data raises concern of the significance of the triphasic trend of E-selectin-mediated dissociation.

The tether lifetime results with the sLe<sup>x</sup>-coated beads matches the tether lifetime trend observed for neutrophils and provides strong evidence to support the triphasic trend of dissociation for E-selectin. When the linear regression for the tether lifetime of sLe<sup>x</sup>-coated beads to E-selectin included the points neighboring the chosen inflection points, most of the data was found to significantly follow a linear curve for all cases. Furthermore, for all tether lifetime measures and  $k_{\text{off}}$  for all cases, the slopes of the first slip and catch bond regimes were demonstrated to be statistically significantly different with  $p < 0.005$  in most cases and  $p < 0.05$  in the rest of the cases. Again, the statistical difference between the slopes of the catch bond regime with the second slip bond regime did not demonstrate to be significant when either of the neighboring points were included in the slope. However, fewer data points were collected in the second slip regime again due to exhaustive studies of E-selectin dissociation in this shear stress range previously. With the limitations of this statistical method, the tether lifetime data for the E-selectin/neutrophil and E-selectin/sLe<sup>x</sup>-coated beads interactions separately may not strongly demonstrate the triphasic force dependence of the dissociation of E-selectin. But collectively, the triphasic transition of the dissociation of E-selectin-mediated adhesion over force seems to be statistically significant. In other words, catch bonds for E-selectin exist because the transition of the E-selectin-mediated tethers from a slip bond to a catch bond and back to a slip bond is statistically significant.

## ***7.2 Relevance of the Triphasic Dissociation Curve to Selectin Studies***

Previous studies with P- and L-selectin also showed catch/slip transitional bonds (Marshall et al. 2003; Sarangapani et al. 2004), which were qualitatively similar to

each other and to the latter two phases of the E-selectin triphasic curves. This similar kinetic behavior reflects the similar structures and functions of the three selectins. The specificity of the different selectin-ligand interactions are revealed by the quantitative differences among their catch/slip bonds, which differ not only in the lifetime levels but also span different ranges of wall shear stresses. As wall shear stress decreased for E-selectin, the catch bonds returned to slip bonds. However, in both cases of P- and L-selectin, the catch bonds returned to slip bonds. However, in both cases of P- and L-selectin, the catch bond regime extended into the lowest forces able to be tested (Marshall et al. 2003; Sarangapani et al. 2004). Although it was difficult to observe tether lifetimes supported by P- and L-selectin at even lower forces, it seems reasonable to predict that their catch bonds would also transit back to slip bonds as force further decreased. Not only would this be consistent with the structural and functional similarities of selectins, but it would also agree with the zero-force lifetimes (reciprocal off-rates) measured by SPR (Mehta et al. 1998; Nicholson et al. 1998), which are much longer than the respective zero-force extrapolations of the lifetime vs. force curves of the P- (Marshall et al. 2003) and L-selectin (Sarangapani et al. 2004).

Using the third order polynomial curve, the unstressed off-rate from the zero-force extrapolation of the E-selectin/neutrophil ligand dissociation can be roughly estimated to be  $1.0\text{s}^{-1}$ . This is slightly higher than the  $k_{\text{off}}^{\circ} = 0.7\text{s}^{-1}$  seen in previous flow chamber studies for neutrophils interacting with E-selectin (Alon et al. 1997). However, their  $k_{\text{off}}^{\circ}$  was determined using the Bell equation to fit data obtained at higher forces. The  $k_{\text{off}}^{\circ}$  obtained with micropipette experiments is in good agreement with the results presented here given that the E-selectin ligand on neutrophils may differ from those on HL-60 cells. For HL-60 cells binding to E-selectin,  $k_{\text{off}}^{\circ} = 0.9\text{-}0.92\text{s}^{-1}$  (Long et al. 2001;

Huang et al. 2004). In order to more accurately determine the  $k_{\text{off}}^0$  for E-selectin-mediated interactions, appropriate models depicting the slip/catch/slip transition need to be developed.

In previous experiments,  $k_{\text{off}}^0$  was determined by using the Bell model which is valid when the bond behaves as a slip bond. However, because a catch regime preceded by an additional slip region has been revealed, new models need to be developed to describe the dependence of off-rate on force. For the catch bond seen with P-selectin, a two pathway model has been proposed where the P-selectin/PSGL-1 bond behaves as a mechanochemical switch that is force sensitive and determines which pathway the bond will dissociate. Using a biomembrane force probe, catch/slip bonds for P-selectin interacting with PSGL-1 were observed but only slip bonds seen for P-selectin interacting with sLe<sup>x</sup> (Evans et al. 2004). The two-pathway model was used to explain these results such that P-selectin dissociates from sLe<sup>x</sup> along a fast but force independent pathway. In contrast, the interaction of P-selectin with the peptide component of PSGL-1 adds another pathway, which is slow but force sensitive. The results obtained with sLe<sup>x</sup>-coated beads binding to E-selectin indicate that the sLe<sup>x</sup> epitope of the ligand is sufficient for mediating slip/catch/slip bonds. Therefore, this model may not be applicable to E-selectin, as its interactions with both neutrophil ligands and sLe<sup>x</sup> exhibited slip/catch/slip bonds.

Force-induced changes in the structure may give rise to the slip/catch/slip bond transition of E-selectin-mediated dissociation. Catch bond behavior has been seen in bacterial adhesion of FimH due to a shear-enhanced conformational change in a regulatory region of FimH (Thomas et al. 2002). The catch bond for L-selectin has been

found to be augmented when a hydrogen bond is eliminated in the interdomain hinge region which may allow ligands to slide along the L-selectin interface (Yago submitted). Furthermore, a recent sliding-rebinding model done on the P-selectin interface with PSGL-1 looks at the force-dependent movement of the hinge region and predicts a triphasic trend of the tether lifetime over force (Lou unpublished data). This theory might thus explain the slip/catch/slip trend of tether lifetime seen with E-selectin.

The catch/slip transition of tether lifetime relates to the flow-enhanced adhesion through L-selectin where a minimum shear is required for cell rolling to occur (Yago et al. 2004). This shear threshold may prevent inappropriate leukocyte aggregation or vessel interaction in low shear conditions (Finger et al. 1996; Yago et al. 2004). The similarity of the catch/slip phase between E-selectin and L-selectin could indicate that the dissociation of E-selectin may be physiologically important in an analogous way. However, this would not explain the preceding slip bond regime found for E-selectin. E-selectin mediates the slower rolling of leukocytes on vascular surfaces compared to P- and L-selectin-mediated rolling. This slower rolling of the leukocytes allows the cell ample exposure time to chemokines that are important in the inflammation cascade. Extending the knowledge of this unique role of E-selectin in inflammation may lead to a better understanding of the physiological role of the triphasic force-dependent dissociation of E-selectin-mediated adhesion. Yet, its biophysical role in determining the rolling velocity of cells on E-selectin has been shown here.

### ***7.3 Triphasic Rolling Velocity for Neutrophils, HL-60 and Colo-205 cells***

The average rolling velocity data obtained for neutrophils, unfixed and fixed, correlates well to triphasic off-rate curve. Regions of decreasing off-rates, meaning prolonged tether lifetimes, had decreased rolling velocities while increasing off-rates were found in areas where rolling velocities were increased. This is consistent with the notion that rolling velocity is predominantly determined by the rate of dissociation of bonds at the rear end of the cell (Alon et al. 1997). This also agrees well with the previous studies with L-selectin where the change in rolling velocity correlated with the change in the dissociation kinetics from catch to slip bonds (Yago et al. 2004). This trend was also displayed when other cell types were utilized. The average rolling velocity of both HL-60 cells and Colo-205 cells rolling on E-selectin demonstrated a triphasic trend.

The triphasic rolling velocity of neutrophils on E-selectin was found to also depend on the E-selectin density on the surface. At 37 sites/ $\mu\text{m}^2$ , neutrophils rolled faster on E-selectin than on 248 sites/ $\mu\text{m}^2$  but both exhibited a triphasic trend. So a triphasic curve that is shifted towards higher velocities is seen as the density of E-selectin is decreased.

Because of early micropipette experiments with Colo-205 cells interacting with E-selectin where a slip-catch transition was seen in the range of 10-28 pN (Piper 1997), the rolling velocity of Colo-205 cells was expected to follow a similar trend. At the lowest shear stresses tested, the rolling velocity results for Colo-205 cells did indicate the existence of a slip regime followed by a catch regime. However, quantitatively, the curve differed from that obtained with micropipette. The lowest shear stress that Colo-205 cells were able to be observed rolling on E-selectin in the flow chamber was 0.05 dynes/ $\text{cm}^2$

which equates to 21.8pN. In this force range, Colo-205 cells interacting with E-selectin in the flow chamber are found to be in a slip bond state whereas micropipette results show catch bonds to exist in this force range.

The variation in the way the bond is loaded between the micropipette and flow chamber experiments could be one cause for this discrepancy. In micropipette experiments, force is applied to the bond at a constant loading rate in a normal direction. Flow chamber experiments load the bond through the shear force of the fluid flowing over the cell at varying loading rates that depend on the shear being applied. Experiments with the atomic force microscope reveal a dependence of the off-rate on not just the force applied but also the force history (Marshall et al. 2005). Other studies with AFM suggest that the loading rate used to apply the force also plays a role in the dissociation of the selectin-mediated bond (Sarangapani unpublished data). So, the distinction in force application between the two systems may result in the observation of slip/catch/slip bonds in both systems but appearing in different force ranges.

Another possibility is that the relationship of off-rate to the rolling velocity with Colo-205 cells is more complex than that seen with neutrophils interacting with E-selectin. Colo-205 cells have sLe<sup>a</sup> in addition to sLe<sup>x</sup>. Perhaps the dissociation of E-selectin-mediated bond during cell rolling and transient tethering differs slightly when both sLe<sup>x</sup> and sLe<sup>a</sup> present.

#### ***7.4 Biphaseic Dissociation Rate of Rolling Adherent Cells***

For cells rolling on E-selectin, the chamber was inverted to study the dissociation of rollingly adherent cells. The number of rolling cells bound over time after inversion

followed an exponential decay that agreed well with first order dissociation kinetics. From first order analysis,  $k_{\text{off(RA)}}$  was found to decrease first and then increase as shear stress was increased for HL-60 cells. This result was unexpected. Additionally, scatter in the early data between experiments created more uncertainty about the results. Factors such as the homogeneity of the E-selectin coated on the surface, human variability in the inversion method and the relatively small number of cells that could be collected in the field of view due to magnification limitations could have been sources of error. However, by pooling the data of multiple experiments, the scatter was greatly reduced. Seeing similar results with HL-60 cells rolling on a lower density of E-selectin as well as with neutrophils rolling on two different densities of E-selectin provided more certainty in the results. The  $k_{\text{off(RA)}}$  with neutrophils rolling on E-selectin actually displayed a triphasic trend with the first two phases very similar to the curve obtained for the HL-60 cells. Furthermore, in the only published study where an inverted flow chamber was utilized, HL-60 cells in the inverted orientation were observed to detach from P- and E-selectin substrates within 15 seconds when the shear stress was changed from 1 dyne/cm<sup>2</sup> to 0.1 dynes/cm<sup>2</sup> (Lawrence et al. 1997). Thus, the quantitative data collected regarding the biphasic, and possibly triphasic, dissociation of rollingly adherent HL-60 cells and neutrophils on E-selectin matches well to what has been previously observed at 0.1 dynes/cm<sup>2</sup> for HL-60 cells rolling on E-selectin. This trend seems real although unsettling when compared to the dissociation results obtained for transiently tethering cells in the normal orientation.

### ***7.5 Relevance of the Dissociation of Rollingly Adherent Cells to Tether Formation***

The trend of the dissociation of rollingly adherent cells over shear stress mirrors the dissociation rate constant curve obtained for neutrophils transiently tethering to E-selectin and the dissociation rate constant suggested from rolling velocity results for HL-60 cells. So at first glance, this may seem to contradict the triphasic trend obtained for the dissociation of transiently tethering cells in Aim 1. However, closer study into the instantaneous rolling velocity reveals that  $k_{\text{off(RA)}}$  may not only reflect off-rate as it does when looking at transiently tethering cells. In the regions where the rolling cells dissociate faster, cell rolling appears to be more irregular with large increases in velocity during rolling. At the very low shear stresses like 0.1 and 0.15 dynes/cm<sup>2</sup> where rolling cells are found to dissociate very fast, cells seem to detach and reattach in between continuous segments of rolling. This was also seen by Lawrence et. al. when the rolling of HL-60 cells at 0.5 and 0.1 dynes/cm<sup>2</sup> was compared for both P- and E-selectin. HL-60 cell rolling on P- and E-selectin at 0.1 dynes/cm<sup>2</sup> was intermittent and of brief duration contrasting the more sustained rolling found at 0.5 dynes/cm<sup>2</sup> (Lawrence et al. 1997).

To look at this rolling discrepancy further, the distance a cell traveled while rolling was measured for HL-60 cells at 0.1, 0.25 and 0.5 dynes/cm<sup>2</sup> (Figure 6-10). The distance a rolling cell traveled was highest for 0.25 dynes/cm<sup>2</sup> and lowest for 0.1 dynes/cm<sup>2</sup>. At 0.25 dynes/cm<sup>2</sup>, slower dissociation of rollingly adherent cells was observed while dissociation was fastest at 0.1 dynes/cm<sup>2</sup>. Thus,  $k_{\text{off(RA)}}$  seems to be linked to the distance that the cell continuously rolls.

For a cell to continuously roll, it has to alternate between at least two bonds. Before the rear bond dissociates, one or more bonds must be formed at the cell front to

allow the cell to remain in contact with the surface. When that rear bond dissociates without a new bond being already formed, the rolling cell detaches. Therefore, the regions where the cells detach faster and rolling is more irregular may indicate a region where tethers are less able to form before the rear bond breaks. So the faster dissociation of rollingly adherent cells at  $0.1 \text{ dynes/cm}^2$  than at  $0.25 \text{ dynes/cm}^2$  may be due to a reduced ability to form tethers.

Finger et al. discovered a shear threshold requirement for L-selectin. A shear of about  $0.4 \text{ dynes/cm}^2$  is required for stable tethers to form and optimal tether formation and cell accumulation occurred at  $1 \text{ dyne/cm}^2$  (Finger et al. 1996). Although this study did not find a shear threshold requirement for E- or P-selectin, it did not focus on adhesion at the very low forces. On the contrary, Lawrence et al. presented data to suggest E-selectin has a shear threshold where below  $0.25 \text{ dynes/cm}^2$ , the adhesion of HL-60 cells to E-selectin is reduced (Lawrence et al. 1997). The data presented here seem to support the idea that a shear threshold exists for E-selectin. By determining  $k_{\text{off(RA)}}$  over the low shear force range with small shear stress intervals, the E-selectin shear threshold was more precisely and quantitatively depicted than previously, providing more confidence of its existence.

For L-selectin, catch bonds have been suggested to govern the rolling velocity of cells through the threshold shear. As the shear is increased to the optimal shear stress of  $1 \text{ dyne/cm}^2$ , slower and more regular rolling is observed. This is where catch bonds have been observed and data by Yago et al suggests that catch bonds explain this rolling stabilization below  $1 \text{ dyne/cm}^2$  (Yago et al. 2004). For E-selectin, the rolling appears to become more regular and stable as the shear is increased to the optimal shear of  $0.25$

dynes/cm<sup>2</sup>. This has been shown in previous studies as well as with the instantaneous rolling velocity and rolling distance data presented here. However, the average rolling velocity data in Chapter 5 shows that the rolling velocity becomes faster as shear is increased to the apparent optimal shear of 0.25 dynes/cm<sup>2</sup>. This matches well to the tether lifetime data obtained for cells transiently tethering to E-selectin that predicts the slip bond regime to exist here. Yet it is quite different from the L-selectin results. For L-selectin, slower velocities with more regular and stable rolling are seen as the shear is increased to the optimal level that seems to be a result of catch bonds. But for E-selectin, faster velocities with more regular and stable rolling are seen as the shear is increased to the optimal shear, which falls in a slip bond regime. Off-rate and the bond type, whether slip or catch, may govern the rolling velocity, which has been strongly shown by Yago et al. (Yago et al. 2004) and suggested here for E-selectin. But, other factors may play a role in additional aspects of the rolling behavior such as the stability of rolling. The instantaneous rolling velocity profile and distance that the cell is able to travel while continuously rolling, presented here for 0.1, 0.25 and 0.5 dynes/cm<sup>2</sup>, could be indicators of the stability of cell rolling. Rolling stabilization has been hypothesized by other to result from shear rate and its movement of the receptors and ligand to promote binding and shear stress induced torque that bring receptors and ligands in closer proximity for binding (Lawrence et al. 1997; Chang et al. 1999; Chen et al. 1999; Chen et al. 2001). These hypotheses tend to suggest that tether formation could be a factor in rolling stabilization. So perhaps for E-selectin, the shear-dependent slip/catch/slip bond determines the rolling velocity of the cell whereas shear-enhanced tether formation

determines the rolling stability of the cell. The data presented in this thesis collectively point to that hypothesis.

### ***7.6 Average Rolling Velocity in the Inverted Orientation***

The discrepancy in the curves obtained for the average rolling velocity of the cells in the normal and inverted orientation was surprising. For the HL-60 cells, the average rolling velocity in the inverted orientation mirrors that seen in the normal orientation. From the plots of the instantaneous rolling velocity for the normal and inverted orientation, cells in the inverted orientation showed some signs of longer pauses while rolling than cells rolling in the normal orientation. If the cells paused longer in the inverted orientation, the average rolling velocity in the inverted orientation would be expected to be lower than the velocity in the normal orientation. However, when the average rolling velocity from those instantaneous rolling velocity plots for the normal and inverted orientation were compared, only at 0.25 dynes/cm<sup>2</sup> was the velocity in the inverted orientation found to be significantly slower than the velocity in the normal orientation. For 0.1 dynes/cm<sup>2</sup> the velocity in the inverted orientation was significantly faster than the velocity in the normal orientation, as well as for 0.5 dynes/cm<sup>2</sup> although not found to have a statistically significant difference. Interestingly, rolling cells dissociated slowly from the substrate at 0.25 dynes/cm<sup>2</sup> where inverted rolling was slower than in the normal orientation while dissociation of rolling cells was fast at 0.1 dynes/cm<sup>2</sup> and moderately fast at 0.5 dynes/cm<sup>2</sup> where cell rolling in the inverted orientation was faster than that in the normal orientation.

One reason for the discrepancy in the rolling velocity between the normal and inverted orientation could be due to different populations of cells being observed in each case. In the normal orientation, the velocities of all cells that are rolling on the substrate are measured at each shear stress. Cell detachment is closely observed during measurements to ensure that the rolling behavior is primarily reflected in the velocity measurement. In the inverted orientation, those cells that are not stably rolling will likely detach quickly after inversion. This will leave cells with more stable rolling to be observed for their rolling velocities. Thus, a coincidental selectivity of the cells in the inverted orientation of the more stably rolling cells could account for the rolling velocity difference in the normal and inverted orientation.

Although gravity appears negligible from the balance of forces analysis ( $\leq 1\text{pN}$ ), perhaps it actually plays a role in the rolling adhesion of the cells. Tensegrity is thought to describe the arrangement of cells and explain their mechanotransduction ability. Cells are able to respond immediately to their mechanical environment, including gravity, through surface receptors that are hard-wired to the load bearing structure in the cell called the cytoskeleton, and transduce signals (Ingber 1997). In plant cells and AtT20 pituitary cells, an altered gravity environment has been shown to influence the oscillation and intracellular levels of  $\text{Ca}^{+2}$  (Ikeda et al. 2000; Kordyum 2003). Microgravity studies have also been done with HL-60 cells where membrane damage and membrane-membrane fusion was inhibited by acute microgravity exposure (Clarke et al. 2001). Additionally, HL-60 cell survival was impaired by a microgravity environment due to alterations in the cellular trafficking and activation of the tyrosine kinase vascular endothelial growth factor receptor-2 (VEGFR-2) and VEGFR-A (Vincent et al. 2005).

Thus, HL-60 cells may be able to sense the change in the gravity environment through PSGL-1 or other surface molecules and as a result modulate their rolling behavior.

The effect of force on the kinetic dissociation of selectin-mediated bonds has not yet been fully resolved. The dissociation rate,  $k_{\text{off}}$ , has been most commonly thought to be a single value function of force (Bell 1978). However, recent studies have indicated that  $k_{\text{off}}$  depends on the entire history of force application and the way force is applied can affect the dissociation pathway the selectin-mediated bond follows (Evans et al. 2004; Marshall et al. 2005). Integrated into these mechanisms may be an indirect effect of the gravitational force on the kinetic rates. The force dependent off-rate and tether formation may be enhanced or suppressed due to gravity. In turn, this may also change the balance between off-rate and tether formation, resulting in a unique rolling behavior. Alternatively, the effect of gravity on the force experienced by the tether extrusions might also be a way in which the gravitational force affects the rolling behavior.

For neutrophils, the rolling behavior of the cells in the inverted orientation is even more peculiar than the results for HL-60 cells. Rolling velocity in the inverted orientation is essentially constant over the shear stress range whereas in the normal orientation, a triphasic trend is seen. In addition, some neutrophils were stationary for an extended period of time before rolling and detaching while inverted. The extended pauses seen with neutrophils rolling on E-selectin while inverted resembles observations made in early experiments with neutrophils rolling on P-selectin while inverted (data not shown). Neutrophils rolling on P-selectin in the normal orientation became stationary when in the inverted orientation. The cells appeared to be firmly adherent. But, when the chamber was returned to the normal orientation, neutrophils resumed rolling on P-

selectin. This was not seen with HL-60 cells rolling on P-selectin in the inverted orientation. So, the same extended pauses seem to occur with neutrophils rolling on P- and E-selectin while inverted. Yet, the time scale of when rolling is resumed for E-selectin appears to be shorter than for P-selectin. Seeing this extended pause with neutrophils rolling on both P- and E-selectin while inverted would suggest that the rolling behavior is modified when the chamber is in the inverted orientation.

The same gravitational effects as discussed for HL-60 cells may also play a role in neutrophil rolling on E-selectin. However, the longer membrane tether extrusions of neutrophils, smaller size of the cells and larger array of cell surface molecules expressed on neutrophils than HL-60 cells may cause the affects of gravity on neutrophils to vary from that for HL-60 cells. This might explain the difference in the trend for the rolling velocity while inverted between the HL-60 cells and neutrophils.

## CHAPTER 8

### CONCLUSIONS AND RECOMMENDATIONS

This work explores the kinetics of E-selectin-mediated adhesion. The tether lifetime of transiently tethering neutrophils on a low density of E-selectin was shown to have a triphasic dependence on shear at low shear stresses where the E-selectin-mediated bond transitions from a slip bond to a catch bond and then returns to a slip bond. With the slip/catch/slip bond transition, the unstressed off-rate,  $k_{\text{off}}^0 = 1.0\text{s}^{-1}$  for the neutrophil ligand dissociation from E-selectin. This agrees well with micropipette measurements of  $k_{\text{off}}^0$  for HL-60 cells interacting with E-selectin. This triphasic behavior of E-selectin-mediated dissociation was also observed with sLe<sup>x</sup>-coated beads transiently tethering to E-selectin. Despite the subtle trends of the data for both neutrophils and sLe<sup>x</sup>-coated beads, the transitions of the curves between slip and catch bonds were found to be statistically significant.

Catch/slip bond transitions have already been seen for P- and L-selectin (Marshall et al. 2003; Sarangapani et al. 2004). With this work, the role of catch bonds in the dissociation kinetics of all three selectins is now known. Furthermore, the slip/catch/slip dissociation of E-selectin reveals that a slip bond regime may precede the catch bond regime for P- and L-selectin. For P- and L-selectin, collecting tether lifetime data at forces lower than the catch bond regime was challenging. However, if a slip bond does precede the catch bond regime, then the lifetime at zero force would be higher and in better agreement with zero-force lifetime measurements done with SPR for P-selectin/PSGL-1. Instrumentation to allow tether lifetime observations at lower forces for

P- and L-selectin would provide additional insight into whether a slip bond does exist before the catch/slip transition.

The trend of the average rolling of neutrophils, fixed and unfixed, on E-selectin also followed a statistically significant triphasic trend. At the very low and higher shear stresses where slip bonds were seen, the average rolling velocity increased as shear was increased. In the moderate shear stress range, which corresponded to the catch bond regime, decreasing rolling velocity as shear stress increased was found. This result fits well with prior studies which prove that faster dissociation kinetics of selectins mediate faster rolling (Alon et al. 1997) and that catch bonds govern the rolling velocity through L-selectin (Yago et al. 2004). The average rolling velocity of HL-60 cells and Colo-205 cells was also observed and found to have a triphasic curve over shear stress as well. The agreement of the tether lifetime measurement and the average rolling velocity data provide strong evidence that the dissociation of E-selectin has a statistically significant triphasic force dependence containing slip/catch/slip bond transitions which determines the rolling velocity of cells on E-selectin substrates.

For expansion of the work on the dissociation kinetics of E-selectin presented here, the following studies would be recommended:

- Studies of the tether lifetime at lower forces for P- and L-selectin that precede the catch/slip transition
- Additional studies using micropipette of the dissociation of E-selectin with neutrophils

- Experiments with SPR to measure the zero-force lifetime of E-selectin with various neutrophil ligands
- Further investigation into the dissociation of Colo-205 from E-selectin using flow chamber
- Investigation into the physiological role of the slip/catch/slip bond transition of E-selectin-mediated dissociation

Investigating the dissociation of Colo-205 cells from E-selectin using the flow chamber is of particular interest. The average rolling velocity of Colo-205 cells displayed a triphasic curve as shear stress was increased. However, the shear stress range of each rolling velocity phase did not completely match the tether lifetime results obtained with micropipette experiments (Piper 1997). Micropipette experiments to observe the tether lifetimes were conducted at forces lower than where rolling velocity measurements were made. Thus, observing the tether lifetime of Colo-205 cells transiently tethering to E-selectin in the flow chamber would be important to resolving this discrepancy. With the current flow chamber design, the lowest shear stress with reliability is  $0.05 \text{ dynes/cm}^2$ . Tether lifetime experiments could be done between  $0.05$  and  $0.8 \text{ dynes/cm}^2$  to start. However, the use of a thicker gasket may allow lower shear stresses to be tested. Further investigation could include conducting similar tether lifetime experiments with sLe<sup>a</sup>-coated beads transiently tethering to E-selectin to delineate the role of sLe<sup>a</sup> compared to sLe<sup>x</sup> in E-selectin-mediated dissociation for Colo-205 cells.

The  $k_{\text{off(RA)}}$ , determined using an invertible flow chamber, was found to decrease as force increased to  $0.25 \text{ dynes/cm}^2$  and then increase with increasing shear stress. These results looked as if they contradicted the triphasic curve obtained for the dissociation of transiently tethering neutrophils and sLe<sup>x</sup>-coated beads on E-selectin. However, closer investigation into the rolling behavior of the cells revealed that  $k_{\text{off(RA)}}$  is related to the rolling stability of the cell, demonstrating quantitatively the shear threshold phenomenon as suggested previously for E-selectin (Lawrence et al. 1997). The work here further discusses how for E-selectin, tether formation may be a larger influence on rolling stability than off-rate due to the region where less stable rolling was found to occur. This varies from what has been found for L-selectin where the off-rate has been shown to govern the slower rolling velocity and the more stable rolling behavior through the shear threshold (Yago et al. 2004). However, the dissociation for L-selectin is biphasic with a catch/slip transition whereas for E-selectin a triphasic dissociation curve with slip/catch/slip bonds is observed. Therefore,  $k_{\text{off(RA)}}$  may be a measure of the shear-dependent tether formation or even reflect the combined effect of both  $k_{\text{off}}$  and tether formation as a function of shear stress. This may provide insight into the cell rolling behavior through the shear threshold for E-selectin and how it differs from that found for L-selectin.

One of the main objectives that drives the studying the kinetics of E-selectin-mediated dissociation is to accurately model the leukocyte rolling on vascular surfaces through selectin-mediated bonds. In this work, the dissociation kinetics of transiently tethering cells on E-selectin in the low shear forces was revealed and shown to correlate to the cell's rolling velocity. This kinetic information could therefore be useful for

modeling the cell rolling velocity in a flow field. The  $k_{\text{off(RA)}}$  provides kinetic information related to how cells sustain rolling in a flow field. This parameter reflects shear-dependent tether formation and may be the net effect of the tether formation of front bonds and the tether lifetime of rear bonds. In using the dissociation kinetic information from these experiments for both transiently tethering and rolling cells, models that depict the continuous rolling of cells on E-selectin in a flow field can be developed.

The inverted flow chamber studies also revealed a difference in the rolling velocity of the cells while inverted from their rolling velocity when the chamber is normally oriented. At 0.25 dynes/cm<sup>2</sup>, where HL-60 cells dissociated the slowest, the rolling velocity of the cells in the inverted orientation was slower than that in the normal orientation. For 0.1 dynes/cm<sup>2</sup>, rolling HL-60 cell dissociation was fastest and the cells rolled faster in the inverted orientation than in the normal orientation. Furthermore, neutrophil rolling on E-selectin while inverted consisted of noticeably long pauses where cells appeared to be firmly adherent but would resume rolling and detach after several seconds of pausing. The modified cell rolling observed for HL-60 cells and neutrophils rolling on E-selectin while inverted could be due to a subpopulation of cells only being observed in the inverted orientation. However, gravity, although assumed negligible, may affect selectin-mediated cell rolling. Previous studies have shown that cells do respond to changes in the microgravity environment (Ikeda et al. 2000; Clarke et al. 2001; Kordyum 2003; Vincent et al. 2005). Yet the results presented here provide new knowledge of how the effect of gravity on the cells may modulate selectin-mediated adhesion.

To further this work on the dissociation of rollingly adherent cells, the following studies would be recommended:

- Experiments with L-selectin using the inverted flow chamber to obtain  $k_{\text{off(RA)}}$
- A more quantitative study of the rolling behavior of cells on E-selectin with higher spatial and temporal resolution
- Additional tethering frequency experiments for E-selectin-mediated binding at low shear stresses
- Studies of cell tethering and rolling using a side view flow chamber as done by Cao et al. (Cao et al. 1997)
- Investigation of the affect of gravity on cellular trafficking and activation of selectin ligands on HL-60 cells and neutrophils and how it affects selectin-mediated adhesion

More is known about L-selectin and its shear threshold phenomenon than about E-selectin. The slower and more stable rolling of cells with L-selectin through the shear threshold has been well shown to be governed by catch bonds. So for L-selectin,  $k_{\text{off(RA)}}$  would be expected to agree well with the catch/slip transition of the  $k_{\text{off}}$  for transiently tethering cells. Thus, obtaining  $k_{\text{off(RA)}}$  with the inverted flow chamber would be a step towards the comprehensive understanding of the relation of the dissociation kinetics to the rolling velocity behavior for selectin-mediated adhesion. Additionally, determining the  $k_{\text{off(RA)}}$  on L-selectin could help validate the method used of inverting the flow

chamber to obtain  $k_{\text{off(RA)}}$  for cells rolling on selectin surfaces while also strengthening the results obtained with E-selectin for rollingly adherent cells.

A closer look into the rolling behavior of cells through E-selectin would also be beneficial. Rolling adhesion experiments with higher spatial and temporal resolution could be done to investigate the E-selectin mediated rolling behavior. The total movement of rolling cells, including the attachment and detachment of the cells, at various shear stresses could be instantaneous tracked. The rolling velocity, acceleration, deceleration, “go” phases and “stop” phases during rolling can be quantified by using Microsoft Excel macros similar to that used for L-selectin rolling studies (Yago et al. 2004). However, enhancing the macros to include the total time that the cell is rollingly adherent to the surface while being tracked and the frequency of detachment and re-attachment while rolling would be needed to make this study useful. With this data, the stability of rolling of E-selectin through the shear threshold can be better quantified.

## REFERENCES

- Alon, R., S. Chen, K. D. Puri, E. B. Finger and T. A. Springer (1997). "The kinetics of L-selectin tethers and the mechanics of selectin-mediated rolling." J Cell Biol **138**(5): 1169-80.
- Alon, R., D. A. Hammer and T. A. Springer (1995). "Lifetime of the P-selectin-carbohydrate bond and its response to tensile force in hydrodynamic flow." Nature **374**(6522): 539-42.
- Bell, G. I. (1978). "Models for the specific adhesion of cells to cells." Science **200**(4342): 618-27.
- Berg, E. L., T. Yoshino, L. S. Rott, M. K. Robinson, R. A. Warnock, T. K. Kishimoto, L. J. Picker and E. C. Butcher (1991). "The cutaneous lymphocyte antigen is a skin lymphocyte homing receptor for the vascular lectin endothelial cell-leukocyte adhesion molecule 1." J Exp Med **174**(6): 1461-6.
- Bevilacqua, M. P., R. M. Nelson, G. Mannori and O. Cecconi (1994). "Endothelial-leukocyte adhesion molecules in human disease." Annu Rev Med **45**: 361-78.
- Bevilacqua, M. P., J. S. Pober, D. L. Mendrick, R. S. Cotran and M. A. Gimbrone, Jr. (1987). "Identification of an inducible endothelial-leukocyte adhesion molecule." Proc Natl Acad Sci U S A **84**(24): 9238-42.
- Borregaard, N., L. Kjeldsen, H. Sengelov, M. S. Diamond, T. A. Springer, H. C. Anderson, T. K. Kishimoto and D. F. Bainton (1994). "Changes in subcellular localization and surface expression of L-selectin, alkaline phosphatase, and Mac-1 in human neutrophils during stimulation with inflammatory mediators." J Leukoc Biol **56**(1): 80-7.
- Bruehl, R. E., K. L. Moore, D. E. Lorant, N. Borregaard, G. A. Zimmerman, R. P. McEver and D. F. Bainton (1997). "Leukocyte activation induces surface redistribution of P-selectin glycoprotein ligand-1." J Leukoc Biol **61**(4): 489-99.
- Brunk, D. K. and D. A. Hammer (1997). "Quantifying rolling adhesion with a cell-free assay: E-selectin and its carbohydrate ligands." Biophys J **72**(6): 2820-33.
- Cao, J., S. Usami and C. Dong (1997). "Development of a side-view chamber for studying cell-surface adhesion under flow conditions." Ann Biomed Eng **25**(3): 573-80.

- Chang, K. C. and D. A. Hammer (1999). "The forward rate of binding of surface-tethered reactants: effect of relative motion between two surfaces." Biophys J **76**(3): 1280-92.
- Chen, S., R. Alon, R. C. Fuhlbrigge and T. A. Springer (1997). "Rolling and transient tethering of leukocytes on antibodies reveal specializations of selectins." Proc Natl Acad Sci U S A **94**(7): 3172-7.
- Chen, S. and T. A. Springer (1999). "An automatic braking system that stabilizes leukocyte rolling by an increase in selectin bond number with shear." J Cell Biol **144**(1): 185-200.
- Chen, S. and T. A. Springer (2001). "Selectin receptor-ligand bonds: Formation limited by shear rate and dissociation governed by the Bell model." Proc Natl Acad Sci U S A **98**(3): 950-5.
- Clarke, M. S., C. R. Vanderburg and D. L. Feedback (2001). "The effect of acute microgravity on mechanically-induced membrane damage and membrane-membrane fusion events." J Gravit Physiol **8**(2): 37-47.
- Dembo, M., D. C. Torney, K. Saxman and D. Hammer (1988). "The reaction-limited kinetics of membrane-to-surface adhesion and detachment." Proc R Soc Lond B Biol Sci **234**(1274): 55-83.
- Dimitroff, C. J., J. Y. Lee, S. Rafii, R. C. Fuhlbrigge and R. Sackstein (2001). "CD44 is a major E-selectin ligand on human hematopoietic progenitor cells." J Cell Biol **153**(6): 1277-86.
- Eriksson, E. E., X. Xie, J. Werr, P. Thoren and L. Lindbom (2001). "Direct viewing of atherosclerosis in vivo: plaque invasion by leukocytes is initiated by the endothelial selectins." Faseb J **15**(7): 1149-57.
- Erlandsen, S. L., S. R. Hasslen and R. D. Nelson (1993). "Detection and spatial distribution of the beta 2 integrin (Mac-1) and L-selectin (LECAM-1) adherence receptors on human neutrophils by high-resolution field emission SEM." J Histochem Cytochem **41**(3): 327-33.
- Evans, E., A. Leung, V. Heinrich and C. Zhu (2004). "Mechanical switching and coupling between two dissociation pathways in a P-selectin adhesion bond." Proc Natl Acad Sci U S A **101**(31): 11281-6.
- Finger, E. B., K. D. Puri, R. Alon, M. B. Lawrence, U. H. von Andrian and T. A. Springer (1996). "Adhesion through L-selectin requires a threshold hydrodynamic shear." Nature **379**(6562): 266-9.

- Firrell, J. C. and H. H. Lipowsky (1989). "Leukocyte margination and deformation in mesenteric venules of rat." Am J Physiol **256**(6 Pt 2): H1667-74.
- Forlow, S. B., E. J. White, S. C. Barlow, S. H. Feldman, H. Lu, G. J. Bagby, A. L. Beaudet, D. C. Bullard and K. Ley (2000). "Severe inflammatory defect and reduced viability in CD18 and E-selectin double-mutant mice." J Clin Invest **106**(12): 1457-66.
- Foxall, C., S. R. Watson, D. Dowbenko, C. Fennie, L. A. Lasky, M. Kiso, A. Hasegawa, D. Asa and B. K. Brandley (1992). "The three members of the selectin receptor family recognize a common carbohydrate epitope, the sialyl Lewis(x) oligosaccharide." J Cell Biol **117**(4): 895-902.
- Frenette, P. S., S. Subbarao, I. B. Mazo, U. H. von Andrian and D. D. Wagner (1998). "Endothelial selectins and vascular cell adhesion molecule-1 promote hematopoietic progenitor homing to bone marrow." Proc Natl Acad Sci U S A **95**(24): 14423-8.
- Geng, J. G., M. P. Bevilacqua, K. L. Moore, T. M. McIntyre, S. M. Prescott, J. M. Kim, G. A. Bliss, G. A. Zimmerman and R. P. McEver (1990). "Rapid neutrophil adhesion to activated endothelium mediated by GMP-140." Nature **343**(6260): 757-60.
- Goetz, D. J., D. M. Greif, H. Ding, R. T. Camphausen, S. Howes, K. M. Comess, K. R. Snapp, G. S. Kansas and F. W. Luscinskas (1997). "Isolated P-selectin glycoprotein ligand-1 dynamic adhesion to P- and E-selectin." J Cell Biol **137**(2): 509-19.
- Goldman, A. J., R. G. Cox and H. Brenner (1967). "Slow viscous motion of a sphere parallel to a plane wall. II. Couette flow." Chem. Engineer. Sci. **22**: 653-660.
- Graves, B. J., R. L. Crowther, C. Chandran, J. M. Rumberger, S. Li, K. S. Huang, D. H. Presky, P. C. Familletti, B. A. Wolitzky and D. K. Burns (1994). "Insight into E-selectin/ligand interaction from the crystal structure and mutagenesis of the lec/EGF domains." Nature **367**(6463): 532-8.
- Greenberg, A. W., D. K. Brunk and D. A. Hammer (2000). "Cell-free rolling mediated by L-selectin and sialyl Lewis(x) reveals the shear threshold effect." Biophys J **79**(5): 2391-402.
- Hensley, P., P. J. McDevitt, I. Brooks, J. J. Trill, J. A. Feild, D. E. McNulty, J. R. Connor, D. E. Griswold, N. V. Kumar, K. D. Kopple and et al. (1994). "The soluble form of E-selectin is an asymmetric monomer. Expression, purification, and characterization of the recombinant protein." J Biol Chem **269**(39): 23949-58.

- Hinds, M. T., Y. J. Park, S. A. Jones, D. P. Giddens and B. R. Alevriadou (2001). "Local hemodynamics affect monocytic cell adhesion to a three-dimensional flow model coated with E-selectin." J Biomech **34**(1): 95-103.
- Huang, J., J. Chen, S. E. Chesla, T. Yago, P. Mehta, R. P. McEver, C. Zhu and M. Long (2004). "Quantifying the effects of molecular orientation and length on two-dimensional receptor-ligand binding kinetics." J Biol Chem **279**(43): 44915-23.
- Ikeda, M., M. Hirono, M. Kishio, J. Matsuura, M. Sakakibara and T. Yoshioka (2000). "Examination of microgravity effects on spontaneous Ca<sup>2+</sup> oscillations in AtT20 pituitary cells using heavy water." J Gravit Physiol **7**(2): P63-4.
- Ingber, D. E. (1997). "Tensegrity: the architectural basis of cellular mechanotransduction." Annu Rev Physiol **59**: 575-99.
- Kansas, G. S. (1996). "Selectins and their ligands: current concepts and controversies." Blood **88**(9): 3259-87.
- Kojima, N., K. Handa, W. Newman and S. Hakomori (1992). "Inhibition of selectin-dependent tumor cell adhesion to endothelial cells and platelets by blocking O-glycosylation of these cells." Biochem Biophys Res Commun **182**(3): 1288-95.
- Kordyum, E. L. (2003). "Calcium signaling in plant cells in altered gravity." Adv Space Res **32**(8): 1621-30.
- Kumar, R., R. T. Camphausen, F. X. Sullivan and D. A. Cumming (1996). "Core2 beta-1,6-N-acetylglucosaminyltransferase enzyme activity is critical for P-selectin glycoprotein ligand-1 binding to P-selectin." Blood **88**(10): 3872-9.
- Kunkel, E. J. and K. Ley (1996). "Distinct phenotype of E-selectin-deficient mice. E-selectin is required for slow leukocyte rolling in vivo." Circ Res **79**(6): 1196-204.
- Larson, R. S. and T. A. Springer (1990). "Structure and function of leukocyte integrins." Immunol Rev **114**: 181-217.
- Lauri, D., L. Needham, I. Martin-Padura and E. Dejana (1991). "Tumor cell adhesion to endothelial cells: endothelial leukocyte adhesion molecule-1 as an inducible adhesive receptor specific for colon carcinoma cells." J Natl Cancer Inst **83**(18): 1321-4.
- Lawrence, M. B., G. S. Kansas, E. J. Kunkel and K. Ley (1997). "Threshold levels of fluid shear promote leukocyte adhesion through selectins (CD62L,P,E)." J Cell Biol **136**(3): 717-27.

- Lawrence, M. B. and T. A. Springer (1991). "Leukocytes roll on a selectin at physiologic flow rates: distinction from and prerequisite for adhesion through integrins." Cell **65**(5): 859-73.
- Lei, X., M. B. Lawrence and C. Dong (1999). "Influence of cell deformation on leukocyte rolling adhesion in shear flow." J Biomech Eng **121**(6): 636-43.
- Ley, K. (2003). "Inflammation: The Leukocyte Adhesion Cascade." University of Virginia Biomedical Engineering Website.
- Ley, K., M. Allietta, D. C. Bullard and S. Morgan (1998). "Importance of E-selectin for firm leukocyte adhesion in vivo." Circ Res **83**(3): 287-94.
- Ley, K., P. Gaetgens, C. Fennie, M. S. Singer, L. A. Lasky and S. D. Rosen (1991). "Lectin-like cell adhesion molecule 1 mediates leukocyte rolling in mesenteric venules in vivo." Blood **77**(12): 2553-5.
- Ley, K., A. Zakrzewicz, C. Hanski, L. M. Stoolman and G. S. Kansas (1995). "Sialylated O-glycans and L-selectin sequentially mediate myeloid cell rolling in vivo." Blood **85**(12): 3727-35.
- Long, M., H. Zhao, K. S. Huang and C. Zhu (2001). "Kinetic measurements of cell surface E-selectin/carbohydrate ligand interactions." Ann Biomed Eng **29**(11): 935-46.
- Lou, J. (unpublished data).
- Lu, H., C. W. Smith, J. Perrard, D. Bullard, L. Tang, S. B. Shappell, M. L. Entman, A. L. Beaudet and C. M. Ballantyne (1997). "LFA-1 is sufficient in mediating neutrophil emigration in Mac-1-deficient mice." J Clin Invest **99**(6): 1340-50.
- Luscinskas, F. W., H. Ding, P. Tan, D. Cumming, T. F. Tedder and M. E. Gerritsen (1996). "L- and P-selectins, but not CD49d (VLA-4) integrins, mediate monocyte initial attachment to TNF-alpha-activated vascular endothelium under flow in vitro." J Immunol **157**(1): 326-35.
- Marshall, B. T., M. Long, J. W. Piper, T. Yago, R. P. McEver and C. Zhu (2003). "Direct observation of catch bonds involving cell-adhesion molecules." Nature **423**(6936): 190-3.
- Marshall, B. T., K. K. Sarangapani, J. Lou, R. P. McEver and C. Zhu (2005). "Force history dependence of receptor-ligand dissociation." Biophys J **88**(2): 1458-66.

- Mazo, I. B., J. C. Gutierrez-Ramos, P. S. Frenette, R. O. Hynes, D. D. Wagner and U. H. von Andrian (1998). "Hematopoietic progenitor cell rolling in bone marrow microvessels: parallel contributions by endothelial selectins and vascular cell adhesion molecule 1." J Exp Med **188**(3): 465-74.
- McEver, R. P. and R. D. Cummings (1997). "Role of PSGL-1 binding to selectins in leukocyte recruitment." J Clin Invest **100**(11 Suppl): S97-103.
- McEver, R. P. and M. N. Martin (1984). "A monoclonal antibody to a membrane glycoprotein binds only to activated platelets." J Biol Chem **259**(15): 9799-804.
- McEver, R. P., K. L. Moore and R. D. Cummings (1995). "Leukocyte trafficking mediated by selectin-carbohydrate interactions." J Biol Chem **270**(19): 11025-8.
- Mehta, P., R. D. Cummings and R. P. McEver (1998). "Affinity and kinetic analysis of P-selectin binding to P-selectin glycoprotein ligand-1." J Biol Chem **273**(49): 32506-13.
- Milstone, D. S., D. Fukumura, R. C. Padgett, P. E. O'Donnell, V. M. Davis, O. J. Benavidez, W. L. Monsky, R. J. Melder, R. K. Jain and M. A. Gimbrone, Jr. (1998). "Mice lacking E-selectin show normal numbers of rolling leukocytes but reduced leukocyte stable arrest on cytokine-activated microvascular endothelium." Microcirculation **5**(2-3): 153-71.
- Moore, K. L. (1998). "Structure and function of P-selectin glycoprotein ligand-1." Leuk Lymphoma **29**(1-2): 1-15.
- Moore, K. L., S. F. Eaton, D. E. Lyons, H. S. Lichenstein, R. D. Cummings and R. P. McEver (1994). "The P-selectin glycoprotein ligand from human neutrophils displays sialylated, fucosylated, O-linked poly-N-acetylactosamine." J Biol Chem **269**(37): 23318-27.
- Moore, T. B., N. Sidell, V. J. Chow, R. H. Medzoyan, J. I. Huang, J. M. Yamashiro and R. K. Wada (1995). "Differentiating effects of 1,25-dihydroxycholecalciferol (D3) on LA-N-5 human neuroblastoma cells and its synergy with retinoic acid." J Pediatr Hematol Oncol **17**(4): 311-7.
- Munoz, F. M., E. P. Hawkins, D. C. Bullard, A. L. Beaudet and S. L. Kaplan (1997). "Host defense against systemic infection with *Streptococcus pneumoniae* is impaired in E-, P-, and E-/P-selectin-deficient mice." J Clin Invest **100**(8): 2099-106.
- Naiyer, A. J., D. Y. Jo, J. Ahn, R. Mohle, M. Peichev, G. Lam, R. L. Silverstein, M. A. Moore and S. Rafii (1999). "Stromal derived factor-1-induced chemokinesis of cord blood CD34(+) cells (long-term culture-initiating cells) through endothelial cells is mediated by E-selectin." Blood **94**(12): 4011-9.

- Nicholson, M. W., A. N. Barclay, M. S. Singer, S. D. Rosen and P. A. van der Merwe (1998). "Affinity and kinetic analysis of L-selectin (CD62L) binding to glycosylation-dependent cell-adhesion molecule-1." J Biol Chem **273**(2): 763-70.
- Norgard, K. E., K. L. Moore, S. Diaz, N. L. Stults, S. Ushiyama, R. P. McEver, R. D. Cummings and A. Varki (1993). "Characterization of a specific ligand for P-selectin on myeloid cells. A minor glycoprotein with sialylated O-linked oligosaccharides." J Biol Chem **268**(17): 12764-74.
- Norman, K. E., A. G. Katopodis, G. Thoma, F. Kolbinger, A. E. Hicks, M. J. Cotter, A. G. Pockley and P. G. Hellewell (2000). "P-selectin glycoprotein ligand-1 supports rolling on E- and P-selectin in vivo." Blood **96**(10): 3585-91.
- O'Brien, K. D., T. O. McDonald, A. Chait, M. D. Allen and C. E. Alpers (1996). "Neovascular expression of E-selectin, intercellular adhesion molecule-1, and vascular cell adhesion molecule-1 in human atherosclerosis and their relation to intimal leukocyte content." Circulation **93**(4): 672-82.
- Patel, K. D., K. L. Moore, M. U. Nollert and R. P. McEver (1995). "Neutrophils use both shared and distinct mechanisms to adhere to selectins under static and flow conditions." J Clin Invest **96**(4): 1887-96.
- Patel, K. D., M. U. Nollert and R. P. McEver (1995). "P-selectin must extend a sufficient length from the plasma membrane to mediate rolling of neutrophils." J Cell Biol **131**(6 Pt 2): 1893-902.
- Phillips, M. L., E. Nudelman, F. C. Gaeta, M. Perez, A. K. Singhal, S. Hakomori and J. C. Paulson (1990). "ELAM-1 mediates cell adhesion by recognition of a carbohydrate ligand, sialyl-Lex." Science **250**(4984): 1130-2.
- Picker, L. J., S. A. Michie, L. S. Rott and E. C. Butcher (1990). "A unique phenotype of skin-associated lymphocytes in humans. Preferential expression of the HECA-452 epitope by benign and malignant T cells at cutaneous sites." Am J Pathol **136**(5): 1053-68.
- Picker, L. J., R. A. Warnock, A. R. Burns, C. M. Doerschuk, E. L. Berg and E. C. Butcher (1991). "The neutrophil selectin LECAM-1 presents carbohydrate ligands to the vascular selectins ELAM-1 and GMP-140." Cell **66**(5): 921-33.
- Piper, J. W. (1997). Force dependence of cell bound E-selectin/carbohydrate ligand binding characteristics. Mechanical Engineering. Atlanta, GA, Georgia Institute of Technology. **Ph.D.**
- Piper, J. W., R. A. Swerlick and C. Zhu (1998). "Determining force dependence of two-dimensional receptor-ligand binding affinity by centrifugation." Biophys J **74**(1): 492-513.

- Polley, M. J., M. L. Phillips, E. Wayner, E. Nudelman, A. K. Singhal, S. Hakomori and J. C. Paulson (1991). "CD62 and endothelial cell-leukocyte adhesion molecule 1 (ELAM-1) recognize the same carbohydrate ligand, sialyl-Lewis x." Proc Natl Acad Sci U S A **88**(14): 6224-8.
- Poppe, L., G. S. Brown, J. S. Philo, P. V. Nikrad and B. H. Shah (1997). "Conformation of sLex Tetrasaccharide, Free in Solution and Bound to E-, P-, and L-Selectin." J. Am. Chem. Society **119**(7): 1727-1736.
- Pouyani, T. and B. Seed (1995). "PSGL-1 recognition of P-selectin is controlled by a tyrosine sulfation consensus at the PSGL-1 amino terminus." Cell **83**(2): 333-43.
- Puri, K. D., S. Chen and T. A. Springer (1998). "Modifying the mechanical property and shear threshold of L-selectin adhesion independently of equilibrium properties." Nature **392**(6679): 930-3.
- Puri, K. D., E. B. Finger and T. A. Springer (1997). "The faster kinetics of L-selectin than of E-selectin and P-selectin rolling at comparable binding strength." J Immunol **158**(1): 405-13.
- Ramachandran, V., M. U. Nollert, H. Qiu, W. J. Liu, R. D. Cummings, C. Zhu and R. P. McEver (1999). "Tyrosine replacement in P-selectin glycoprotein ligand-1 affects distinct kinetic and mechanical properties of bonds with P- and L-selectin." Proc Natl Acad Sci U S A **96**(24): 13771-6.
- Ramachandran, V., M. Williams, T. Yago, D. W. Schmidtke and R. P. McEver (2004). "Dynamic alterations of membrane tethers stabilize leukocyte rolling on P-selectin." Proc Natl Acad Sci U S A **101**(37): 13519-24.
- Rodgers, S. D., R. T. Camphausen and D. A. Hammer (2000). "Sialyl Lewis(x)-mediated, PSGL-1-independent rolling adhesion on P-selectin." Biophys J **79**(2): 694-706.
- Rodgers, S. D., R. T. Camphausen and D. A. Hammer (2001). "Tyrosine sulfation enhances but is not required for PSGL-1 rolling adhesion on P-selectin." Biophys J **81**(4): 2001-9.
- Sako, D., K. M. Comess, K. M. Barone, R. T. Camphausen, D. A. Cumming and G. D. Shaw (1995). "A sulfated peptide segment at the amino terminus of PSGL-1 is critical for P-selectin binding." Cell **83**(2): 323-31.
- Sarangapani, K. K. (unpublished data).
- Sarangapani, K. K., T. Yago, A. G. Klopocki, M. B. Lawrence, C. B. Fieger, S. D. Rosen, R. P. McEver and C. Zhu (2004). "Low force decelerates L-selectin dissociation from P-selectin glycoprotein ligand-1 and endoglycan." J Biol Chem **279**(3): 2291-8.

- Schmits, R., T. M. Kundig, D. M. Baker, G. Shumaker, J. J. Simard, G. Duncan, A. Wakeham, A. Shahinian, A. van der Heiden, M. F. Bachmann, P. S. Ohashi, T. W. Mak and D. D. Hickstein (1996). "LFA-1-deficient mice show normal CTL responses to virus but fail to reject immunogenic tumor." J Exp Med **183**(4): 1415-26.
- Schweitzer, K. M., A. M. Drager, P. van der Valk, S. F. Thijsen, A. Zevenbergen, A. P. Theijssmeijer, C. E. van der Schoot and M. M. Langenhuijsen (1996). "Constitutive expression of E-selectin and vascular cell adhesion molecule-1 on endothelial cells of hematopoietic tissues." Am J Pathol **148**(1): 165-75.
- Smith, M. J., E. L. Berg and M. B. Lawrence (1999). "A direct comparison of selectin-mediated transient, adhesive events using high temporal resolution." Biophys J **77**(6): 3371-83.
- Somers, W. S., J. Tang, G. D. Shaw and R. T. Camphausen (2000). "Insights into the molecular basis of leukocyte tethering and rolling revealed by structures of P- and E-selectin bound to SLe(X) and PSGL-1." Cell **103**(3): 467-79.
- Springer, T. A. (1994). "Traffic signals for lymphocyte recirculation and leukocyte emigration: the multistep paradigm." Cell **76**(2): 301-14.
- Springer, T. A. (1995). "Traffic signals on endothelium for lymphocyte recirculation and leukocyte emigration." Annu Rev Physiol **57**: 827-72.
- Thomas, W. E., E. Trintchina, M. Forero, V. Vogel and E. V. Sokurenko (2002). "Bacterial adhesion to target cells enhanced by shear force." Cell **109**(7): 913-23.
- Ushiyama, S., T. M. Laue, K. L. Moore, H. P. Erickson and R. P. McEver (1993). "Structural and functional characterization of monomeric soluble P-selectin and comparison with membrane P-selectin." J Biol Chem **268**(20): 15229-37.
- Vincent, L., P. Avancena, J. Cheng, S. Rafii and S. Y. Rabbany (2005). "Simulated microgravity impairs leukemic cell survival through altering VEGFR-2/VEGF-A signaling pathway." Ann Biomed Eng **33**(10): 1405-10.
- Voermans, C., P. M. Rood, P. L. Hordijk, W. R. Gerritsen and C. E. van der Schoot (2000). "Adhesion molecules involved in transendothelial migration of human hematopoietic progenitor cells." Stem Cells **18**(6): 435-43.
- von Andrian, U. H., J. D. Chambers, L. M. McEvoy, R. F. Bargatze, K. E. Arfors and E. C. Butcher (1991). "Two-step model of leukocyte-endothelial cell interaction in inflammation: distinct roles for LECAM-1 and the leukocyte beta 2 integrins in vivo." Proc Natl Acad Sci U S A **88**(17): 7538-42.

- Weninger, W., L. H. Ulfman, G. Cheng, N. Souchkova, E. J. Quackenbush, J. B. Lowe and U. H. von Andrian (2000). "Specialized contributions by alpha(1,3)-fucosyltransferase-IV and FucT-VII during leukocyte rolling in dermal microvessels." *Immunity* **12**(6): 665-76.
- Wild, M. K., M. C. Huang, U. Schulze-Horsel, P. A. van der Merwe and D. Vestweber (2001). "Affinity, kinetics, and thermodynamics of E-selectin binding to E-selectin ligand-1." *J Biol Chem* **276**(34): 31602-12.
- Xia, L., J. M. McDaniel, T. Yago, A. Doeden and R. P. McEver (2004). "Surface fucosylation of human cord blood cells augments binding to P-selectin and E-selectin and enhances engraftment in bone marrow." *Blood* **104**(10): 3091-6.
- Yago, T., A.G. Klopocki, J. Lou, P. Mehta, W. Chen, V. Zarnitsyna, N.V. Bovin, C. Zhu and R.P. McEver (submitted). "Selectin catch bonds regulated by an interdomain hinge."
- Yago, T., A. Leppanen, H. Qiu, W. D. Marcus, M. U. Nollert, C. Zhu, R. D. Cummings and R. P. McEver (2002). "Distinct molecular and cellular contributions to stabilizing selectin-mediated rolling under flow." *J Cell Biol* **158**(4): 787-99.
- Yago, T., J. Wu, C. D. Wey, A. G. Klopocki, C. Zhu and R. P. McEver (2004). "Catch bonds govern adhesion through L-selectin at threshold shear." *J Cell Biol* **166**(6): 913-23.
- Yang, J., B. C. Furie and B. Furie (1999). "The biology of P-selectin glycoprotein ligand-1: its role as a selectin counterreceptor in leukocyte-endothelial and leukocyte-platelet interaction." *Thromb Haemost* **81**(1): 1-7.
- Yang, J., T. Hirata, K. Croce, G. Merrill-Skoloff, B. Tchernychev, E. Williams, R. Flaumenhaft, B. C. Furie and B. Furie (1999). "Targeted gene disruption demonstrates that P-selectin glycoprotein ligand 1 (PSGL-1) is required for P-selectin-mediated but not E-selectin-mediated neutrophil rolling and migration." *J Exp Med* **190**(12): 1769-82.
- Zar, J. (1974). *Biostatistical Analysis*. Englewood Cliffs, N.J., Prentice-Hall, Inc.
- Zhou, Q., K. L. Moore, D. F. Smith, A. Varki, R. P. McEver and R. D. Cummings (1991). "The selectin GMP-140 binds to sialylated, fucosylated lactosaminoglycans on both myeloid and nonmyeloid cells." *J Cell Biol* **115**(2): 557-64.
- Zhu, C., M. Long, S. E. Chesla and P. Bongrand (2002). "Measuring receptor/ligand interaction at the single-bond level: experimental and interpretative issues." *Ann Biomed Eng* **30**(3): 305-14.

Zimmerman, G. A., T. M. McIntyre and S. M. Prescott (1985). "Thrombin stimulates the adherence of neutrophils to human endothelial cells in vitro." J Clin Invest **76**(6): 2235-46.